

TABLE OF CONTENTS

	Page	
SUMMARY	1	1/A7
Test and Analysis	1	1/A7
Steady State Response	1	1/A7
Undamped Blade-Loss Tests	1	1/A7
Damped Blade-Loss Tests	2	1/A8
Conclusions	2	1/A8
INTRODUCTION	3	1/A9
TEST AND ANALYTICAL PROCEDURES	4	1/A10
Test Rig	4	1/A10
Instrumentation and Data Acquisition	4	1/A10
Data Reduction	6	1/A12
Analyses and Dynamic Model	6	1/A12
DISCUSSION OF RESULTS	8	1/A14
Undamped Steady State Response	8	1/A14
Damped Steady State Response	8	1/A14
Undamped Transient Response	15	1/B9
Damped Transient Response	17	1/B11
CONCLUSIONS AND OBSERVATIONS	19	1/B13
REFERENCES	20	1/B14

Microfilmed From
Best Available Copy

COMPLETED
ORIGINAL

Transient Dynamics of a Flexible Rotor With Squeeze Film Dampers

D. F. Buono, L. D. Schlitzer,
R. G. Hall III, and D. H. Hibner

CONTRACT NAS3-18523
SEPTEMBER 1978

NASA

830-H-14 NAS 1.26:3050
NASA Contractor Report 3050

**Microfilmed From
Best Available Copy**

Transient Dynamics of a Flexible Rotor With Squeeze Film Dampers

**D. F. Buono, L. D. Schlitzer,
R. G. Hall III, and D. H. Hibner**
*United Technologies Corporation
East Hartford, Connecticut*

**Prepared for
Lewis Research Center
under Contract NAS3-18523**



**National Aeronautics
and Space Administration**

**Scientific and Technical
Information Office**

1978

Blank Page

FOREWORD

This final report describes the dynamic response characteristics of a flexible rotor investigated by Pratt & Whitney Aircraft, East Hartford, Conn., under Contract NAS3-18523, Modification 3. Mr. D. H. Hibner served as Program Manager and Messers. D. F. Buono, L. D. Schlitzer, and R. G. Hall participated in the program for Pratt & Whitney Aircraft. Mr. A. F. Kascak was Program Manager for NASA. Acknowledgement is given to Dr. R.G. Kirk of the Ingersoll Rand Corporation for his assistance in modifying the transient forced response analysis used in the program.

This report is in compliance with the report requirements of the contract and was prepared under the Contractor's Reference No. PWA 5548-9.

Blank Page

SUMMARY

This report presents the results of a program performed by Pratt & Whitney Aircraft under NASA Contract NASA-18523, Modification 3. The program had two major objectives:

- (1) Obtain the experimental response of a flexible rotor operating under simulated blade-loss conditions, both with and without squeeze film damped bearing supports.
- (2) Correlate the experimental data with theoretical predictions from the transient forced response analysis described in Ref. 2.

These objectives were successfully accomplished. The program and its results are summarized as follows:

Test and Analyses

The test rig used in Ref. 1 was modified to include squeeze film dampers on the bearing supports and to allow operation above the rotor second bending critical speed. The rig was instrumented with five sets of horizontal/vertical proximity probes along the length of the shaft and at the dampers to measure dynamic response. The instrumentation used to record and document the response was the same as described in Ref. 1.

The critical speeds and steady state response of the rig were predicted using the analysis described in Ref. 3. The transient forced response analysis, Ref. 2, was used to predict the rig response during blade-loss as specified by the contract. The computer program based on this analysis was modified to include the characteristics of the spring-centered dampers used in the test rig.

Steady State Response

The rig was balanced to minimize the residual imbalance response in preparation for the steady state and transient testing. Small imbalance was then applied to the blade-loss disk and the peak response speeds for the first and second bending modes were recorded at approximately 1500 rpm and 2950 rpm, respectively. The steady-state baseline response of the rotor was measured at each of several speeds selected to provide mode shapes representative of the rotor response throughout the operating speed range. Both undamped and damped mode shapes were thus obtained and compared to predicted values.

Undamped Blade-Loss Tests

Simulated blade-loss tests without dampers were conducted at 5 speeds; 1500 rpm, 1550 rpm, 2000 rpm, 2950 rpm, and 3100 rpm. The speeds and amounts of imbalance selected for the tests were based on the steady state sensitivity of the rotor. The speeds selected included two speeds between 80% and 120% of each critical, and one speed midway between them. The experimental transient response was correlated with the corresponding predicted response using the aforementioned transient forced response analysis.

Damped Blade-Loss Tests

Damped blade-loss tests were conducted at the same 5 speeds as the undamped blade-loss tests. The imbalance selected for each test was based on the damped steady state sensitivity of the rotor. Two additional damped blade-loss tests were conducted at 1520 rpm and 3050 rpm, respectively, where the rotor sensitivity was high. These tests were conducted to investigate rotor response with large, transient eccentricity ratios of the damper. Again, the experimental data were correlated with the corresponding predicted transient response.

Conclusions

Two main conclusions resulting from the program are:

- (1) The overall response of both damped and undamped flexible rotors is predictable using analytical methods presently available.
- (2) Squeeze film dampers are effective in reducing the sensitivity of flexible rotors to imbalance.

INTRODUCTION

Modern gas turbine engines require light weight flexible rotors to meet the demanding objectives of high performance and efficiency, low cost, and minimum weight. Flexible rotors, however, can be sensitive to imbalance and produce unacceptable transient and steady state dynamic response characteristics. This response can cause high cyclic stresses within engine static structures, high bearing loads, and large rotor excursions which, in turn, produce blade and seal rubs and a loss of performance. Control of this unacceptable response can be obtained by proper use of squeeze film dampers to absorb rotor vibrational energy and make the engine less sensitive to inherent or transient (blade-loss) imbalance.

Under NASA Contract NAS3-18523, Pratt & Whitney Aircraft experimentally measured and studied the transient dynamics of an undamped flexible rotor rig. This program was extended to investigate squeeze film damped as well as undamped transient response of a flexible rotor, and to compare the experimental response with theoretical predictions from a transient response analysis reported in Ref. 2.

The experimental and theoretical transient behavior of a two-bearing flexible rotor subjected to sudden imbalance loads at several speeds up to 120% of its second bending critical speed are discussed herein. The sudden imbalance loads simulate the loss of blades from a high speed turbine or compressor. The transient blade loss response is presented both with and without squeeze film dampers at the bearing locations. The results of this program provide an increased understanding of flexible rotor dynamics technology and aid in the verification and development of analytical methods which can be applied to the design of more complex rotor systems.

TEST FACILITIES AND ANALYTICAL PROCEDURES

Test Rig

The test rig shown in Figures 1 and 2 is a single rotor system with three major masses on a 15.88 mm diameter steel shaft. The shaft is mounted on self-aligning ball bearings 737 mm apart and the bearings are supported from rigid pedestals via flexible cantilevered bearing supports.

Each squeeze film damper comprises a bearing support and housing. The damper housing is designed with large annular cavities on either side of the oil film to act as oil reservoirs and allow damper end leakage. The dampers are identical, having diameters of 114.3 mm and length to diameter ratios of .11, so they can be analytically treated with short bearing theory. Oil is introduced into each damper via reservoirs fed through holes at the bottom and scavenged from oil holes at the top. The oil used in the damper is a jet engine lubrication oil with a viscosity of $.0165 \text{ N}\cdot\text{s}/\text{m}^2$ at 20°C . Oil is supplied to the dampers at a constant pressure of $4.14 \text{ N}/\text{cm}^2$ for all tests. The damper housings are mounted such that they can be centered with respect to the bearing support to compensate for the gravity sag of the support.

The major mass disks shown in Figure 2 are symmetrically placed on the rotor. Each disk has 36 balance holes and the two end disks are designed to release balance weights from axial rim slots to simulate a sudden blade loss. The end disks are also designed to have high polar inertia and thereby produce a large gyroscopic stiffening effect.

The shaft is driven by a frequency controlled induction motor through a 3.18 mm diameter quill shaft 101 mm long. The slender quill shaft has sufficient torsional strength but offers negligible shear and moment restraint to the shaft.

Instrumentation and Data Acquisition

The vertical and horizontal vibratory displacements of the test rotor were measured by pairs of non-contacting proximity probes at five stations along the shaft. The axial position of the probes is listed in Table I and shown schematically in Figure 2. During the steady state testing, the displacement signals and a once-per-rev keyphasor signal were processed by a trim balance analyzer. This provided a digital readout of the running speed, the component of displacement synchronous with running speed, and the phase of the synchronous component. During the transient testing, the displacement signals and the once-per-rev keyphasor signal were captured and recorded by a high speed data memory system. A description of this memory system is given in Ref. 1. The data in the memory system was stored in digital format which could be plotted in analog form or put on magnetic tape for computer reduction and plotting.

The damper oil temperature and supply pressure were also monitored for all tests. Thermocouples were installed in the oil inlet and outlet lines of each damper and mechanical pressure gages were inserted in the oil supply lines close to the damper housings. The pressures were monitored to allow maintaining a constant supply pressure of $4.14 \text{ N}/\text{cm}^2$ for all tests. The temperatures were recorded for each test to provide the proper oil viscosity values in the analyses.

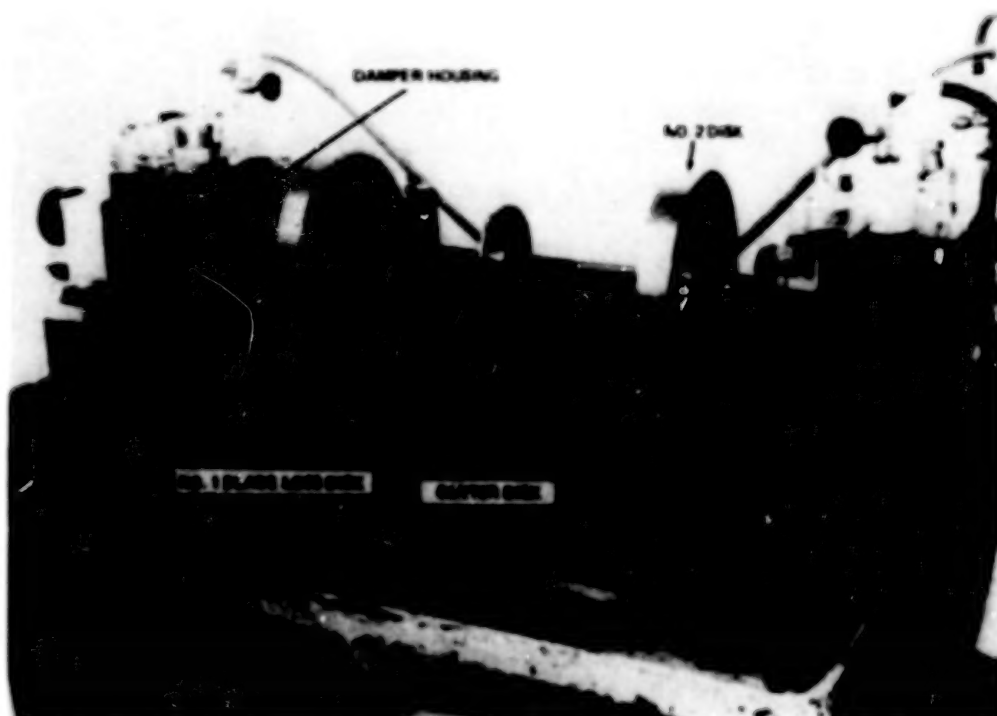


Figure 1 Test Rig Designed For Transient Testing at Speeds Above the Second Bending Critical Speed

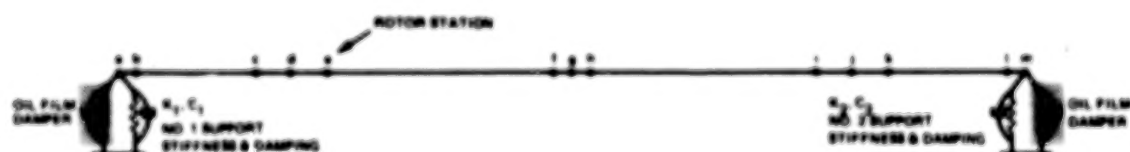
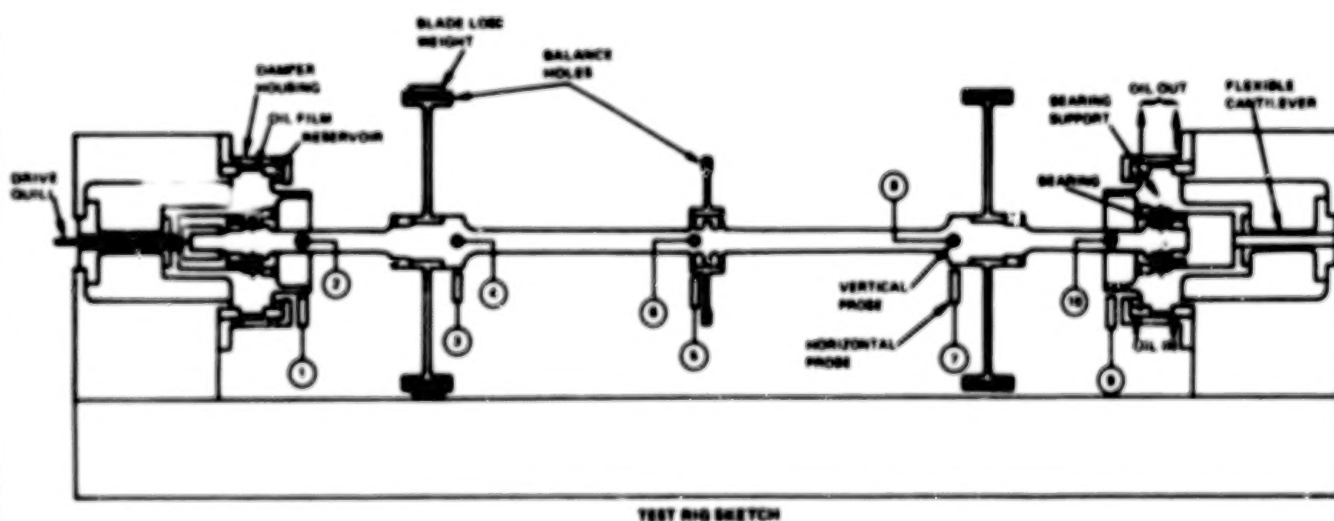


Figure 2 Sketch of Test Rig and Schematic of Analytical Model

TABLE I

DISPLACEMENT PROXIMITY PROBE LOCATION AND ORIENTATION

Data Station	1*		2		3		4		5*	
Probe No.	1	2	3	4	5	6	7	8	9	10
Direction	Vert	Horiz	Vert	Horiz	Vert	Horiz	Vert	Horiz	Vert	Horiz
Axial Location ~ cm	3.2	3.2	18.2	18.2	35.9	35.9	57.5	57.5	70.5	70.5

*Steady state and transient data taken at these stations is corrected to indicate the displacements at the bearing center line.

Data Reduction

The unprocessed displacement data taken during both the steady state and transient tests include vibration due to the applied imbalance as well as any mechanical runout and residual imbalance. Comparison between test and analysis required that the displacement be known for the applied imbalance alone. The steady-state data taken as vibration amplitude and phase were reduced by vector subtraction of that portion of the total signal due to mechanical runout and residual imbalance.

The transient data were recorded as amplitude versus time and stored on magnetic tape in a digital format. Each channel of data represented the vibration signal for a given displacement pickup for a short time before and a longer time after the blade loss occurred. The signal recorded before the blade loss was used as the "As Is" response and subtracted from the response after the blade loss event. This test data processing and reduction, as well as the plotting of the time traces, was automated by a computer program which presented the data in the same format as the transient analysis.

The displacement pickups at data stations 1 and 5, Table I and Figure 2, were located some distance away from the number 1 and 2 bearings. All displacements recorded at these stations were corrected to read the bearing displacements by accounting for the axial location of the pickup relative to the bearing. The bearing stations will hence be called stations 1 and 5.

Analyses and Dynamic Model

The test rig was modeled and analyzed with the critical speed and forced response analyses cited in Ref. 3 and with the transient response analysis cited in Ref. 2. All three analyses are transfer matrix methods which treat the shaft as a beam reduced to a series of masses connected by massless springs. For consistency, the same model was used for all three analyses. The initial design geometries and material properties were used to establish the first dynamic model from which the predicted system response was obtained. During fabrication, assembly and initial running of the test rig, static and dynamic tests were run to verify the shaft and bearing support stiffnesses. Dynamic testing was also conducted to define the level of damping produced by the bearing supports without the squeeze film dampers.

Figure 2 shows a schematic of the analytical model. The lettered stations designate the positions on the rotor where masses were lumped or where the shaft cross section changed. The sections between these stations were modeled as massless uniform beam sections. The bearings were considered as rigid in comparison with the flexible bearing support and the bearing support masses were added directly to the shaft at stations "a" and "m". The stiffness of the drive quill was neglected but a small amount of mass was included at station "a" to account for the drive coupling. The details of the rig model are specified in Table II. It should be noted that two different values of support damping C_1 and C_2 are listed depending on which mode is analyzed. This is required because C_1 and C_2 are lumped approximations to the overall system damping and, as such, they take on different values for each mode.

As shown by the model in Figure 2, the squeeze film dampers were spring supported. This was readily handled on the steady state analysis but the transient analysis as published did not have the capability to model a linear spring and damper in parallel with a squeeze film damper. The computer program was therefore modified to handle this configuration. The modification was straight forward and only required that the forces proportional to the instantaneous displacement and velocity be added to the squeeze film forces.

TABLE II
TEST RIG PHYSICAL PROPERTIES FOR ANALYTICAL MODEL SHOWN IN FIGURE 2

	Rotor Station	Rotor Segment	Weight kg	Mass Moment of Inertia		Segment Length mm	Segment Diameter mm	Young's Modulus $N/cm^2 \times 10^{-6}$
				Polar $kg \cdot cm^2$	Transverse $kg \cdot cm^2$			
No. 1 Bearing	a	—	2.921	—	—	—	—	—
		a - b	—	—	—	12.45	20.07	20.7
		b - c	—	—	—	101.35	15.88	20.7
		c - d	—	—	—	28.45	27.94	20.7
No. 1 Blade Loss Disk	d	—	3.393	281.7	143.2	—	—	—
		d - e	—	—	—	26.67	27.94	20.7
		e - f	—	—	—	186.69	15.88	20.7
		f - g	—	—	—	12.70	16.87	20.7
Center Disk	g	—	.848	—	—	—	—	—
		g - h	—	—	—	12.70	16.87	20.7
		h - i	—	—	—	186.69	15.88	20.7
		i - j	—	—	—	26.67	27.94	20.7
No. 2 Disk	j	—	3.393	281.7	143.2	—	—	—
		j - k	—	—	—	28.45	27.94	20.7
		k - l	—	—	—	101.35	15.88	20.7
		l - m	—	—	—	12.45	20.07	20.7
No. 2 Bearing	m	—	2.785	—	—	—	—	—

Support Characteristics

$$K_1 = K_2 = 4450 \text{ N/cm}$$

$$C_1 = C_2 = 1.31 \text{ N s/cm} \quad \text{At Speeds Near 1st Critical}$$

$$C_1 = C_2 = 0.65 \text{ N s/cm} \quad \text{At Speeds Near 2nd Critical}$$

Squeeze Film Damper Characteristics

$$\text{Diameter} = 114.30 \text{ mm}$$

$$\text{Length} = 12.70 \text{ mm}$$

$$\text{Radial Clearance} = 0.2298 \text{ mm}$$

$$\text{Damper Oil} = \text{Jet Engine Lubricant} \\ \text{Military Spec. MIL-L-6811C (ASG)}$$

DISCUSSION OF RESULTS

Undamped Steady State Response

A two-plane balancing program, specifically written for the HP-65 programmable calculator, was used to balance the rig. Weights were applied to the large end disks and balancing was accomplished at speeds near the undamped first and second bending peak responses. The center disk, as well as the end disks, were then used throughout the experimental program for fine adjustments to the state of balance. The resulting balanced response at 5 speeds is given in Table III.

Using the analytical model of the rig, the first two forward and backward modes were predicted as a function of shaft speed, as shown on Figure 3(a). The first two forward synchronous modes were predicted at 1500 rpm and 2950 rpm respectively. The corresponding mode shapes shown in Figure 3(b) are typical first and second bending.

To obtain the steady-state undamped response and experimental mode shapes of the rig, imbalance was applied to the blade-loss disk and the vibration amplitudes of the shaft were recorded over the speed range. An imbalance of 4.26 g cm on the blade-loss disk was used to obtain the response through the first mode. Since the sensitivity of the rotor was lower for the second mode, a higher imbalance of 5.93 g cm was used to characterize the second mode response. For comparison, corresponding predictions were obtained from a steady-state forced response analysis of the test system. Figure 4(a, b) shows the response, both experimental and analytical, at the blade-loss disk (station 2.). The experimental response agreed quite well with the analytical predictions. However, a small discrepancy was observed between the test and analytically predicted second peak response speed, where the experimental peak was approximately 50 rpm higher. As shown on Figure 3(b), the normalized deflections of the rig shaft at the peak response speeds agreed well with the predicted mode shapes. The experimental and analytical response is given in Table III for each of 5 speeds. Based on the steady-state sensitivity of the rotor, these speeds were selected for transient blade-loss testing. The discrepancies between the experimental and analytical values in this table are due to the apparent differences in peak response speeds.

Damped Steady-State Response

The damped steady-state response of the rig and mode shapes for the first and second peak response speeds were obtained experimentally and predicted with the forced response analysis. The predicted and experimentally observed response of the damped system at the 5 blade loss speeds is shown in Table IV. To characterize the first damped mode, a 7.10 g cm imbalance was applied to the blade-loss disk and the response was determined up to 2200 rpm. The amount of imbalance was higher than for the corresponding undamped response since the damper was effective in reducing the sensitivity of the first mode. Figure 5(a) shows the response at the blade-loss disk. As shown, the test damper was somewhat more effective than predicted analytically and produced significantly lower peak response amplitude than the analytical model. In addition the observed peak response speed was approximately 30 rpm higher than predicted. The first bending mode shape showed excellent agreement, as can be seen from Figure 6(a).

TABLE III

UNDAMPED STEADY STATE RESPONSE ANALYTICALLY PREDICTED AND EXPERIMENTALLY OBSERVED

Speed rpm		Data Station	1		2		3		4		5	
			Vert	Horiz	Vert	Horiz	Vert	Horiz	Vert	Horiz	Vert	Horiz
1500	Experimental Balanced	Ampl. Phase	0.889 170	1.067 273	5.680 176	6.121 265	6.529 177	7.569 268	4.978 191	5.334 271	1.143 185	1.270 278
	Experimental 4.26 g cm	Ampl. Phase	22.479 97	19.964 189	85.508 101	80.645 186	106.985 100	108.915 186	86.893 102	80.833 192	23.419 101	20.168 193
	Predicted 4.26 g cm	Ampl. Phase	19.152 268	19.152 358	79.858 270	79.858 0	112.420 270	112.420 0	79.756 270	79.756 0	18.948 267	18.948 357
1550	Experimental Balanced	Ampl. Phase	0.762 356	0.940 77	0.838 326	1.422 59	1.829 320	2.286 51	2.591 301	2.489 45	0.584 326	0.686 59
	Experimental 4.26 g cm	Ampl. Phase	4.978 173	5.944 263	20.472 171	22.327 260	24.308 171	30.048 266	19.533 174	23.063 269	5.553 174	6.198 262
	Predicted 4.26 g cm	Ampl. Phase	3.861 190	3.861 280	16.612 192	16.612 282	23.724 192	23.724 282	17.609 192	17.069 282	4.242 189	4.242 279
2000	Experimental Balanced	Ampl. Phase	0.381 345	0.432 73	1.270 155	0.991 236	0.813 177	0.559 259	1.575 261	0.991 359	0.229 290	0.356 40
	Experimental 5.93 g cm	Ampl. Phase	3.203 157	0.305 269	2.591 185	2.946 271	4.089 182	4.953 271	4.140 182	4.420 268	1.549 188	1.676 277
	Predicted 5.93 g cm	Ampl. Phase	0.178 187	0.178 277	2.667 182	2.667 272	4.801 181	4.801 271	4.242 180	4.242 270	1.626 178	1.626 268
2950	Experimental Balanced	Ampl. Phase	1.143 285	1.270 300	1.909 170	2.870 247	1.372 167	1.473 244	1.727 264	1.854 20	0.457 334	1.676 48
	Experimental 5.93 g cm	Ampl. Phase	21.996 72	26.010 159	19.279 75	20.244 157	2.769 160	2.667 241	18.110 245	25.273 336	22.428 259	30.734 341
	Predicted 5.93 g cm	Ampl. Phase	25.552 268	25.552 358	21.209 267	21.209 357	2.845 203	2.845 293	21.869 97	21.869 187	24.816 91	24.816 181
3100	Experimental Balanced	Ampl. Phase	2.286 320	4.445 32	0.940 167	1.067 342	1.473 162	1.651 234	2.108 223	1.753 247	0.813 179	1.702 240
	Experimental 5.93 g cm	Ampl. Phase	13.640 151	18.237 249	11.608 155	14.478 245	2.388 180	2.464 259	9.373 327	11.735 59	12.395 332	16.180 64
	Predicted 5.93 g cm	Ampl. Phase	10.490 199	10.490 289	9.423 199	9.423 289	2.921 185	2.921 275	6.198 29	6.198 119	8.788 22	8.788 112

Amplitude ~ mm X 10² P-P, Phase ~ Degrees

Experimental imbalanced response is the change in response due to an imbalance applied at the blade loss disk.

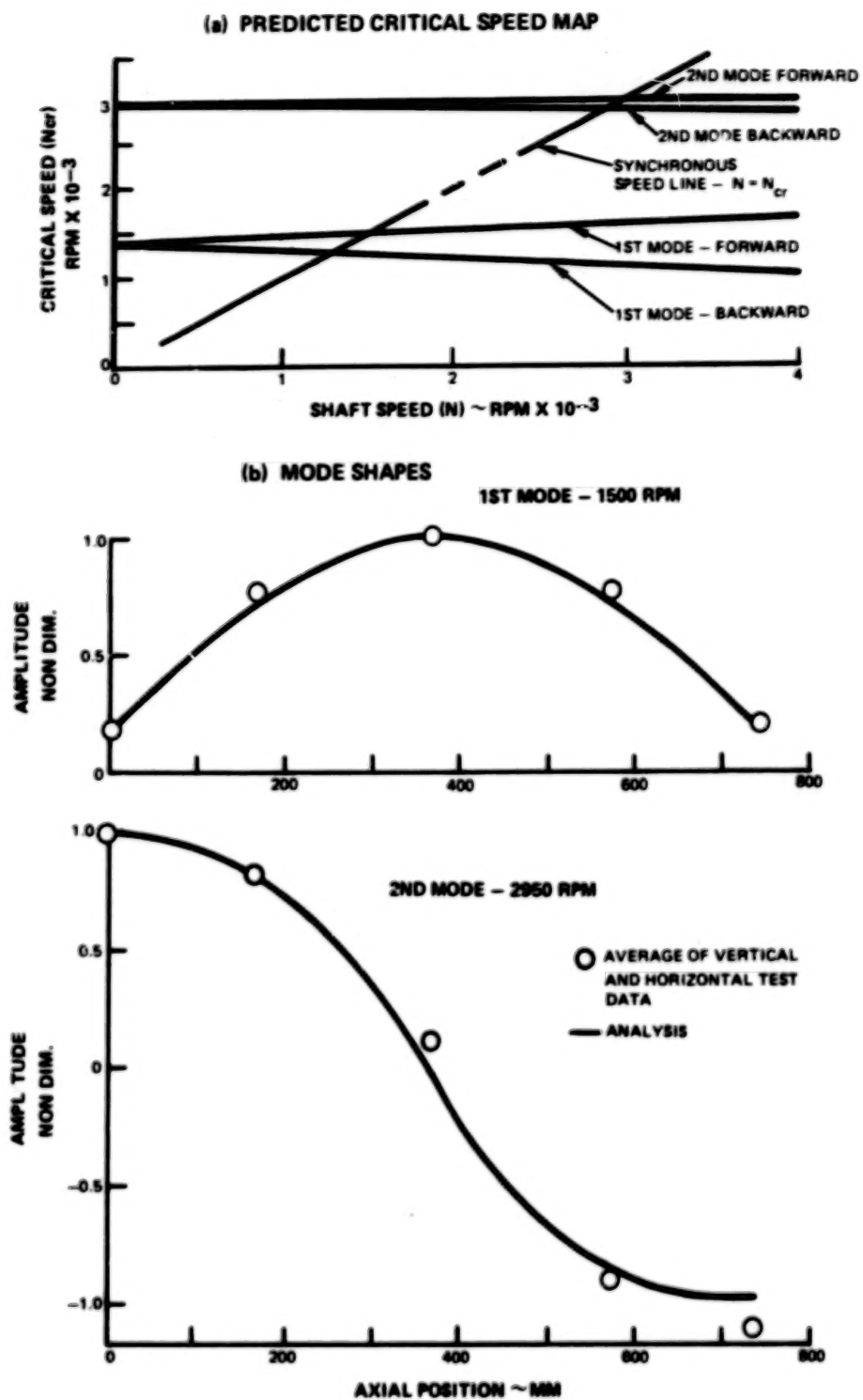


Figure 3 Critical Speed Map and Mode Shapes of the Undamped System

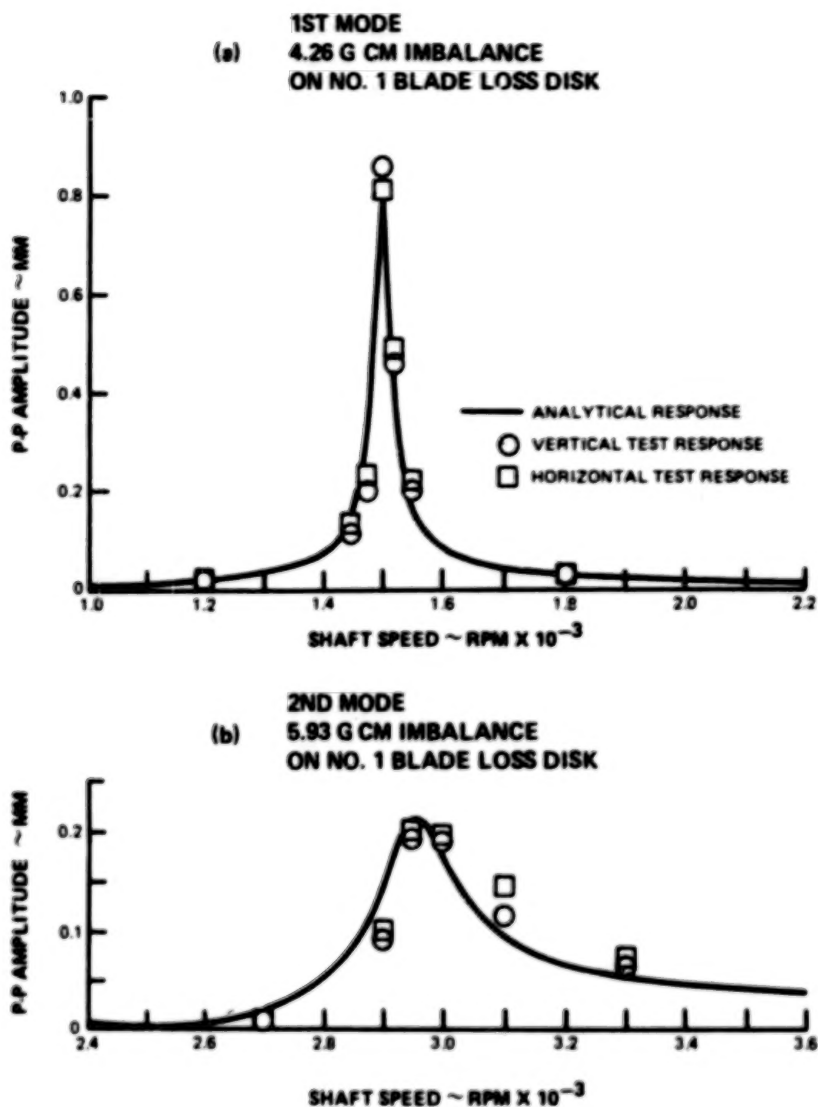


Figure 4 Steady State Response of the Undamped System at Data Station 2

TABLE IV

DAMPED STEADY STATE RESPONSE ANALYTICALLY PREDICTED AND EXPERIMENTALLY OBSERVED

rpm		Data Station	1		2		3		4		5		No. 1 Damper Oil		No. 2 Damper Oil	
			Vert	Horiz	Vert	Horiz	Vert	Horiz	Vert	Horiz	Vert	Horiz	Temp °C	Viscosity N-s/m ²	Temp °C	Viscosity N-s/m ²
1500	Experimental	Ampl.	1.194	0.533	4.089	3.962	4.521	4.750	2.718	2.769	0.559	0.457	24.4	0.0141	23.9	0.145
	Balanced	Phase	58	191	132	221	132	220	139	240	145	226				
	Experimental	Ampl.	4.470	5.182	22.606	21.336	27.076	27.940	19.304	21.438	3.429	3.632				
	7.10 g cm	Phase	54	138	48	127	47	129	57	130	59	142				
1550	Predicted	Ampl.	11.201	11.201	47.752	47.752	67.208	67.208	47.396	47.396	10.871	10.871	24.4	0.0141	23.9	0.0145
	7.10 g cm	Phase	282	12	288	18	288	18	287	17	279	9				
	Experimental	Ampl.	0.965	1.473	4.699	5.309	6.274	7.214	4.877	5.158	0.838	0.965				
	Balanced	Phase	112	253	176	286	176	269	176	263	192	275				
2000	Experimental	Ampl.	5.944	6.198	26.467	23.185	33.426	32.029	26.289	22.504	5.842	5.436	25.6	0.0134	27.2	0.0124
	7.10 g cm	Phase	120	208	109	202	108	200	109	204	126	219				
	Predicted	Ampl.	6.248	6.248	27.280	27.280	38.913	38.913	27.889	27.889	6.756	6.756				
	7.10 g cm	Phase	208	298	213	303	213	303	212	302	204	294				
2000	Experimental	Ampl.	1.016	0.610	1.092	1.118	1.346	1.422	2.616	2.692	0.330	0.356	25.6	0.0134	27.2	0.0124
	Balanced	Phase	4	123	178	286	235	317	267	351	289	39				
	Experimental	Ampl.	1.270	1.727	13.995	14.859	20.828	24.863	18.183	21.209	6.579	5.232				
	27.65 g cm	Phase	150	259	174	262	173	275	186	277	204	297				
2950	Predicted	Ampl.	1.219	1.219	12.979	12.979	22.835	22.835	19.736	19.736	7.239	7.239	25.6	0.0134	27.2	0.0124
	27.65 g cm	Phase	203	293	188	278	185	275	182	272	171	261				
	Experimental	Ampl.	1.295	0.762	2.007	1.854	1.245	1.676	2.743	2.540	1.168	1.219				
	Balanced	Phase	12	85	152	237	181	267	267	349	294	19				
3100	Experimental	Ampl.	12.878	13.251	13.767	12.878	12.167	12.979	13.792	11.913	13.360	8.839	25.6	0.0134	27.2	0.0124
	27.65 g cm	Phase	122	220	132	219	176	264	231	250	279	8				
	Predicted	Ampl.	18.720	18.720	15.392	15.392	12.929	12.929	25.933	25.933	21.387	21.387				
	27.65 g cm	Phase	290	20	277	7	187	277	145	235	123	213				
3100	Experimental	Ampl.	1.092	0.884	2.388	2.032	1.422	1.778	2.388	2.540	1.245	1.549	25.6	0.0134	27.2	0.0124
	Balanced	Phase	356	59	158	235	179	261	275	352	309	35				
	Experimental	Ampl.	13.310	13.995	14.453	13.538	11.405	12.220	10.897	11.252	12.294	8.611				
	27.65 g cm	Phase	140	240	140	228	172	257	234	322	297	25				
3100	Predicted	Ampl.	22.073	22.073	20.422	20.422	12.649	12.649	25.705	25.705	23.343	23.343	25.6	0.0134	27.2	0.0124
	27.65 g cm	Phase	270	0	264	354	190	280	129	219	104	194				

Amplitude ~ mm X 10² P-P, Phase ~ Degrees

Experimental imbalanced response is the change in response due to an imbalance applied at the blade loss disk.

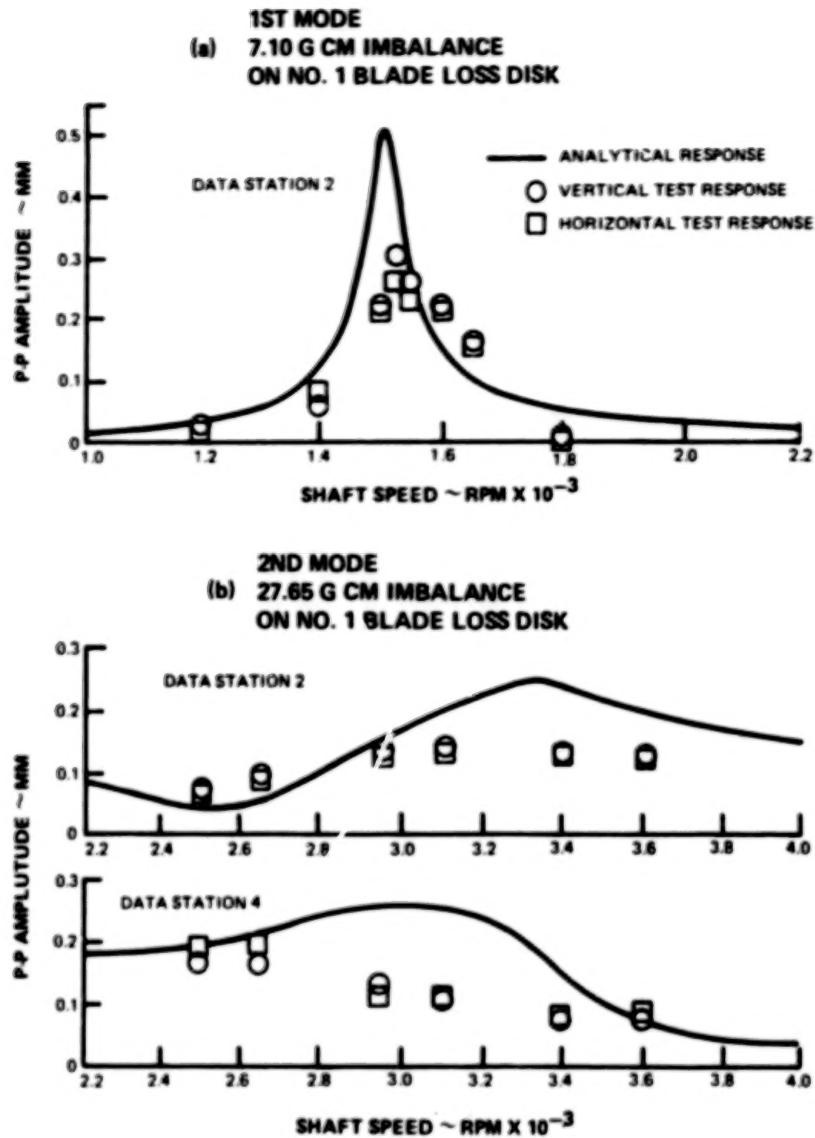
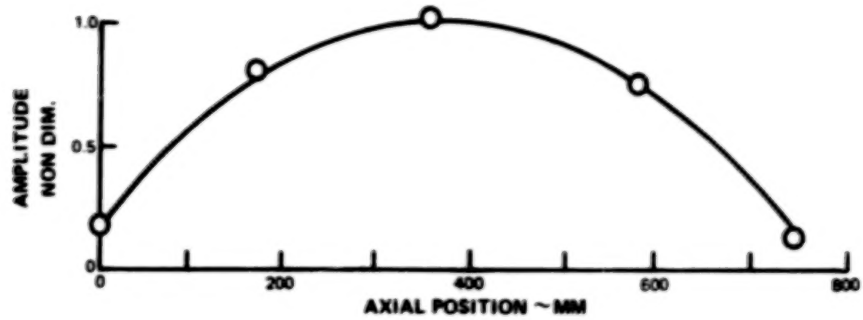


Figure 5 *Steady State Damped Response of the Damped System at Data Stations 2 and 4*

(a) 1ST MODE - 1500 RPM



(b) 2ND MODE - 3100 RPM
TWO PLANE REPRESENTATION

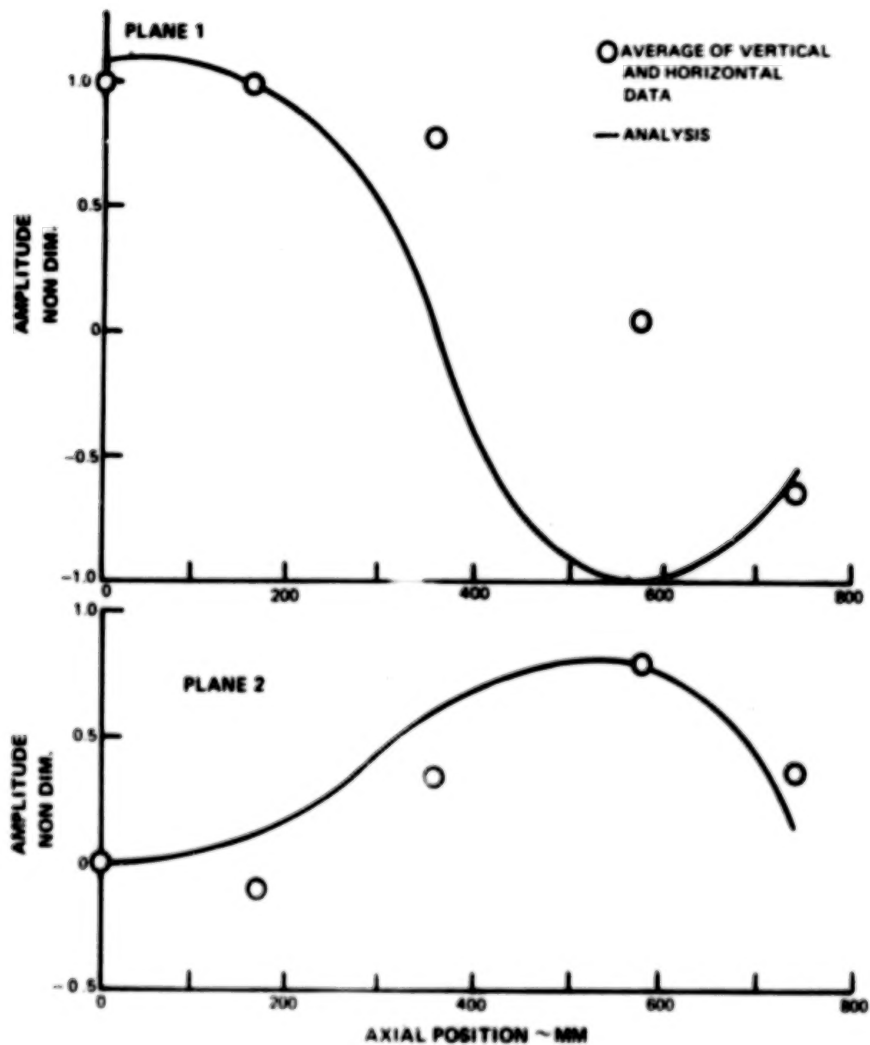


Figure 6 Mode Shapes of the Damped System

A 27.65 g cm imbalance on the blade-loss disk was used to determine the damped steady-state characteristics of the second mode. This large amount of imbalance was used since the dampers were more effective in reducing the second mode sensitivity than the first mode. Figure 5(b) shows the damped second mode response at stations 2 and 4. The response at these stations is presented to illustrate two effects of the dampers at the second mode. Comparison of the two plots shows that the peak response speeds were different for each and consequently at a given speed the amplitudes at the two stations were unequal. Since these two stations are symmetrically placed with respect to the shaft midspan this further indicates that the damped mode shape was not symmetric with respect to the midspan as was the case without the dampers. The phase data in Table IV for the second mode shows that the additional damping also caused out of plane deflection of the shaft such that the mode shape could no longer be represented in a single plane. The test and analytical mode shapes are presented in Figure 6(b) and show the nonsymmetry and twisting are both predicted and experimentally observed.

The test and analytical mode shapes for the second mode show some discrepancy. Also, the analytically predicted amplitudes for both modes were considerably higher than observed in test. Since the differences in mode shape and amplitudes were apparent in much of the damped blade loss testing, a brief analysis was subsequently performed to estimate the pressure and forces produced by the dampers. The predicted forces were small, on the order of 1 to 2 kg, even at high eccentricity ratios and speeds. It is probable, therefore, that the oil supply pressure in the dampers increased the pressure and extent of the uncavitated film from what was predicted. In reality a 2π film probably existed instead of the π film used in the analysis.

Undamped Transient Response

Blade-loss testing without dampers was conducted at five speeds; 1500 rpm, 1550 rpm, 2000 rpm, 2950 rpm, and 3100 rpm. The speeds selected include two speeds between 80% and 120% of each of the two criticals and one speed midway between them. The imbalance applied for each test was based on the steady state sensitivity of the rotor. Each imbalance produced peak-to-peak amplitudes of at least five times the corresponding amplitudes under balanced conditions. Figures 7 through 31 show time traces of the transient response. Experimental horizontal and vertical response and the corresponding predicted results at the station, speed, and imbalance are indicated in the figures. All the time traces have once-per-rev keyphasor marks which show the phase variation with time. The experimental time traces show small steady state response for 1 to 3 revolutions before the blade loss occurs. This pre-blade loss response is zero for the analysis and is not shown. The conditions for the tests are also summarized in Table V.

The transient results at 1500 rpm are shown in Figures 7 through 11. At this speed, the test response was somewhat greater than predicted. In addition, the analytically predicted transient response seemed to reach steady state sooner than the test indicated. However, the discrepancies were small. Both test and analysis showed amplitude and phase consistent with the first bending mode.

TABLE V
TEST CONDITIONS FOR BLADE LOSS TESTS

	Fig. No.*	Speed RPM	Imbalance g cm	Time Duration Sec.	No. 1 Damper Oil		No. 2 Damper Oil	
					Temp. °C	Viscosity N-s/m ²	Temp. °C	Viscosity N-s/m ²
Undamped	7-11	1500	4.26	4.096	—	—	—	—
	12-16	1550	4.26	4.096	—	—	—	—
	17-21	2000	5.93	2.048	—	—	—	—
	22-26	2950	5.93	2.048	—	—	—	—
	27-31	3100	5.93	2.048	—	—	—	—
Damped	32-36	1500	7.41	2.048	25.0	.0138	16.8	.0203
	37-41	1550	7.41	2.048	25.0	.0138	25.6	.0134
	42-46	2000	27.65	2.048	25.3	.0136	27.6	.0123
	47-51	2950	27.65	.819	23.2	.0150	25.1	.0137
	52-56	3100	27.65	.819	23.6	.0147	25.6	.0134
Damped	57-61	1520	22.22	2.048	21.9	.0159	26.4	.0129
High Load	62-66	3050	66.07	.819	23.7	.0146	26.6	.0118

*Refers to transient time traces on pages 21 through 80.

At 1550 rpm (Figures 12 through 16) both test and analysis showed amplitude overshoot which is a transient amplitude greater than the steady state response caused by the blade-loss impact load. The test and analysis also show a beating phenomenon which as described in Ref. 1 is produced by the difference between the running speed and the first bending critical speed. Again, as at 1500 rpm, the predicted response was somewhat smaller and reached steady state sooner than test, and showed first bending mode characteristics.

Figures 17 through 21 show the results at 2000 rpm. Here, a rapid beat frequency was observed since the blade loss was conducted high above the first critical. The mode shape is difficult to distinguish, but seems to be closer to the first bending mode. Again, both analysis and test show similar response characteristics.

The blade loss test at 2950 rpm was conducted at the predicted speed of the second peak response. As shown on figures 22 through 26 both test and analysis produced second bending mode shapes and similar beat characteristics which show the influence of both first and second bending modes. The test horizontal response agreed well with predicted though the phase angles were different due to the 50 rpm difference between the predicted and observed second peak response speeds. The vertical test response was, in general, lower than predicted.

The transient results of the blade loss test at 3100 rpm are shown in Figures 27-31. These results show the response to be predominantly second mode with some first mode participation as indicated by the half running speed beat frequency. There is also a lower beat frequency which results from the interaction of the running speed and the second mode critical speed. Comparison of test and analysis shows this frequency to be higher analytically indicating the natural frequency of the analytical model is lower than that of the real system. The phase angles and relative amplitude of both the test and analytical time traces agree well and show the mode shape to be clearly second mode. However, the test amplitudes are higher than predicted because of the 50 rpm difference between the predicted and observed second peak response speeds.

Damped Transient Response

Damped blade loss tests were conducted at the same five speeds as the undamped tests. Two additional tests were performed at 1520 rpm and 3050 rpm where the sensitivity of the rotor was high. These two tests investigated rotor response with high eccentricity ratios of the damper. Figures 32 through 66 show the experimental and predicted transient response of the rotor during the damped blade-loss tests. The imbalance and other conditions of the tests are summarized in Table V.

Figures 32 through 36 show the results at 1500 rpm. Compared to the corresponding undamped response shown in Figures 7 through 11, both the experimental and analytical results showed that the dampers were very effective in reducing the imbalance sensitivity of the rotor. In general, the test results showed that the dampers were more effective than predicted and produced response with smaller amplitudes and different phase angles. In addition, the test data showed overshoot which was not predicted at that speed. This was not as apparent analytically since the analytical peak response speed was closer to the test speed than to the experimental peak response speed. These effects were consistent with the damped steady state response results.

The response at 1550 rpm, shown in Figures 37 through 41, was in better agreement with the predicted response than at 1500 rpm. Referring to the steady-state response curve given in Figure 5(a), this is expected since both test and analysis at 1550 rpm show similar rotor amplitudes. Again, as previously mentioned, differences in phase angles and overshoot from the predicted to the experimental results can be attributed to slight differences in the analytical model as compared to the actual system.

The damped transient response at 2000 rpm is shown in Figures 42 through 46. Results of the test and analysis are in good agreement and show similar amplitudes and phase. A beat frequency is also apparent similar to the undamped transient response results.

The results at 2950 rpm are shown in Figures 47 through 51. Both the experimental and analytical results showed that the dampers were very effective in reducing the sensitivity of the second mode. The analysis also predicts that the mode shape is nonsymmetric and out of plane. This was verified by the damped test results, and shows that the analysis was capable of simulating the highly damped system. However, the predicted amplitudes are larger than observed experimentally. As previously discussed, differences between the analytical model and the experimental dampers accounts for this discrepancy and makes it consistent with the damped steady-state results.

As shown in Figures 52 through 56, the predicted damped transient response at 3100 shows similar characteristics to the test response. Both have comparable time traces and phase angles. Again, the predicted amplitudes are higher than the experimental test indicated.

The damped transient response at 1520 rpm is shown in Figures 57 through 61. This test was predicted to produce a transient damper eccentricity ratio of 0.55. The test response was similar in character to that predicted. However, the maximum damper eccentricity ratio was approximately .4. This indicates that the test damper was more effective than predicted.

The test at 3050 rpm was predicted to produce a transient damper eccentricity ratio of 0.73. As shown by the results in Figures 62 through 66, the maximum damper eccentricity ratio produced by the test was also approximately .73, although the mode shapes were somewhat different. The agreement between the analysis and experimental response appeared to be somewhat better than the correlation for the lower loads in the vicinity of the second mode.

CONCLUSIONS AND OBSERVATIONS

The successful completion of NASA Contract NAS3-18523, Modification 3, has produced results which significantly extend the understanding of transient rotor dynamics. The response of a flexible rotor under simulated blade loss loads both with and without squeeze film dampers has been studied experimentally and analytically. The results of both the tests and analyses have led to two main conclusions:

- (1) The overall response of both damped and undamped flexible rotors is predictable using analytical methods presently available.
- (2) Viscous dampers are effective in reducing the sensitivity of flexible rotors to imbalance.

In general, the correlation between the transient test response and the predicted response using the analysis of Ref. 2 was good. Both showed similar critical speeds, mode shapes, and time traces. Major characteristics of the response such as the overshoot during transient blade-loss and the beating frequencies between the running speed and the peak response speeds were predicted analytically as well as observed in the test data. The predicted response without dampers showed better correlation than the corresponding damped response. This has been attributed in part to certain aspects of the viscous dampers such as oil viscosity variation and oil supply pressure effects which are not included in the analytical model.

Although there were apparent differences between the test dampers and the analytical model, both test and analysis showed the dampers to be very effective in reducing the sensitivity of the rotor to imbalance. The dampers were more effective at the second mode where motion at the damper was greater than at the first mode. In addition, the level of damping produced at the second mode was sufficient to change the mode shape from the undamped second beating to an out of plane nonsymmetric shape. Moreover, these effects were expected and predicted from the analysis.

The test program and the correlation with the analytical prediction have also pointed out an area for further investigation and improvement. Specifically, the damper model used in the analysis might be improved by including the effect of the oil supply pressure. An investigation described in Ref. 4 has shown that the supply oil pressure can increase the pressures and extent of the uncavitated film in viscous dampers. This effect could account for the higher than predicted experimental damper effectiveness which was observed in certain of the damped transient tests.

The results presented in this report, though obtained from a simple rotor system, represent a major step towards a thorough understanding of flexible rotor steady state and transient dynamics. Technological advances of this kind are a primary requirement for the future development of gas turbine engines where high performance and efficiency, low cost, and minimum weight are major objectives.

REFERENCES

- (1) Hibner, D. H. and Buono, D. F., "Experimental Study of Transient Dynamics of a Flexible Rotor", NASA CR-2703, June 1976.
- (2) Kirk, R. G. and Gunter, E. J., "Transient Response of Rotor Bearing System", Journal of Engineering for Industry, Vol. 96 No. 2, May, 1974, Pgs. 682-693.
- (3) Hibner, D. H., "Dynamic Response of Viscous-Damped Multi-Shaft Jet Engines", Journal of Aircraft, Vol. 12 No. 4, April, 1975.
- (4) Feder, E., Bansal, P. K., and Blanco, A., "Investigation of Squeeze Film Damper Forces Produced by Circular Centered Orbits", ASME. Paper No. 77-GT-30, 1977.

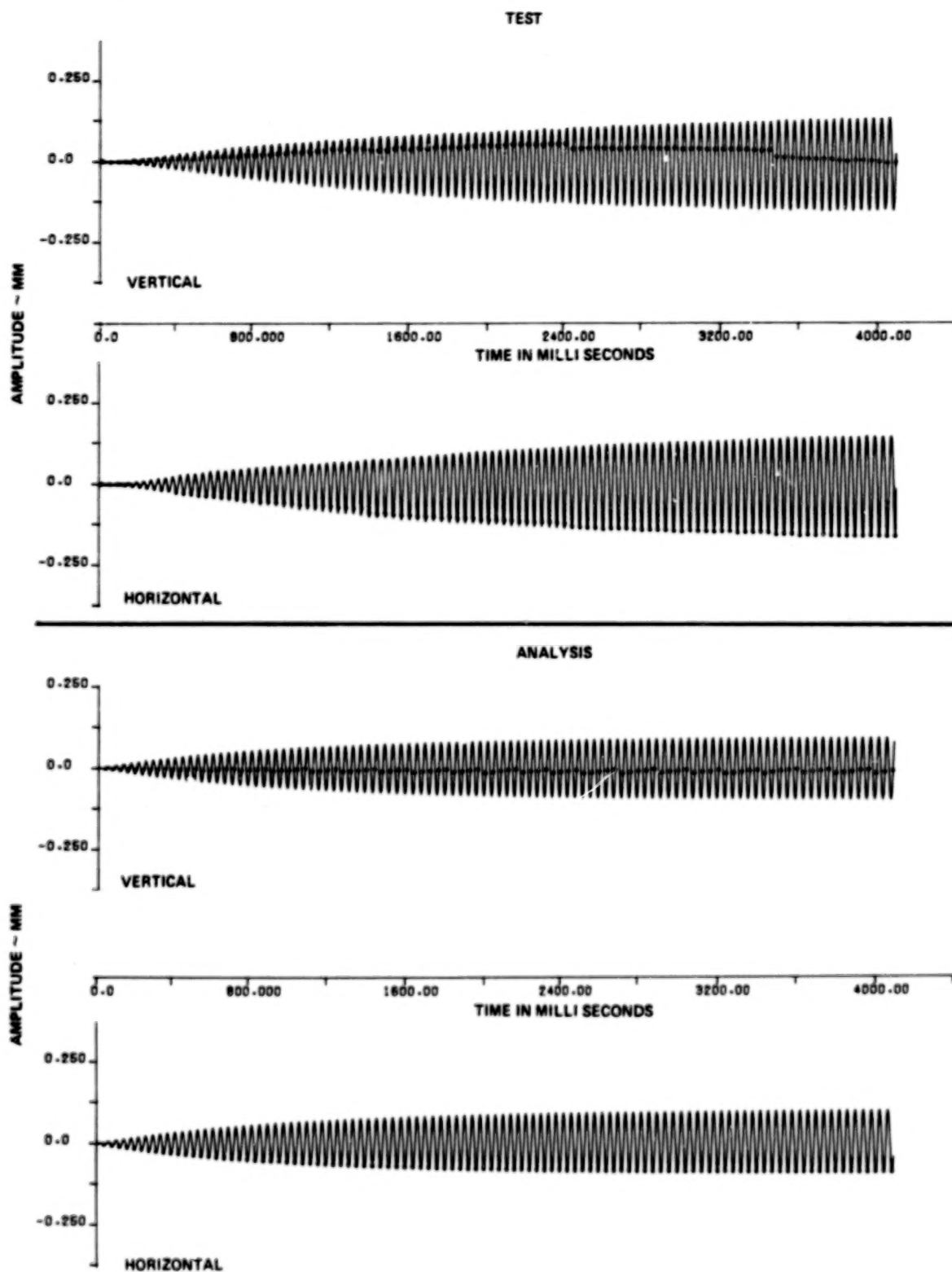


Figure 7 Experimental and Analytical Response From Data Station 1 During Un-damped Blade Loss At 1500 RPM With 4.26 g cm Imbalance

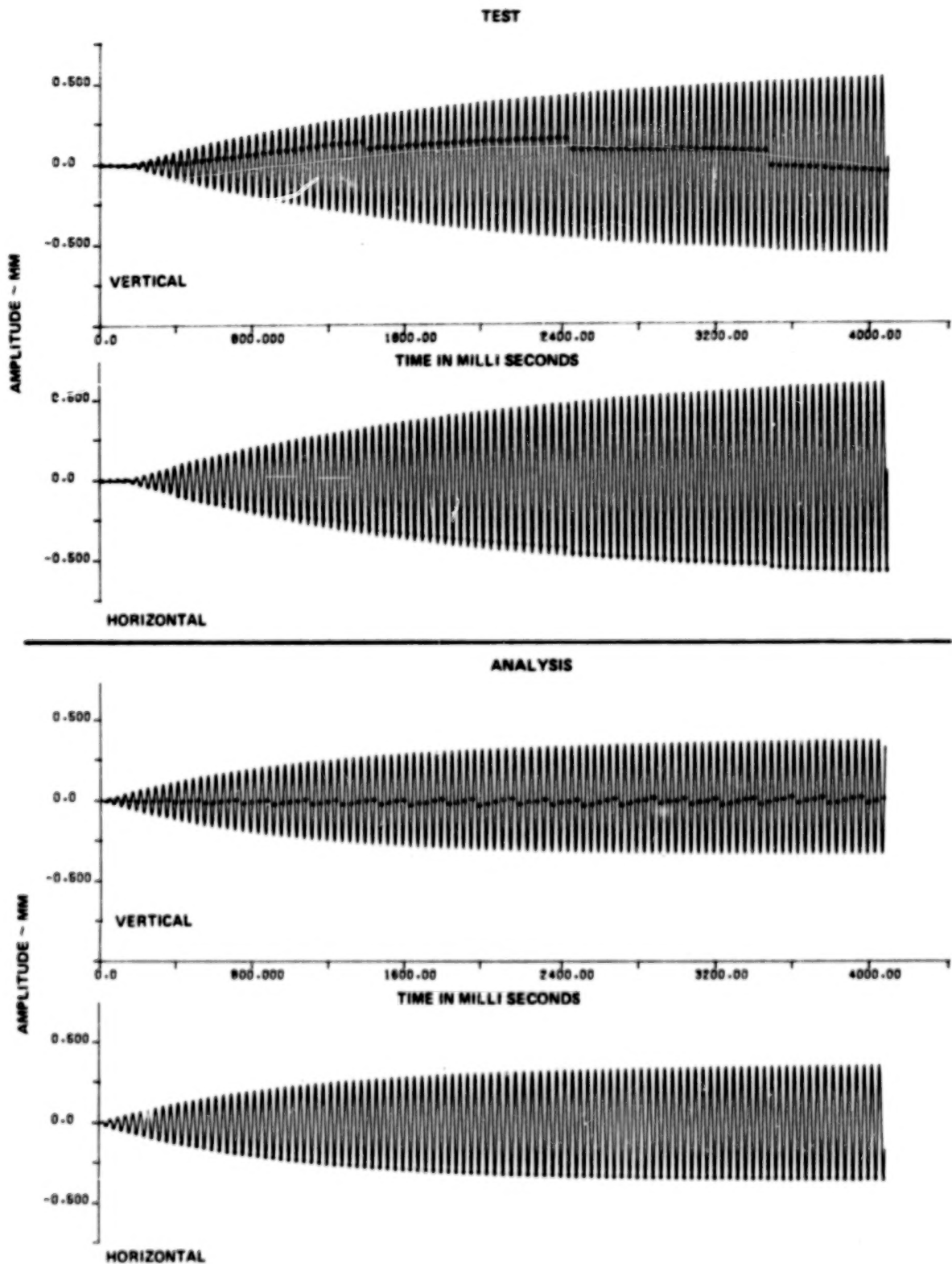


Figure 8 Experimental and Analytical Response From Data Station 2 During Undamped Blade Loss At 1500 RPM With 4.26 g cm Imbalance

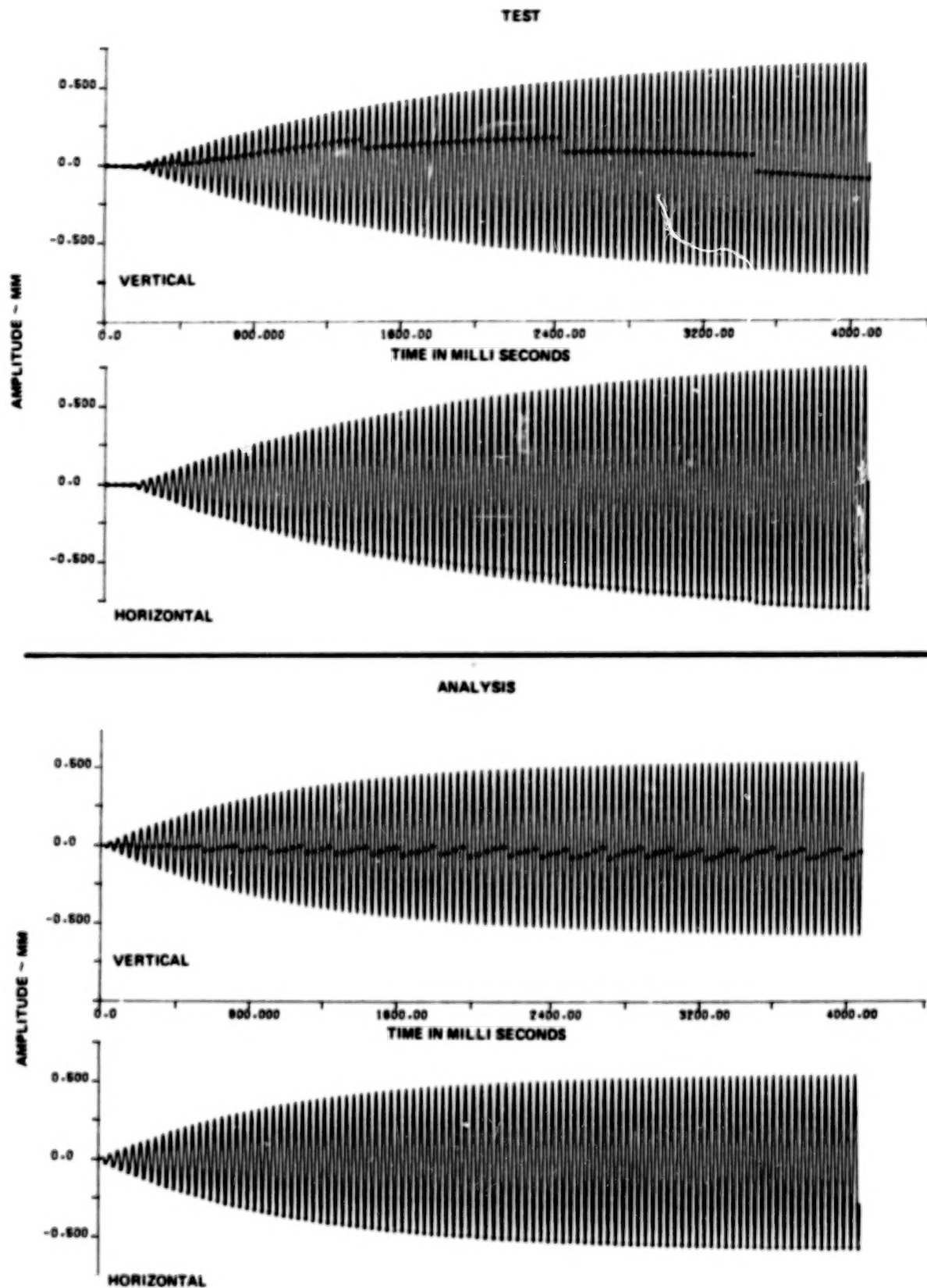


Figure 9 Experimental and Analytical Response From Data Station 3 During Undamped Blade Loss At 1500 RPM With 4.26 g cm Imbalance

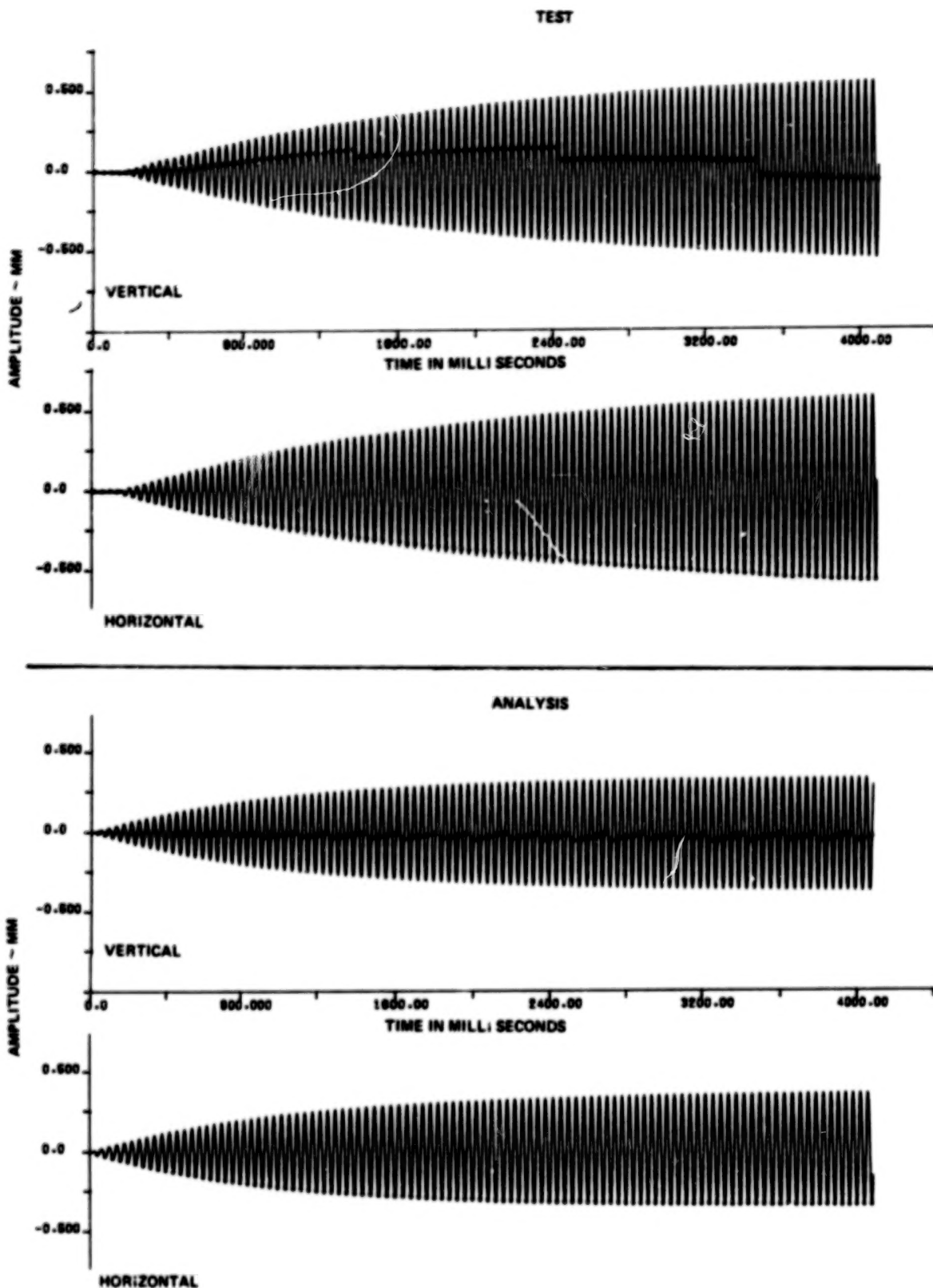


Figure 10 Experimental and Analytical Response From Data Station 4 During Undamped Blade Loss At 1500 RPM With 4.26 g cm Imbalance

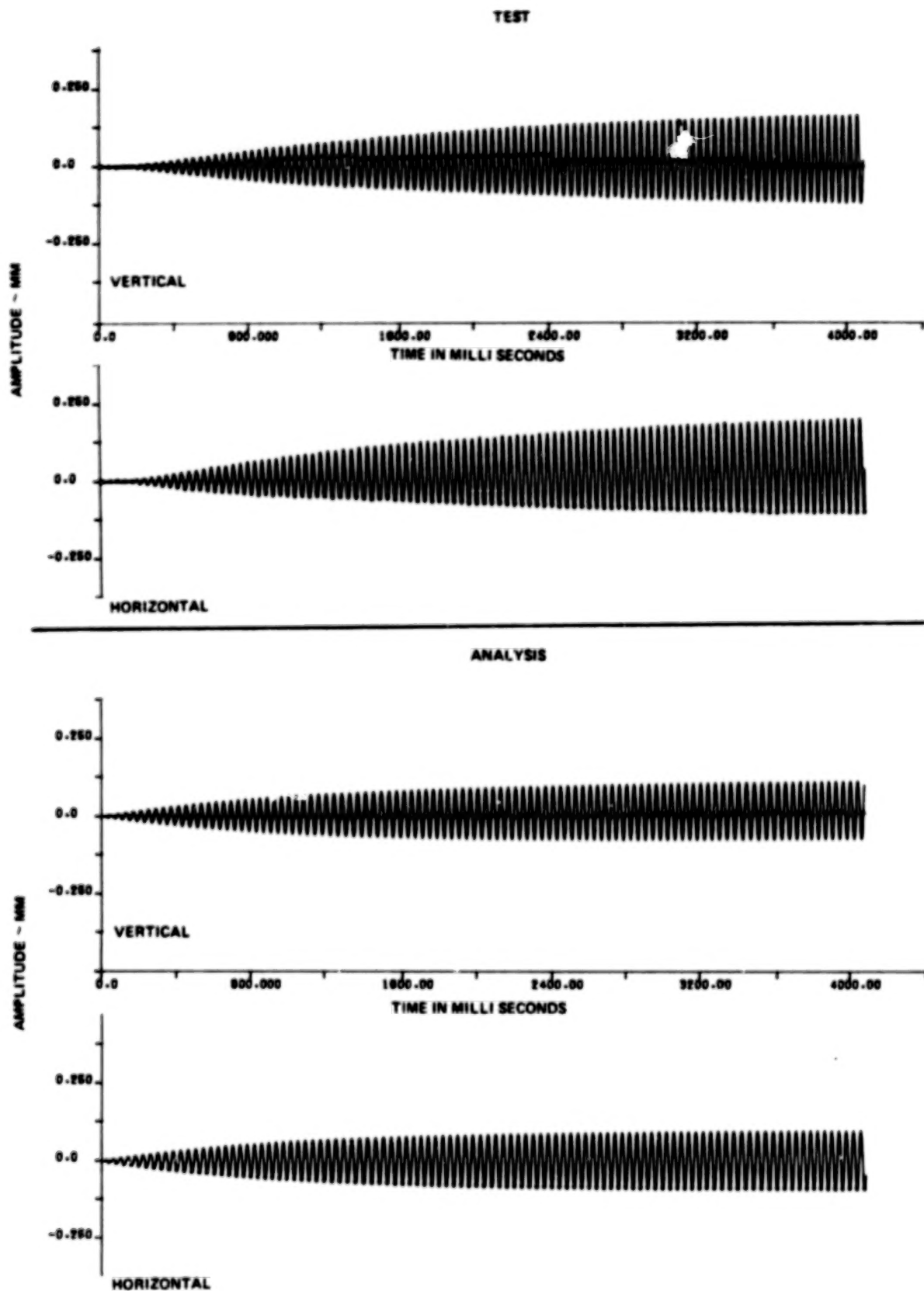


Figure 11 Experimental and Analytical Response From Data Station 5 During Undamped Blade Loss At 1500 RPM With 4.26 g cm Imbalance

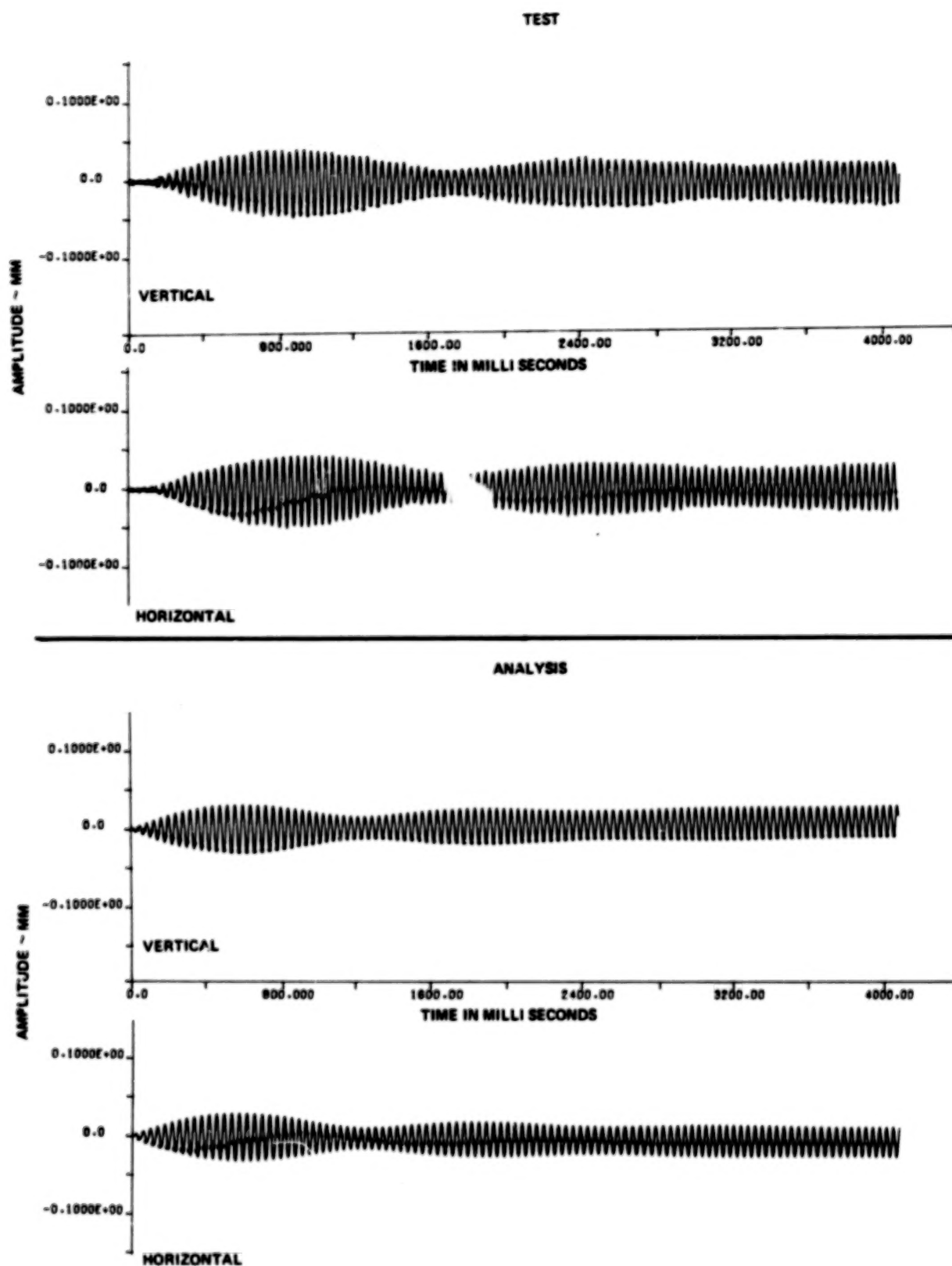


Figure 12 *Experimental and Analytical Response From Data Station 1 During Undamped Blade Loss At 1550 RPM With 4.26 g cm Imbalance*

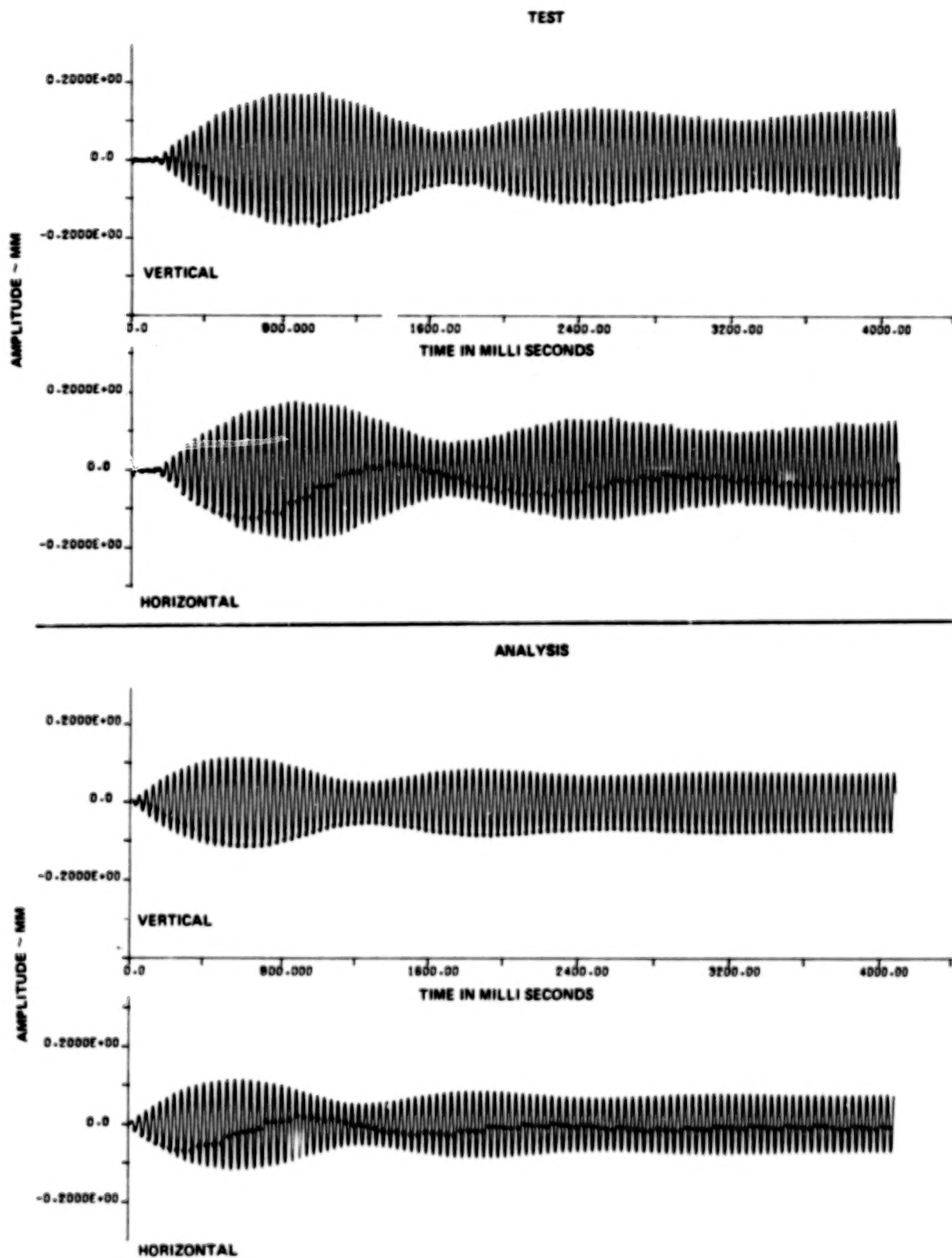


Figure 13 *Experimental and Analytical Response From Data Station 2 During Undamped Blade Loss At 1550 RPM With 4.26 g cm Imbalance*

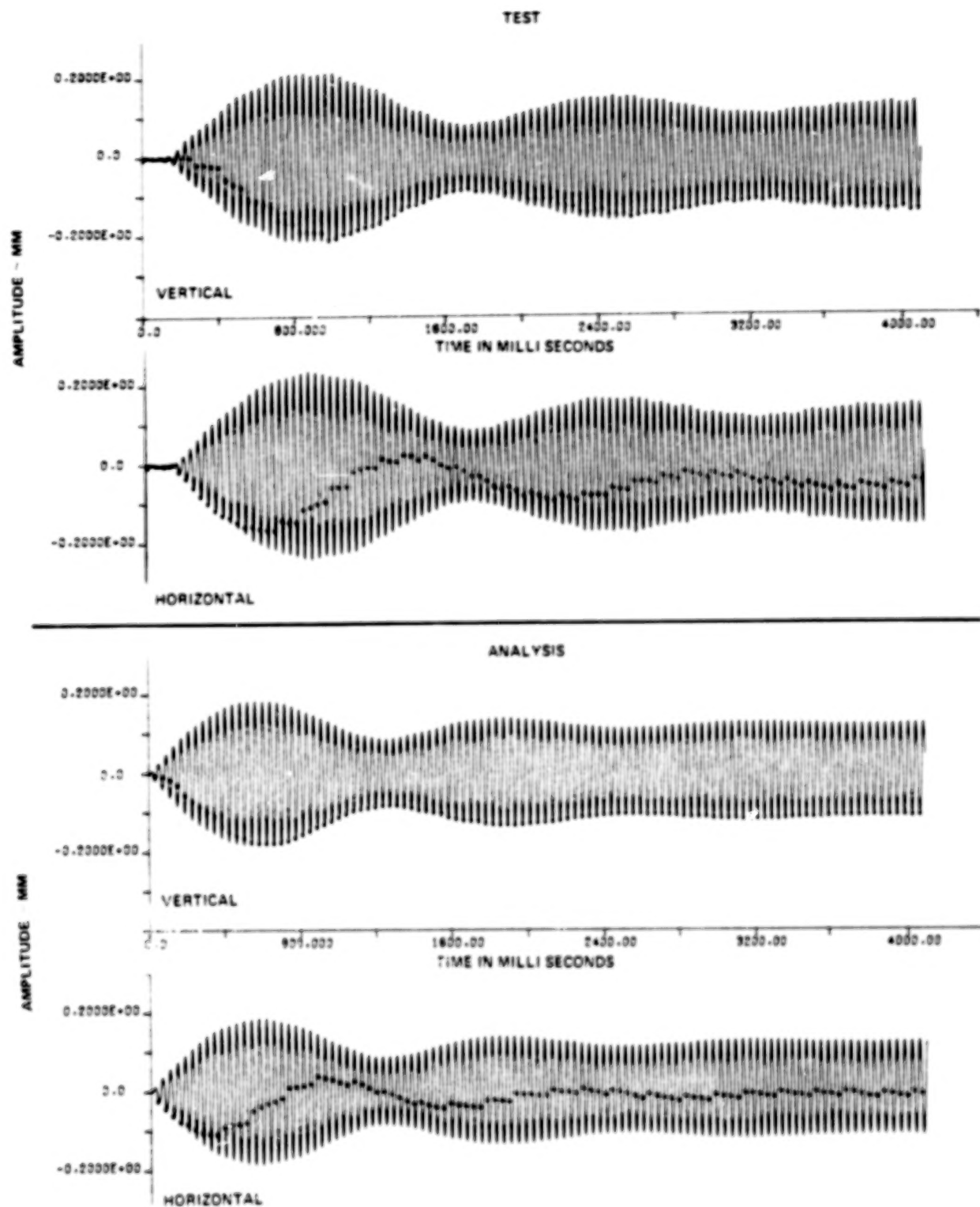


Figure 14 Experimental and Analytical Response From Data Station 3 During Undamped Blade Loss At 1550 RPM With 4.26 g cm Imbalance

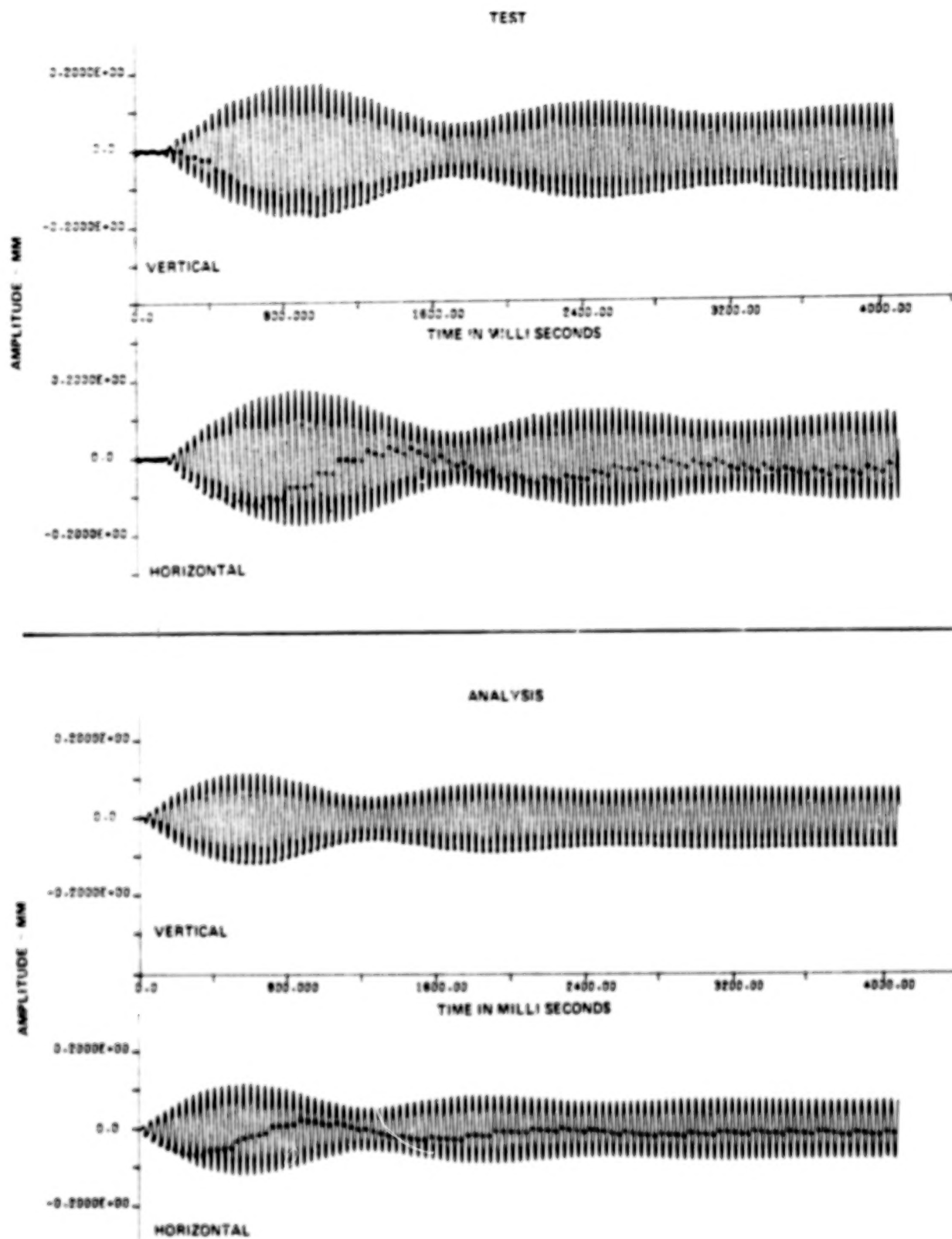


Figure 15 Experimental and Analytical Response From Data Station 4 During Undamped Blade Loss At 1550 RPM With 4.26 g cm Imbalance

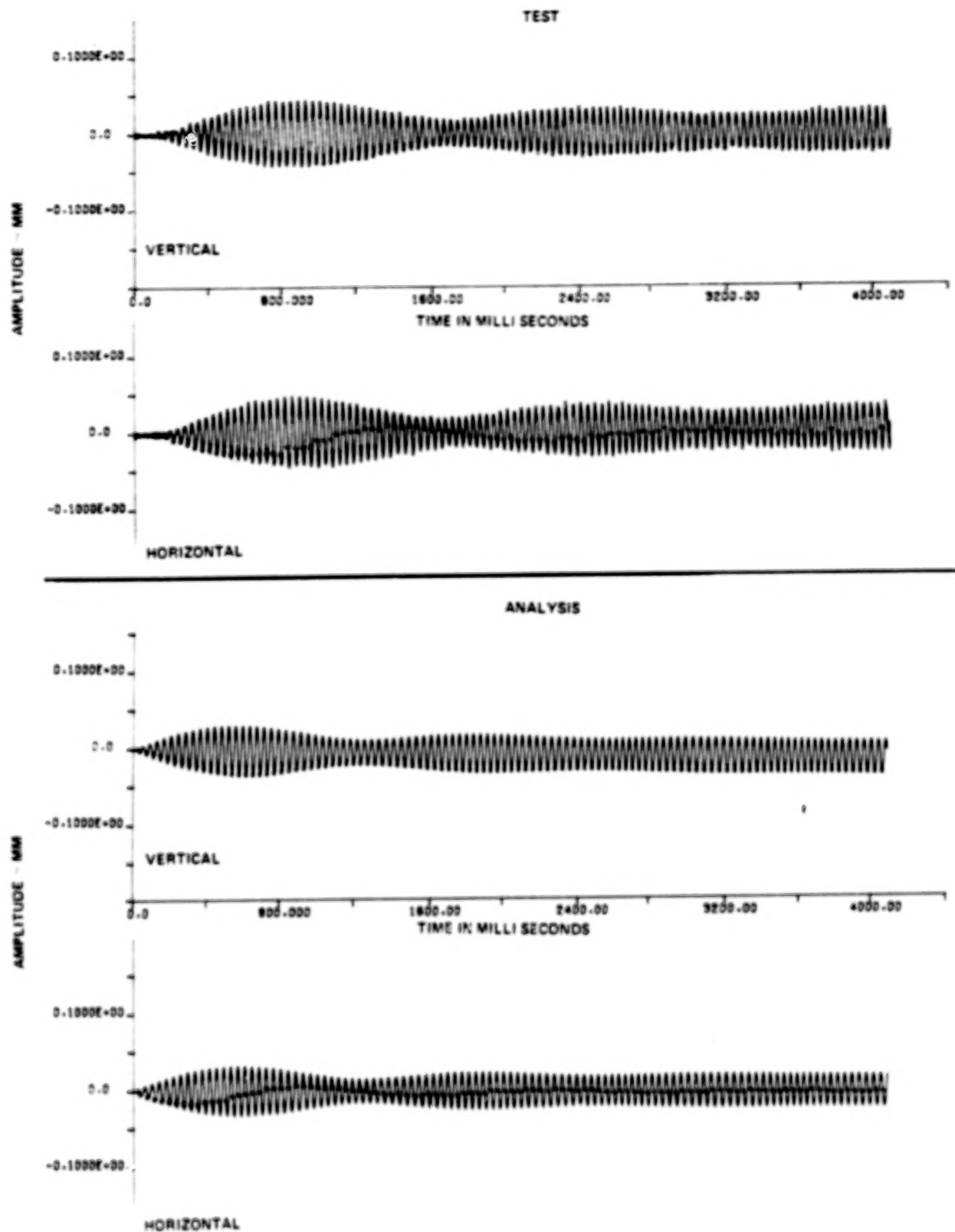


Figure 16 Experimental and Analytical Response From Data Station 5 During Un-damped Blade Loss At 1550 RPM With 4.26 g cm Imbalance

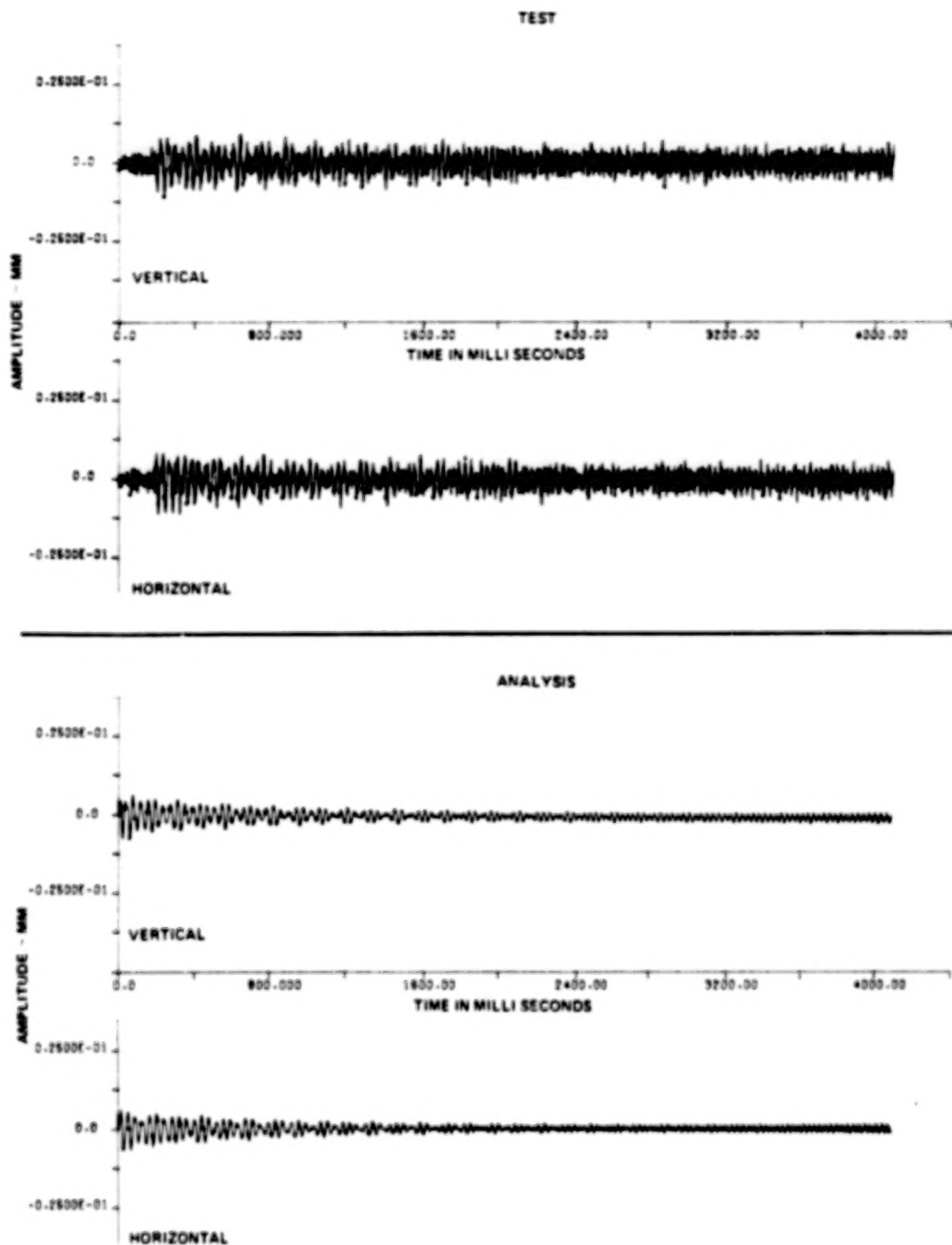


Figure 17 *Experimental and Analytical Response From Data Station 1 During Un-damped Blade Loss At 2000 RPM With 5.93 g cm Imbalance*

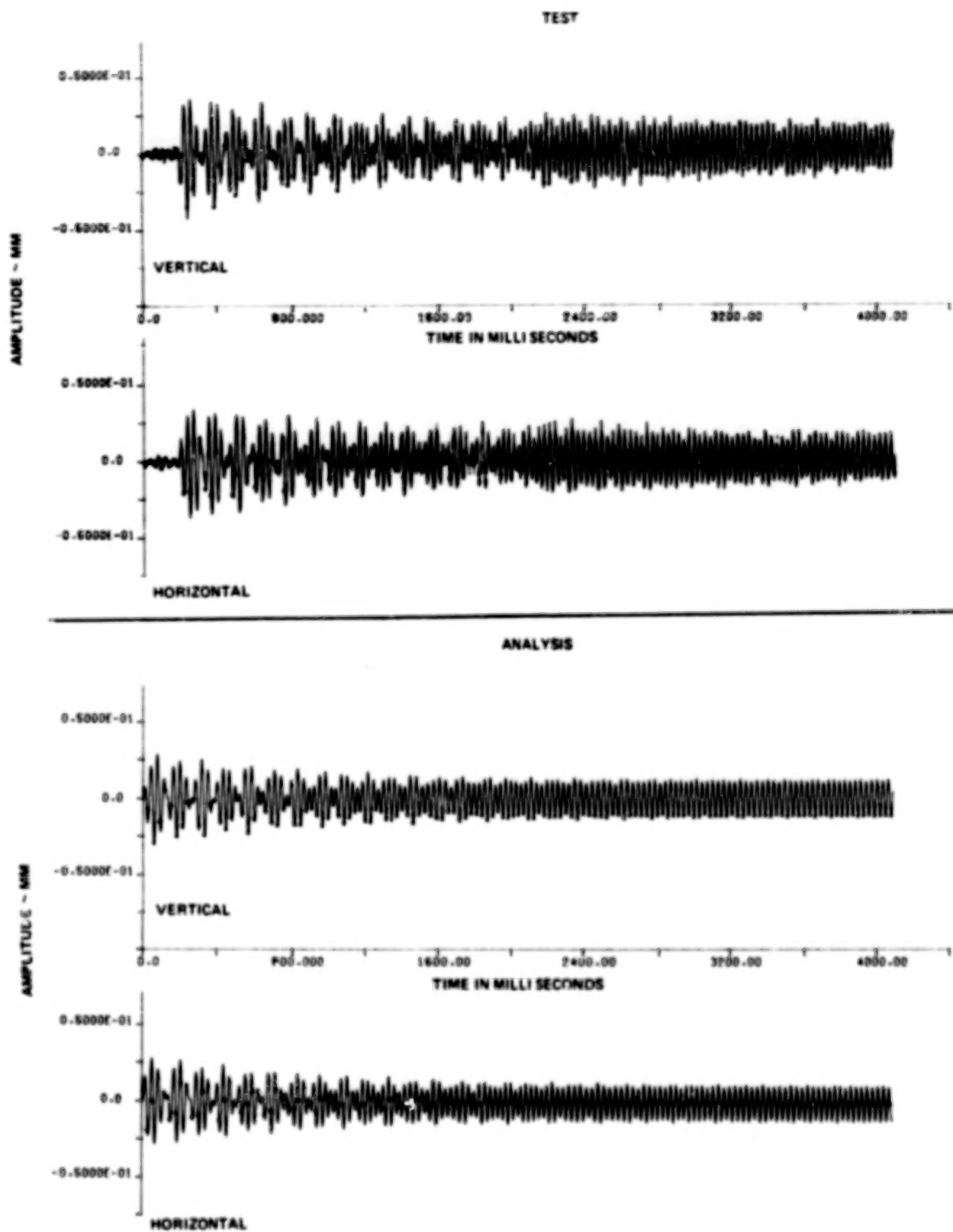
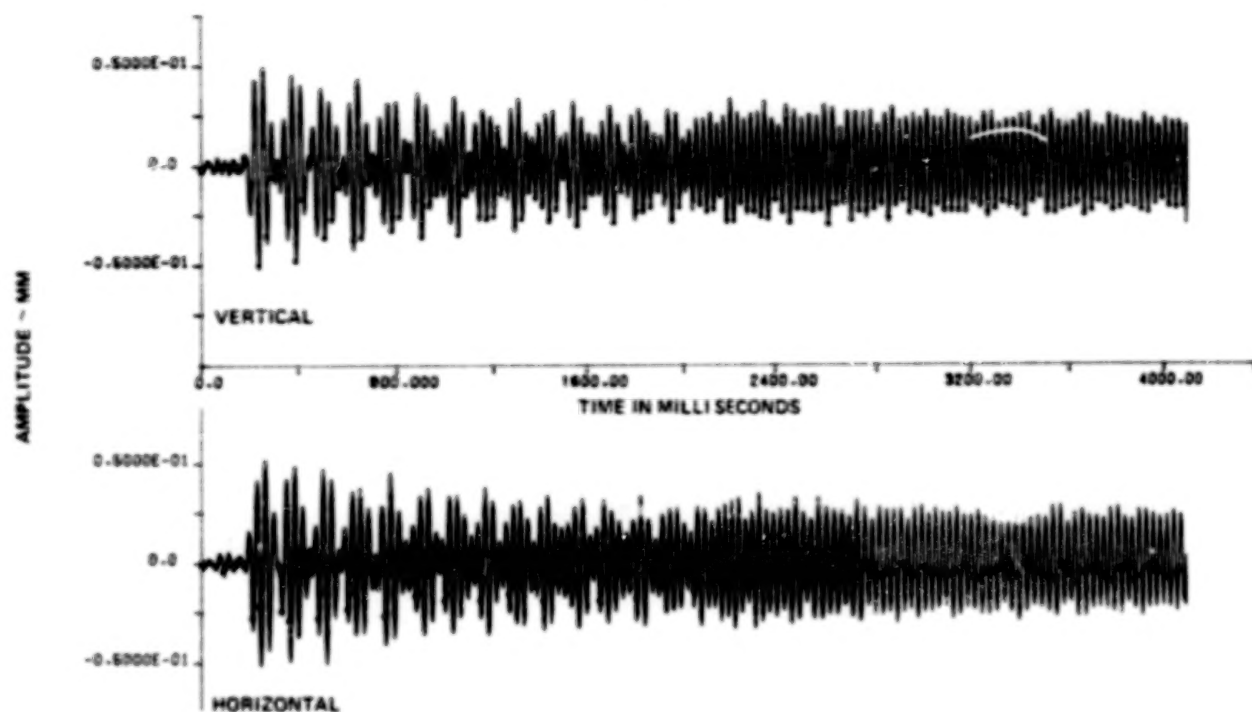


Figure 18 Experimental and Analytical Response From Data Station 2 During Undamped Blade Loss At 2000 RPM With 5.93 g cm Imbalance

TEST



ANALYSIS

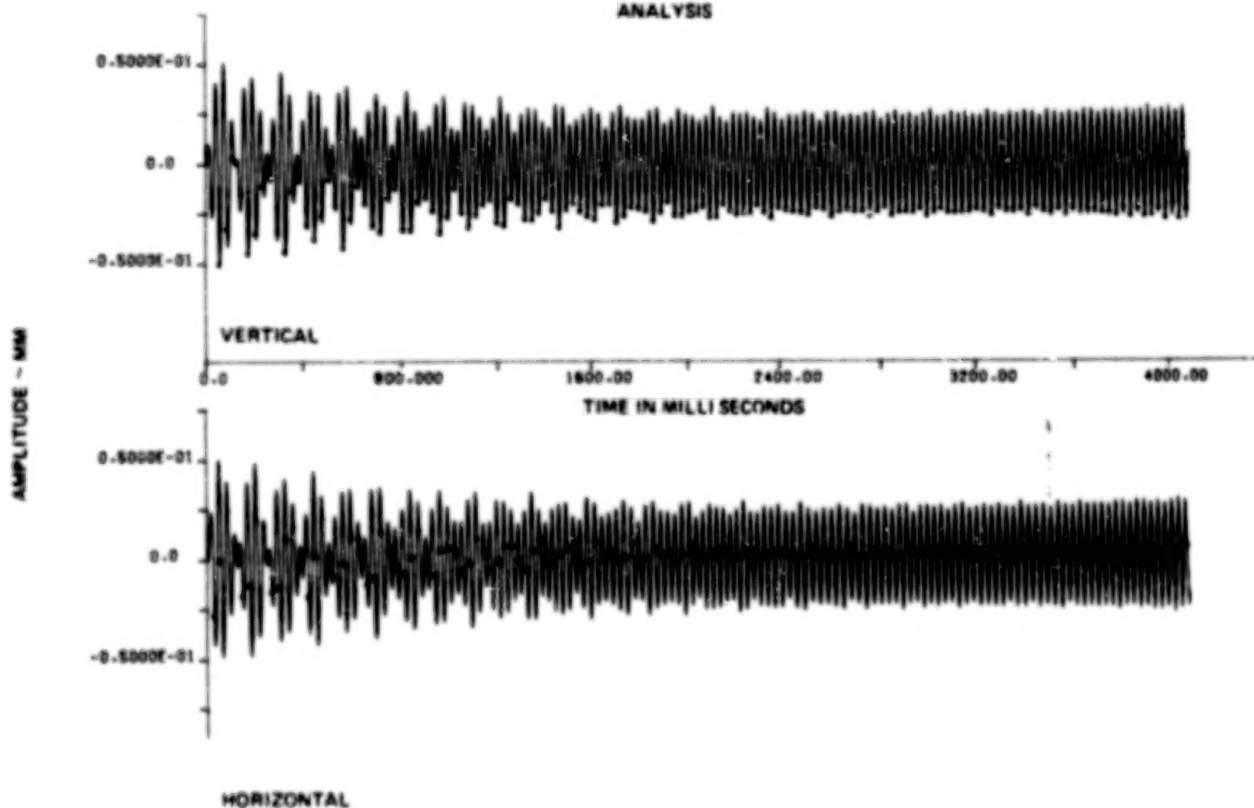


Figure 19 Experimental and Analytical Response From Data Station 3 During Undamped Blade Loss At 2000 RPM With 5.93 g cm Imbalance

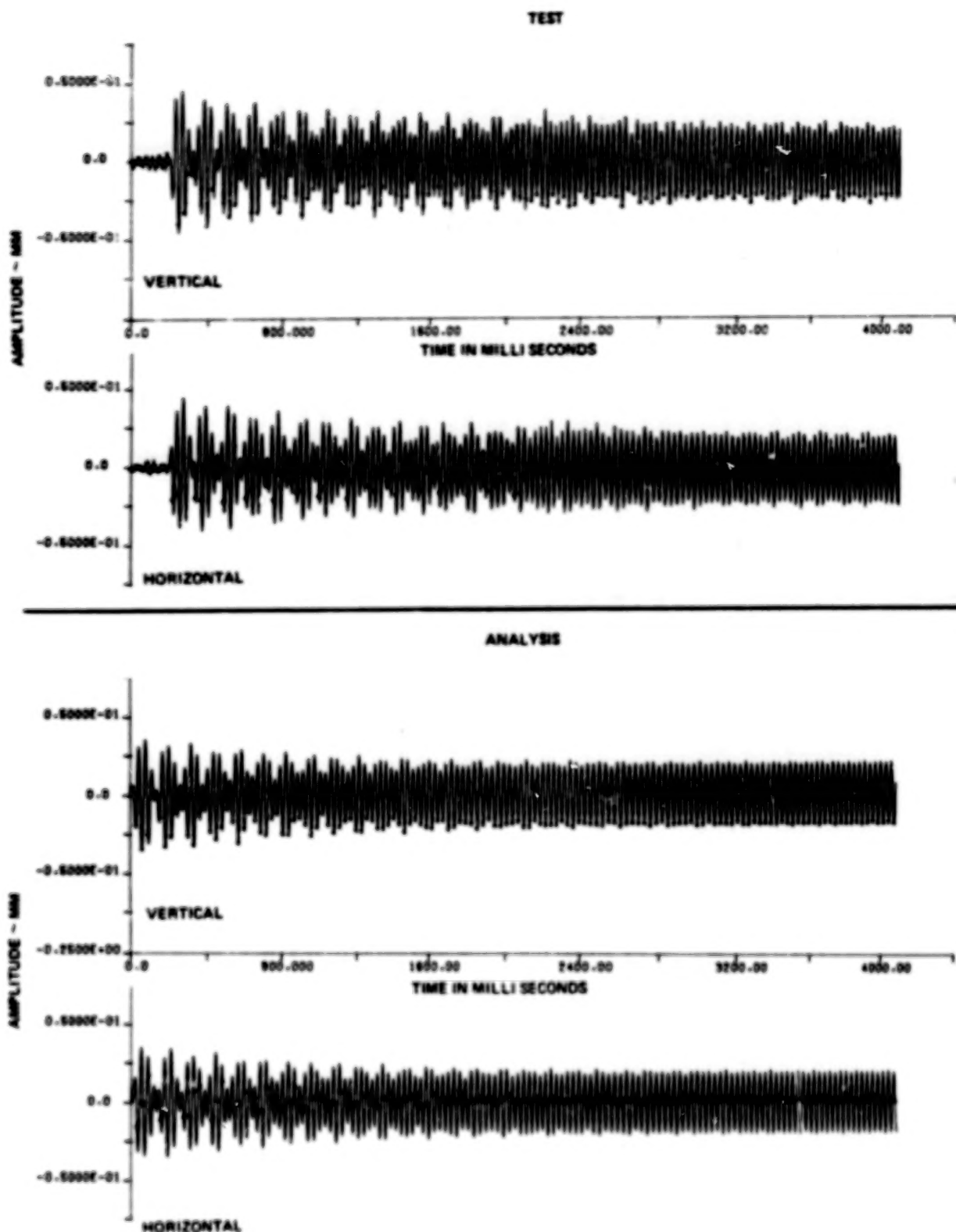
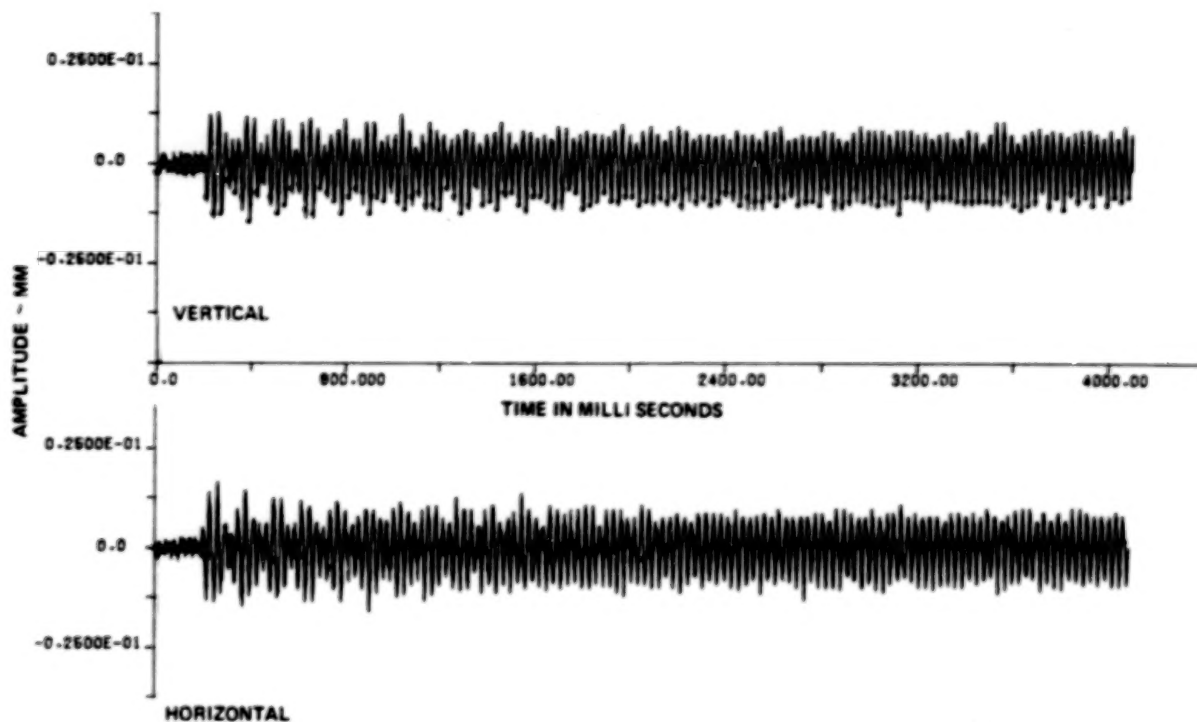


Figure 20 Experimental and Analytical Response From Data Station 4 During Un-damped Blade Loss At 2000 RPM With 5.93 g cm Imbalance

TEST



ANALYSIS

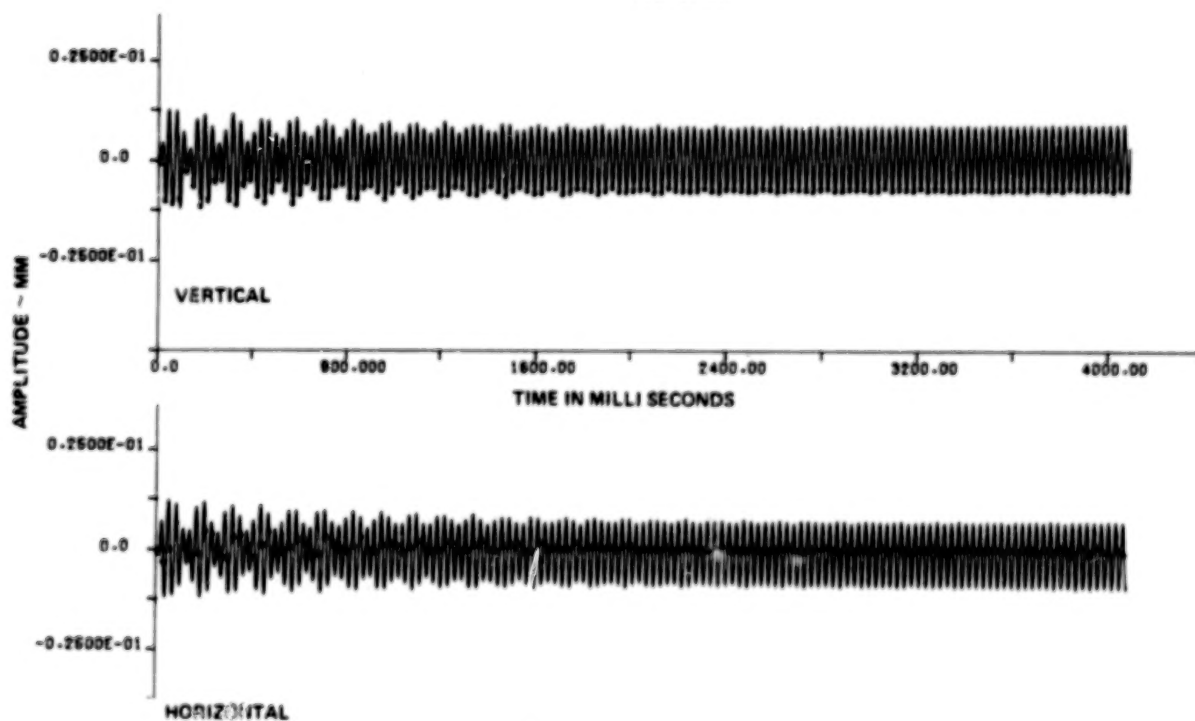


Figure 21 Experimental and Analytical Response From Data Station 5 During Un-damped Blade Loss At 2000 RPM With 5.93 g cm Imbalance

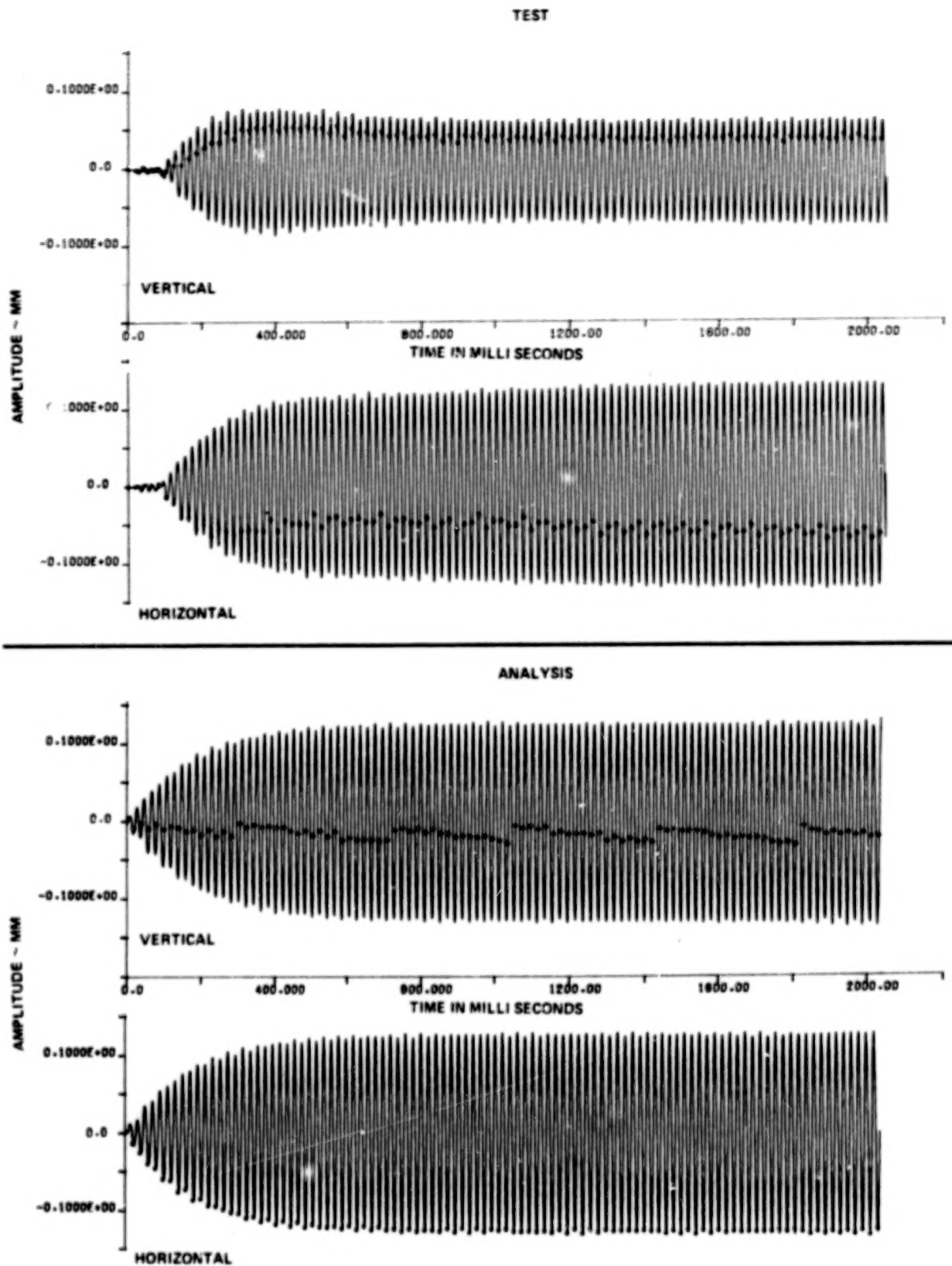


Figure 22 *Experimental and Analytical Response From Data Station 1 During Undamped Blade Loss At 2950 RPM With 5.93 g cm Imbalance*

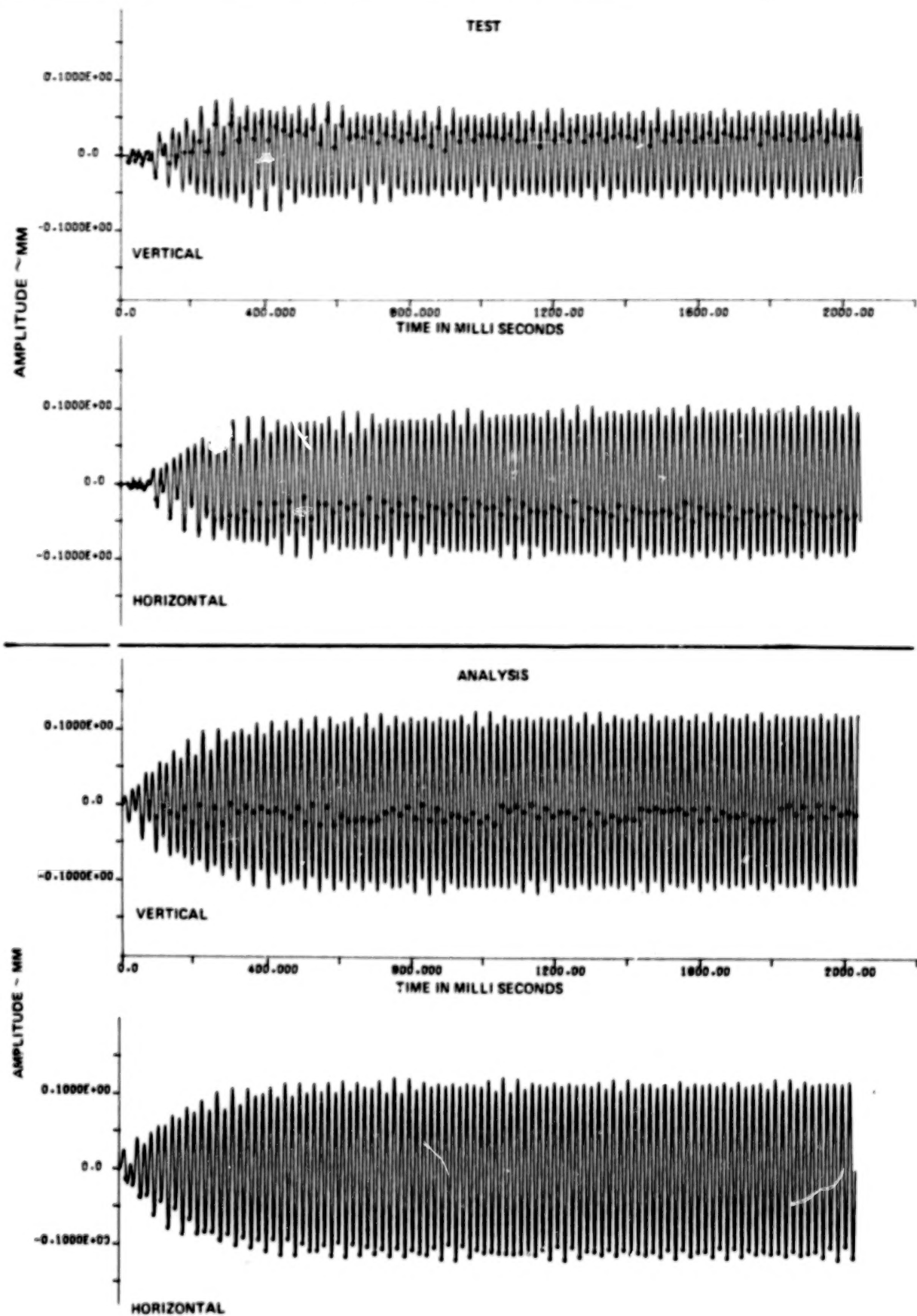


Figure 23 Experimental and Analytical Response From Data Station 2 During Undamped Blade Loss At 2950 RPM With 5.93 g cm Imbalance

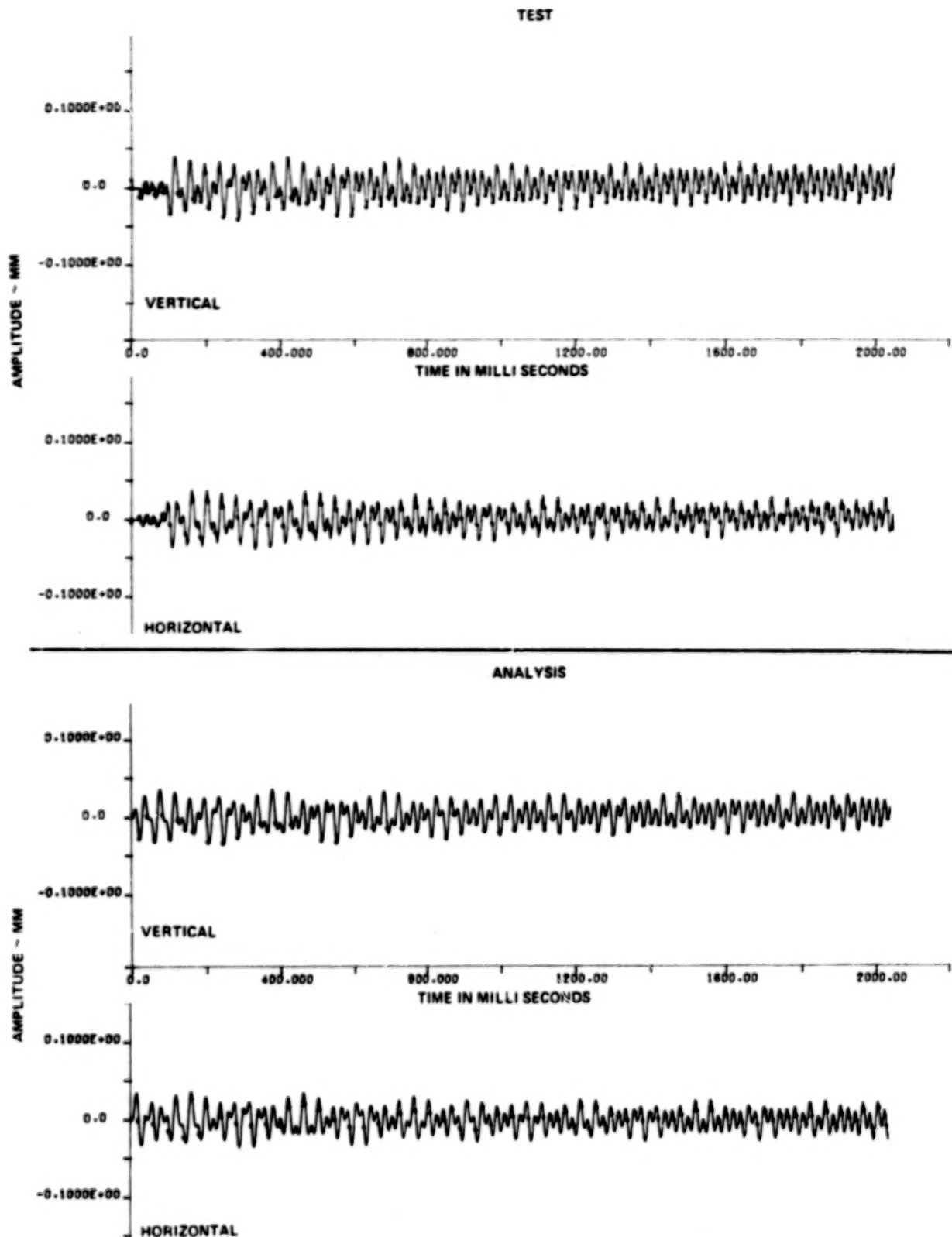


Figure 24 Experimental and Analytical Response From Data Station 3 During Undamped Blade Loss At 2950 RPM With 5.93 g cm Imbalance

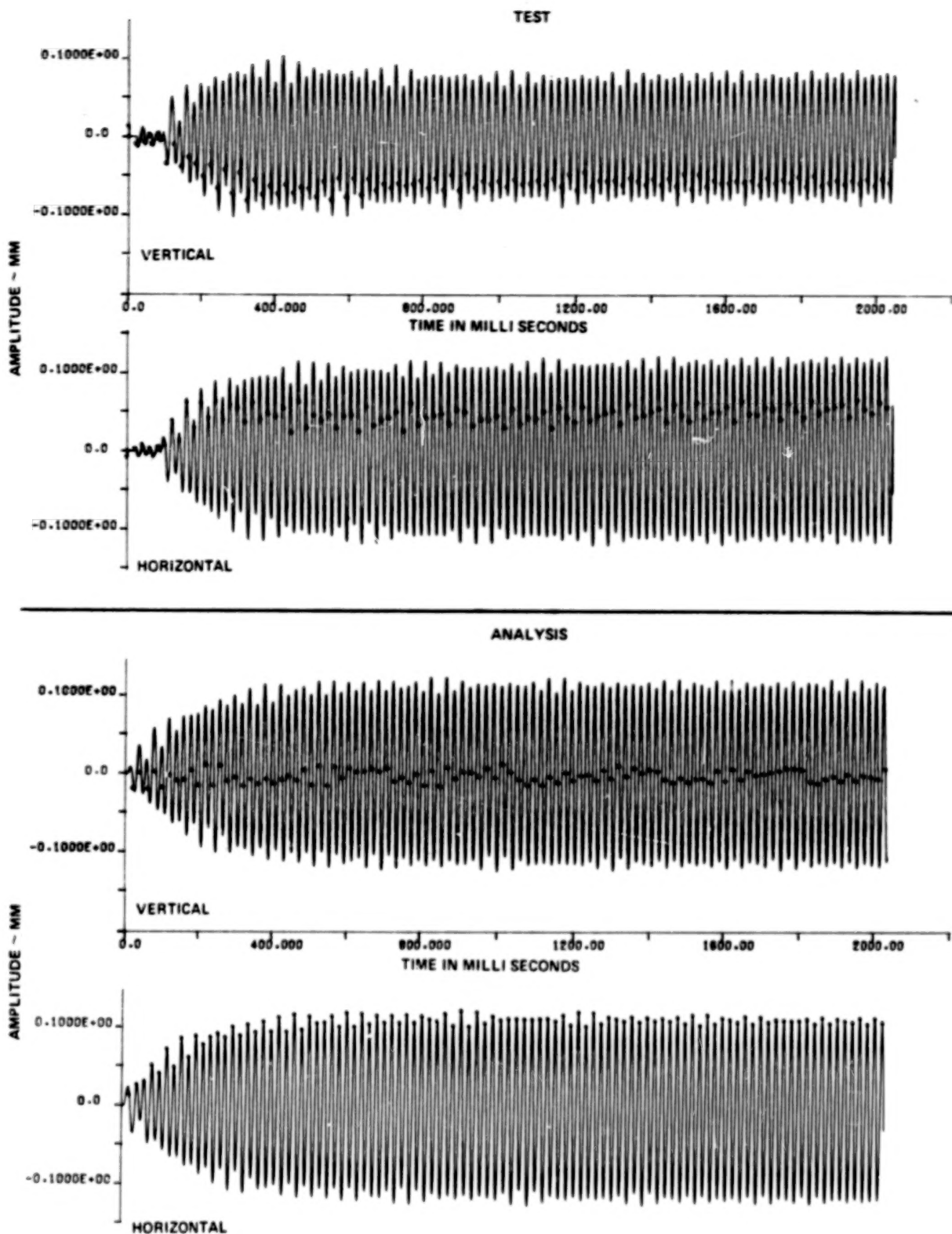
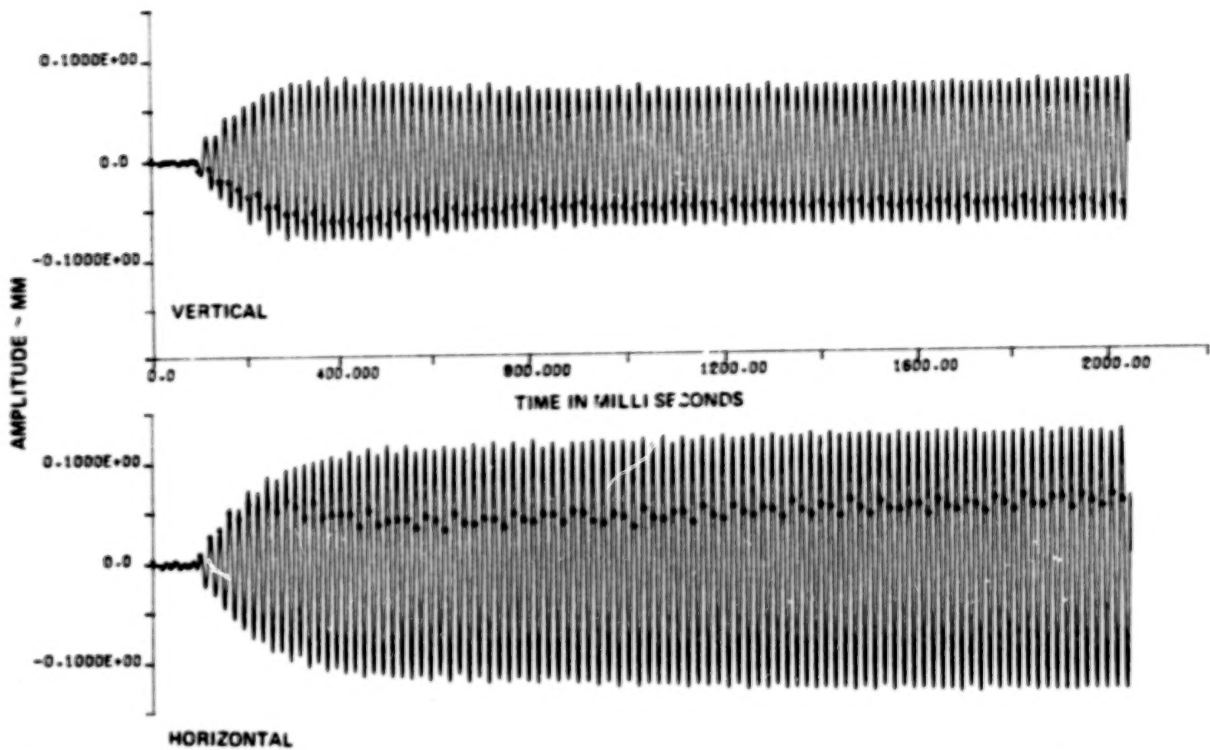


Figure 25 Experimental and Analytical Response From Data Station 4 During Undamped Blade Loss At 2950 RPM With 5.93 g cm Imbalance

TEST



ANALYSIS

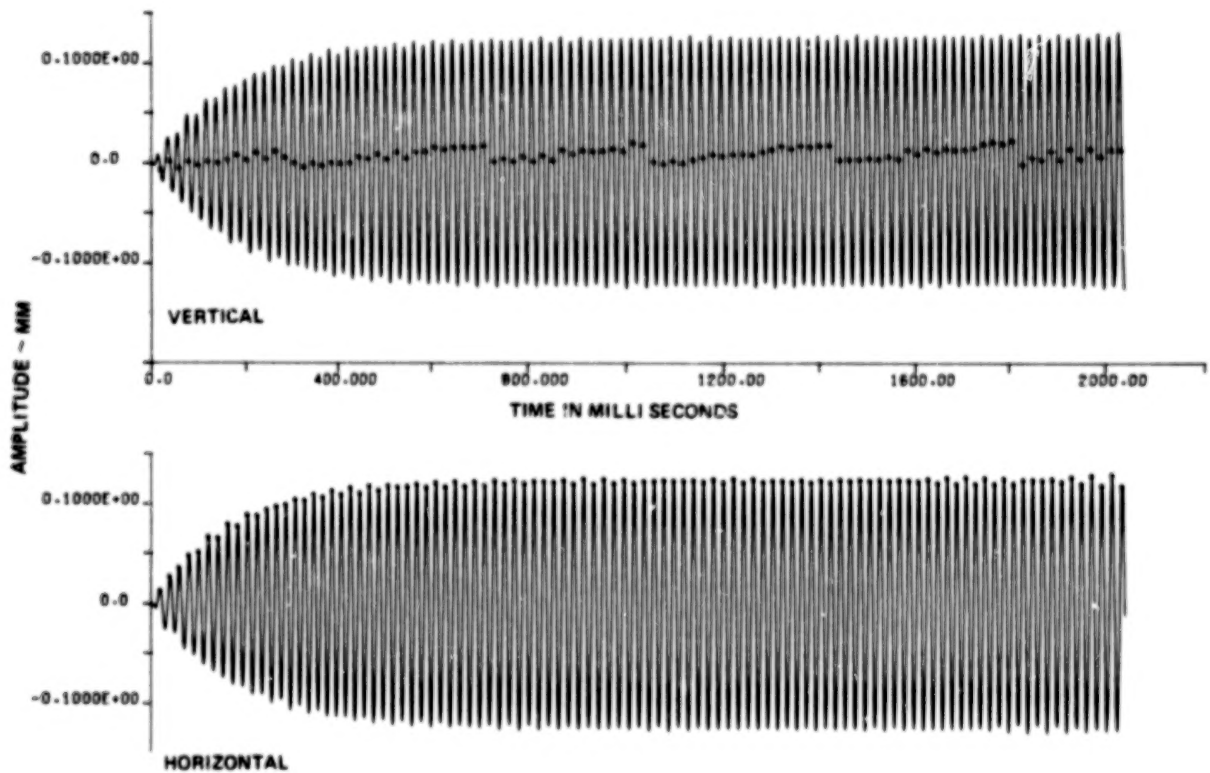


Figure 26 Experimental and Analytical Response From Data Station 5 During Undamped Blade Loss At 2950 RPM With 5.93 g cm Imbalance

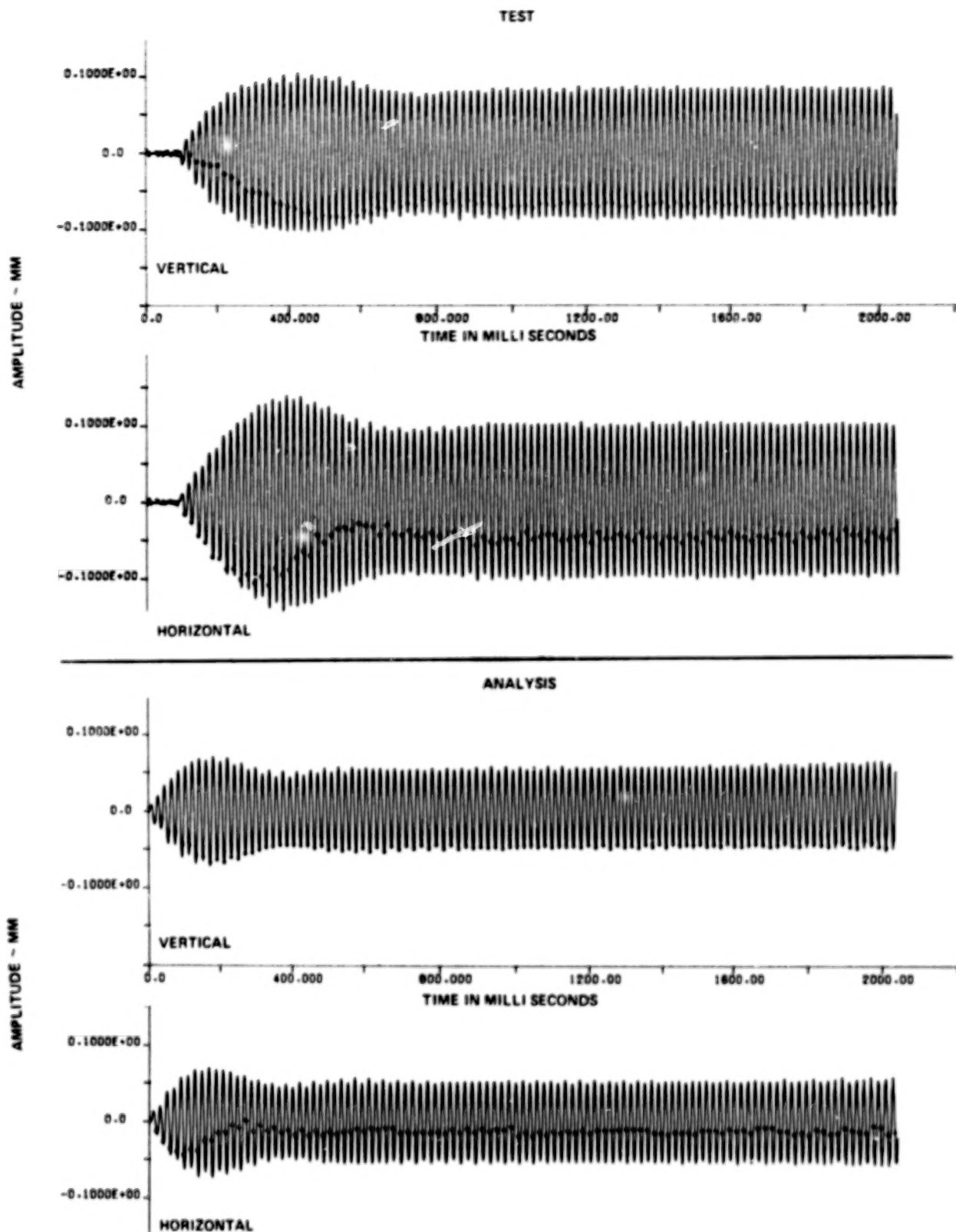


Figure 27 Experimental and Analytical Response From Data Station 1 During Undamped Blade Loss At 3100 RPM With 5.93 g cm Imbalance

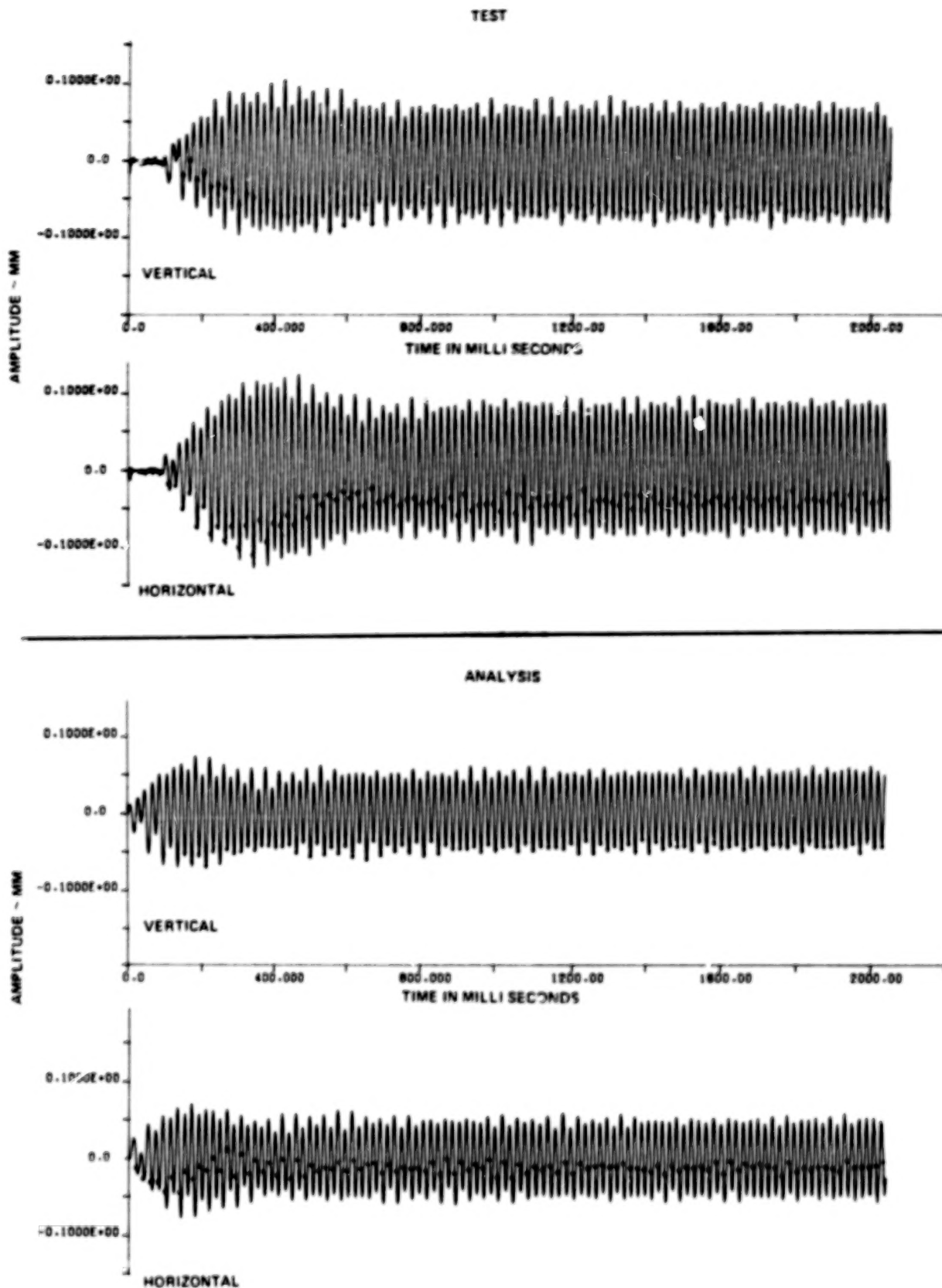
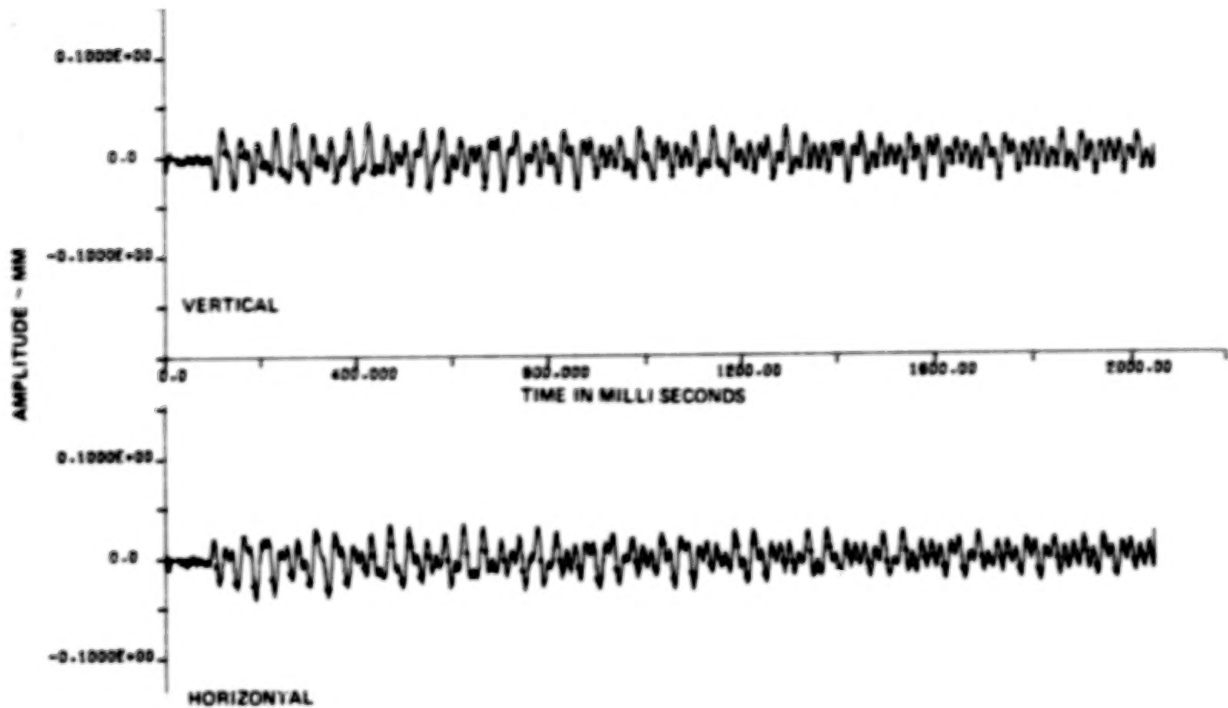


Figure 28 *Experimental and Analytical Response From Data Station 2 During Undamped Blade Loss At 3100 RPM With 5.93 g cm Imbalance*

TEST



ANALYSIS

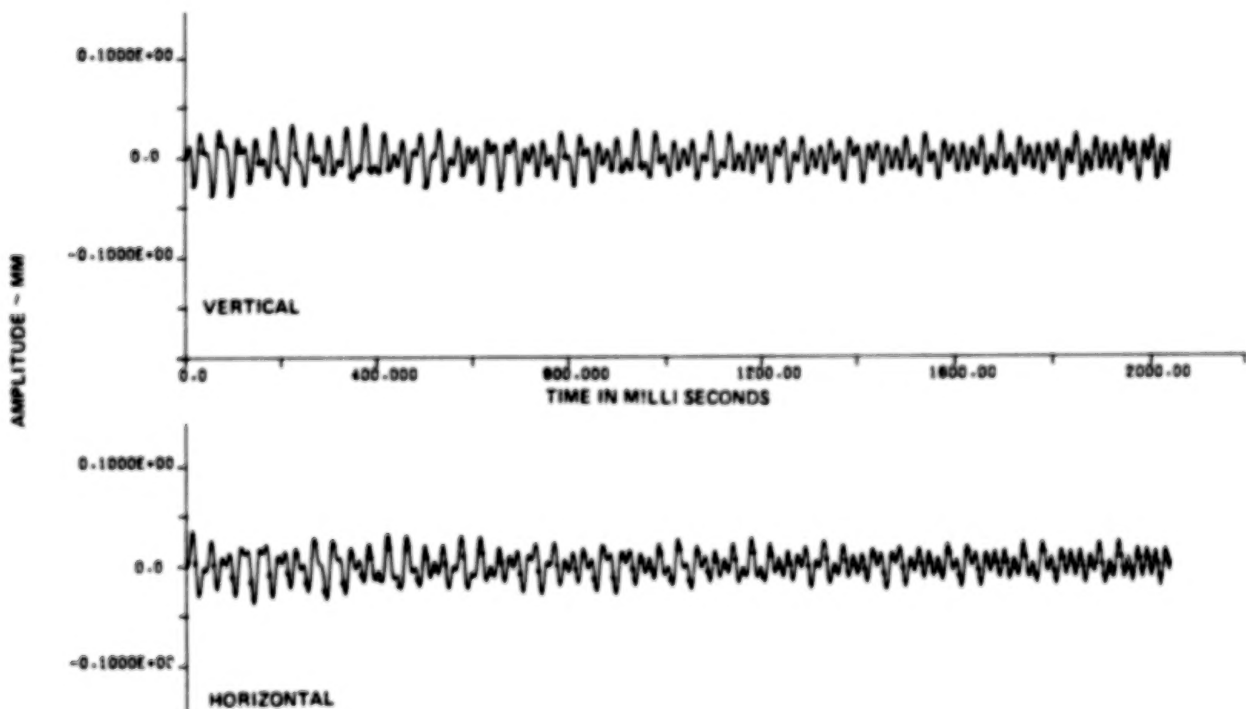


Figure 29 Experimental and Analytical Response From Data Station 3 During Undamped Blade Loss At 3100 RPM With 5.93 g cm Imbalance

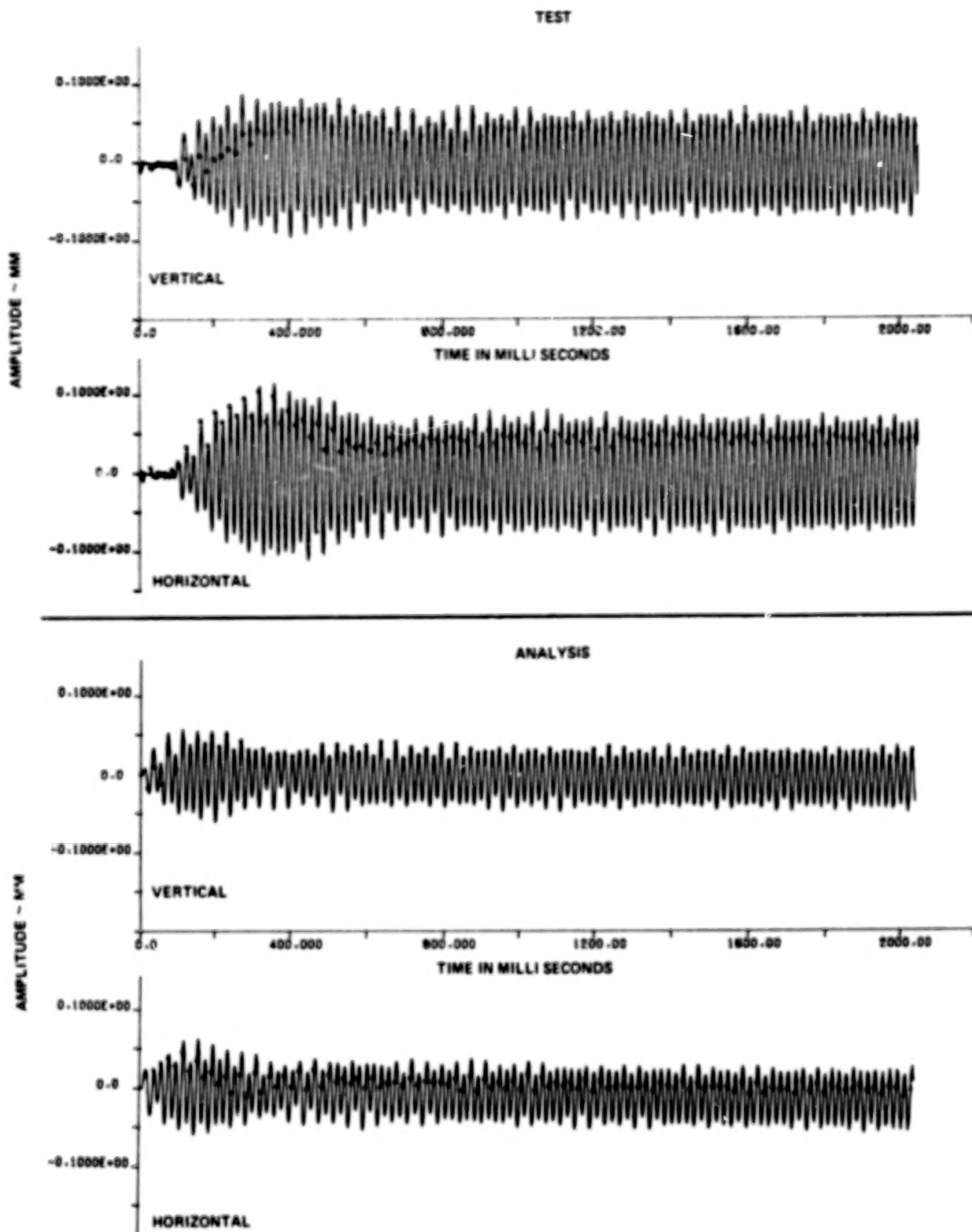


Figure 30 Experimental and Analytical Response From Data Station 4 During Un-damped Blade Loss At 3100 RPM With 5.93 g cm Imbalance

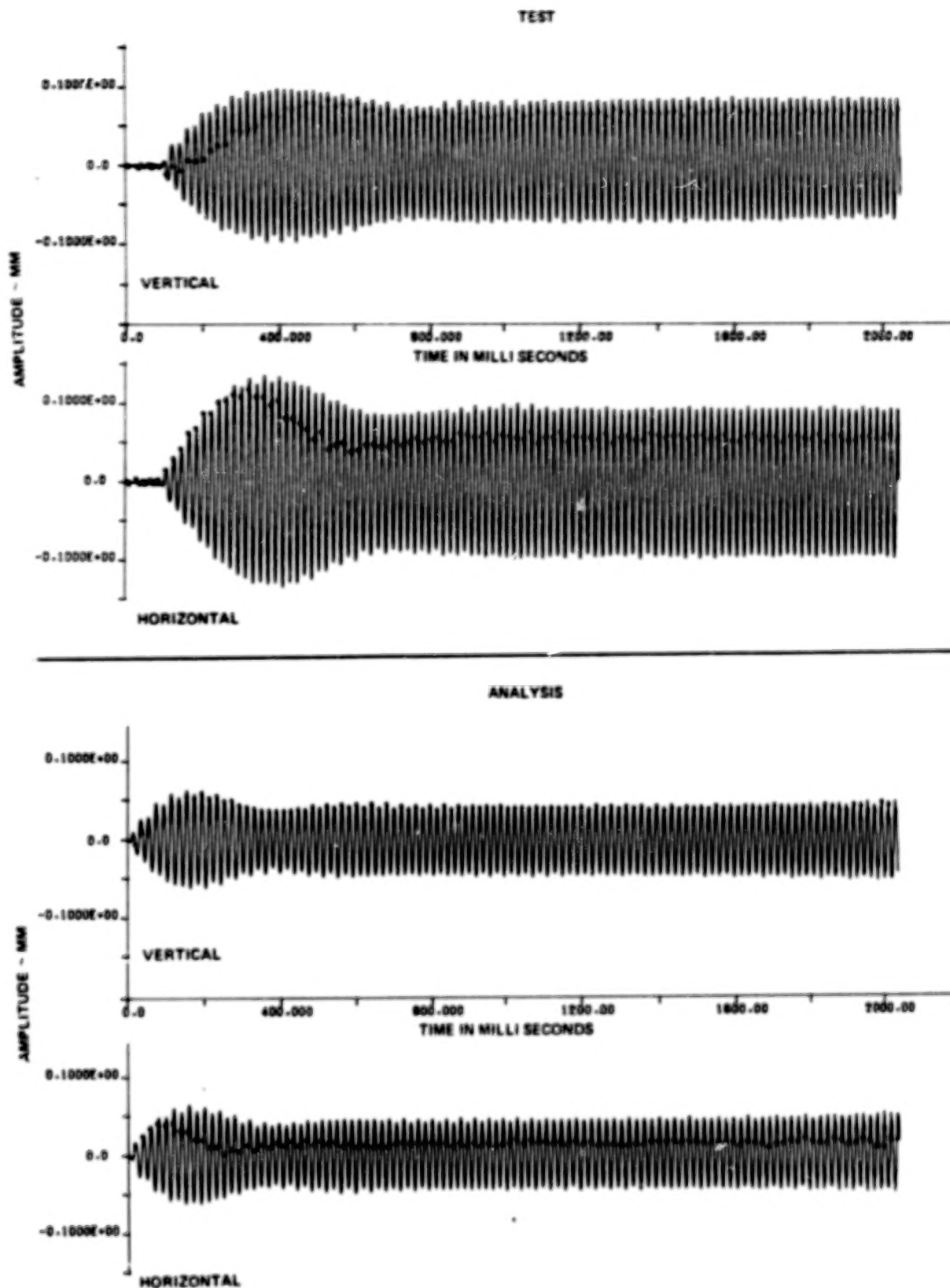


Figure 31 Experimental and Analytical Response From Data Station 5 During Undamped Blade Loss At 3100 RPM With 5.93 g cm Imbalance

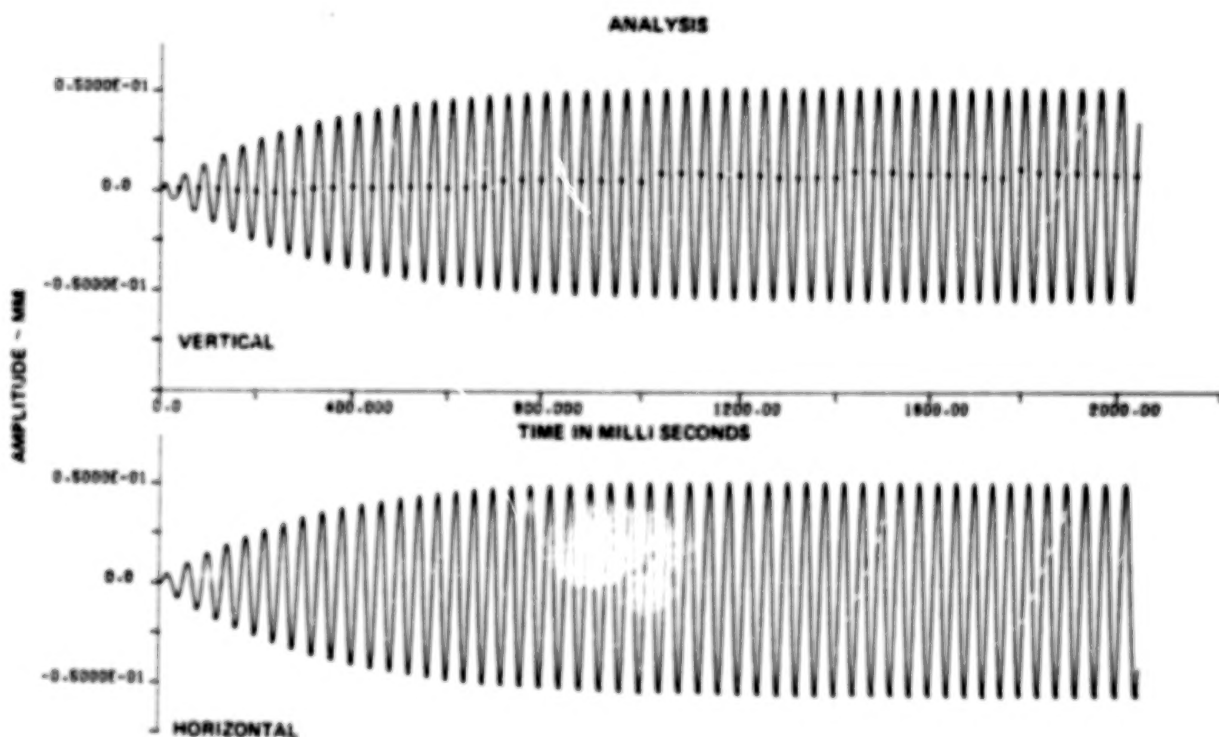
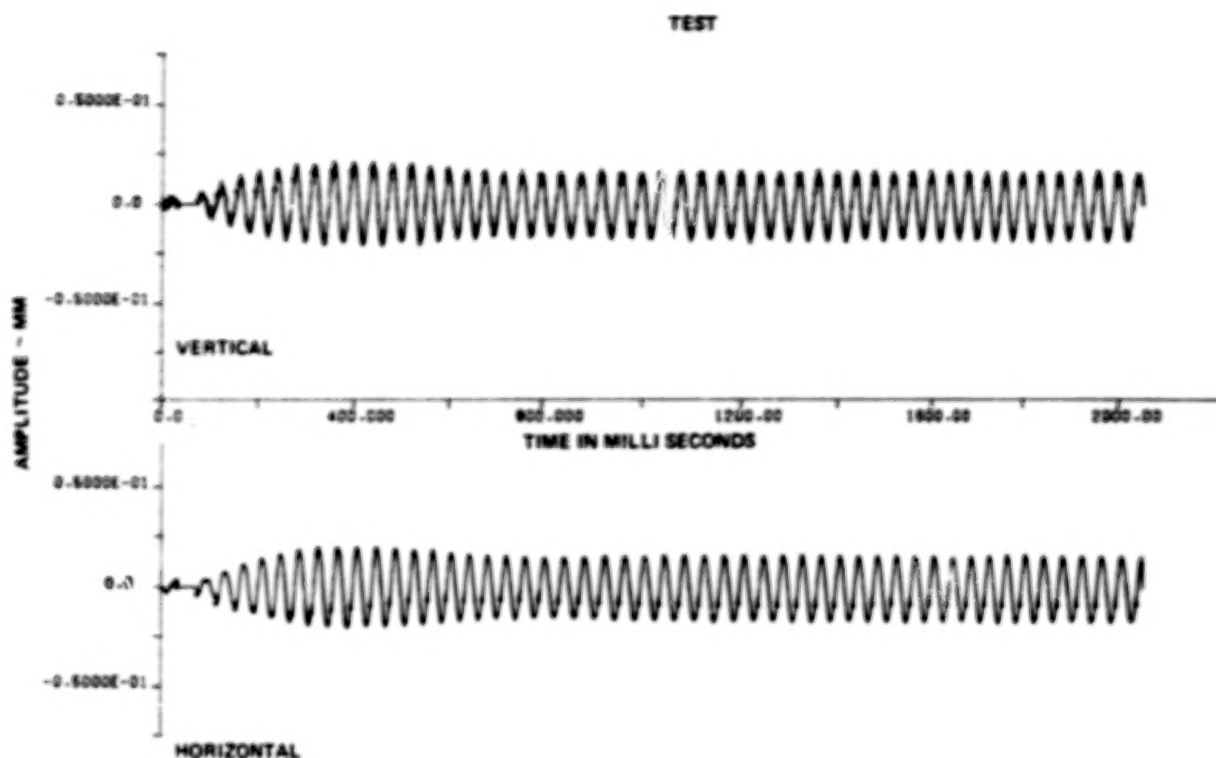


Figure 32 Experimental and Analytical Response From Data Station 1 During Damped Blade Loss At 1500 RPM With 7.41 g cm Imbalance

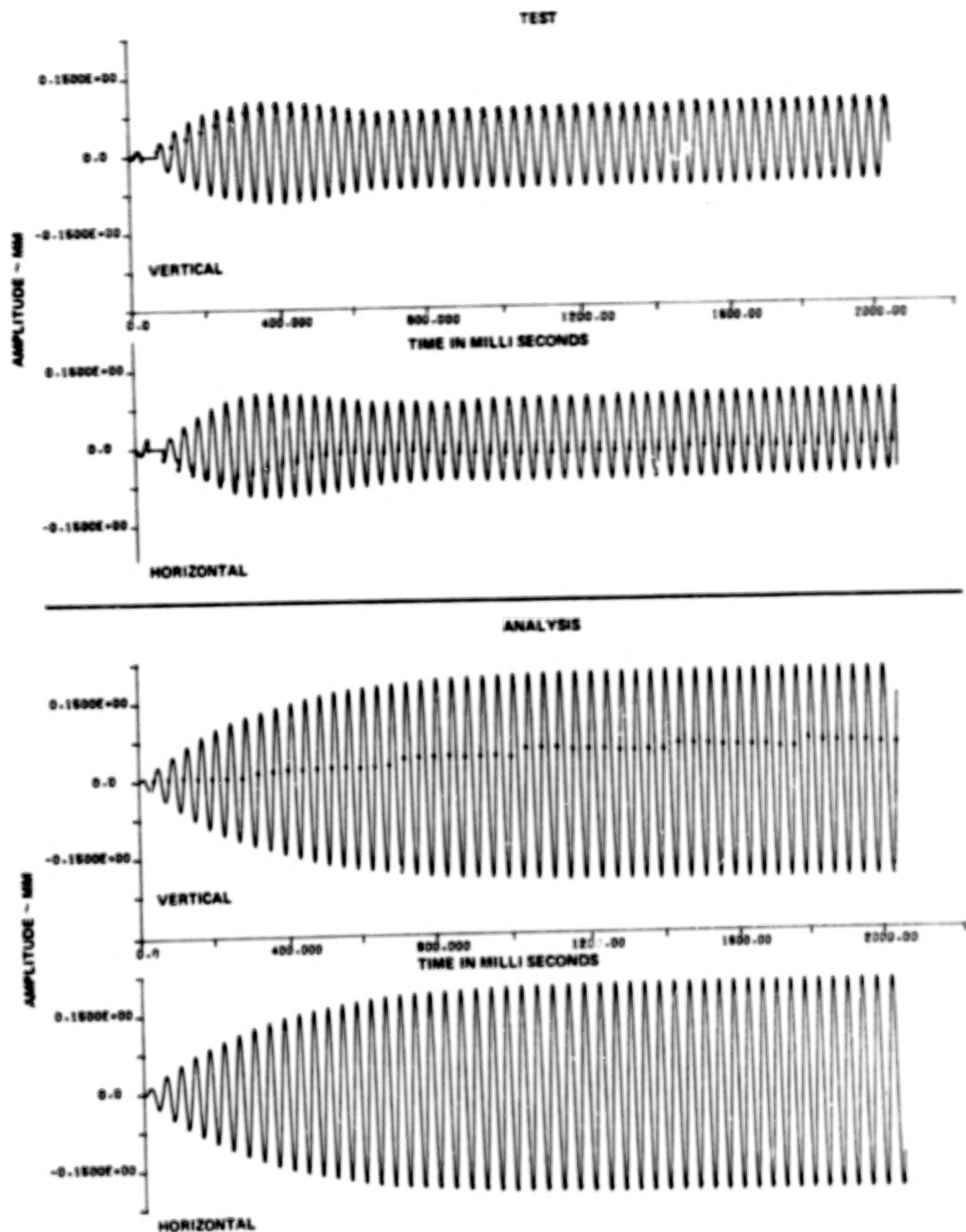


Figure 33 Experimental and Analytical Response From Data Station 2 During Damped Blade Loss At 1500 RPM With 7.41 g cm Imbalance

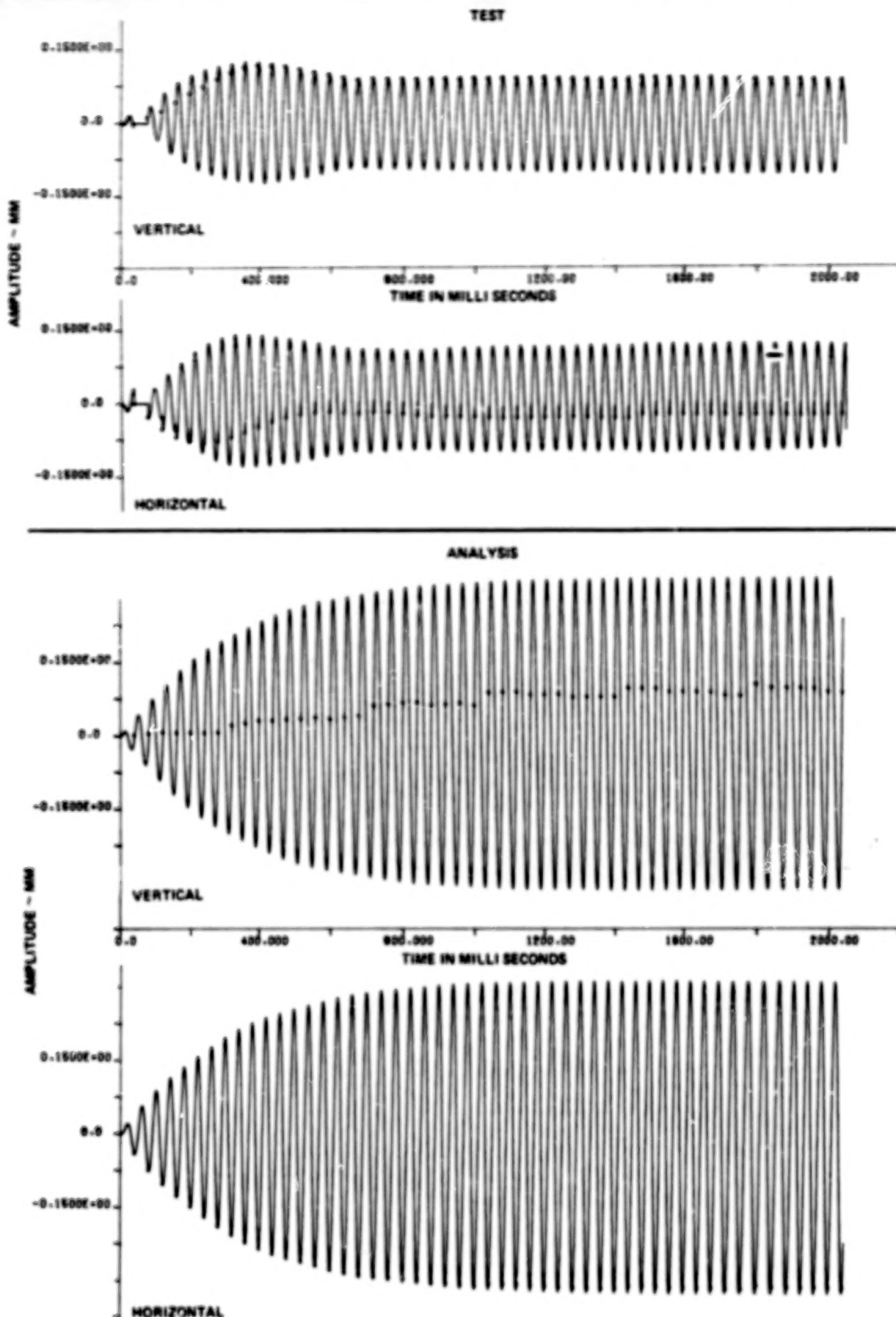


Figure 34 Experimental and Analytical Response From Data Station 3 During Damped Blade Loss At 1500 RPM With 7.41 g cm Imbalance

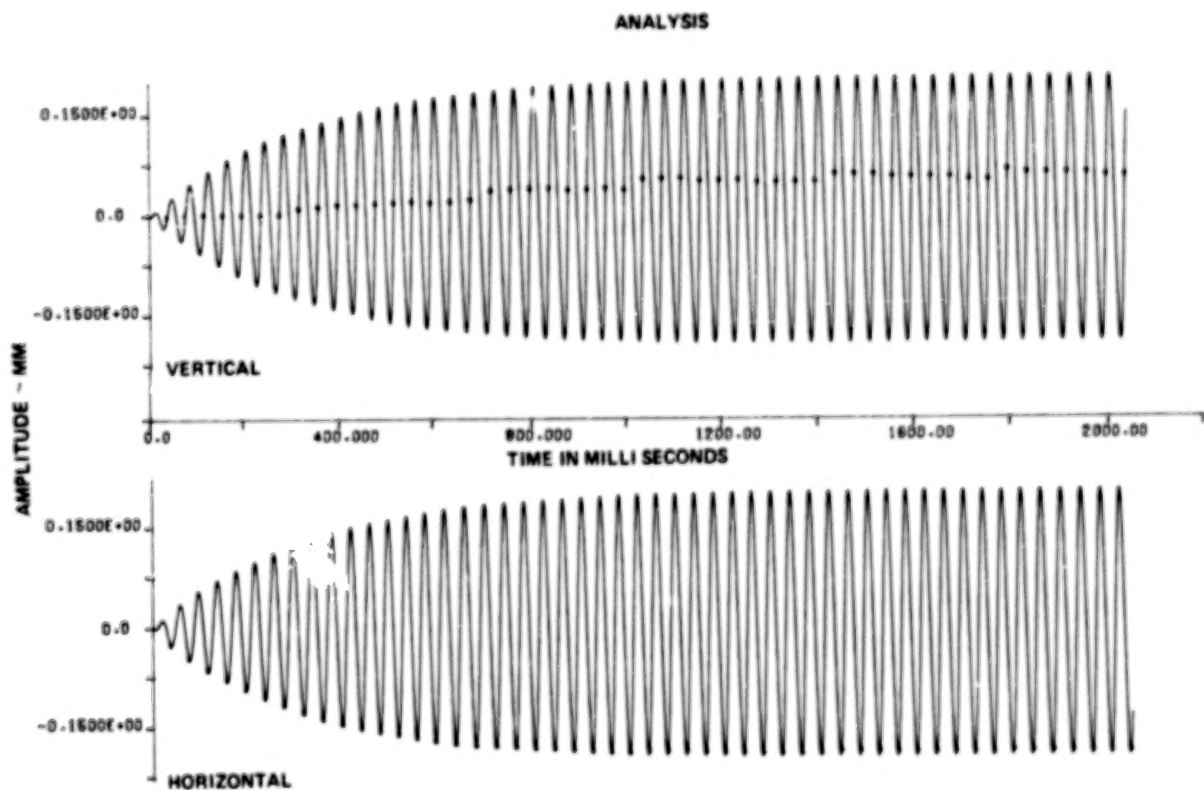
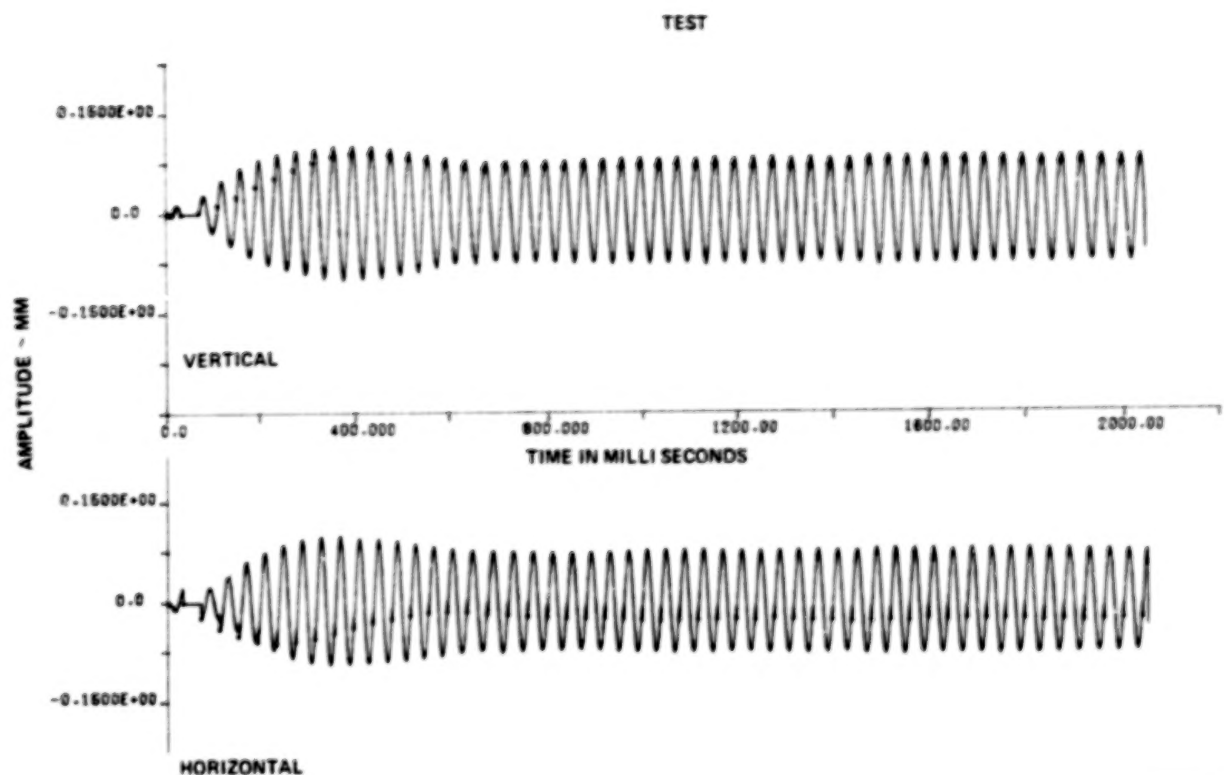


Figure 35 Experimental and Analytical Response From Data Station 4 During Damped Blade Loss At 1500 RPM With 7.41 g cm Imbalance

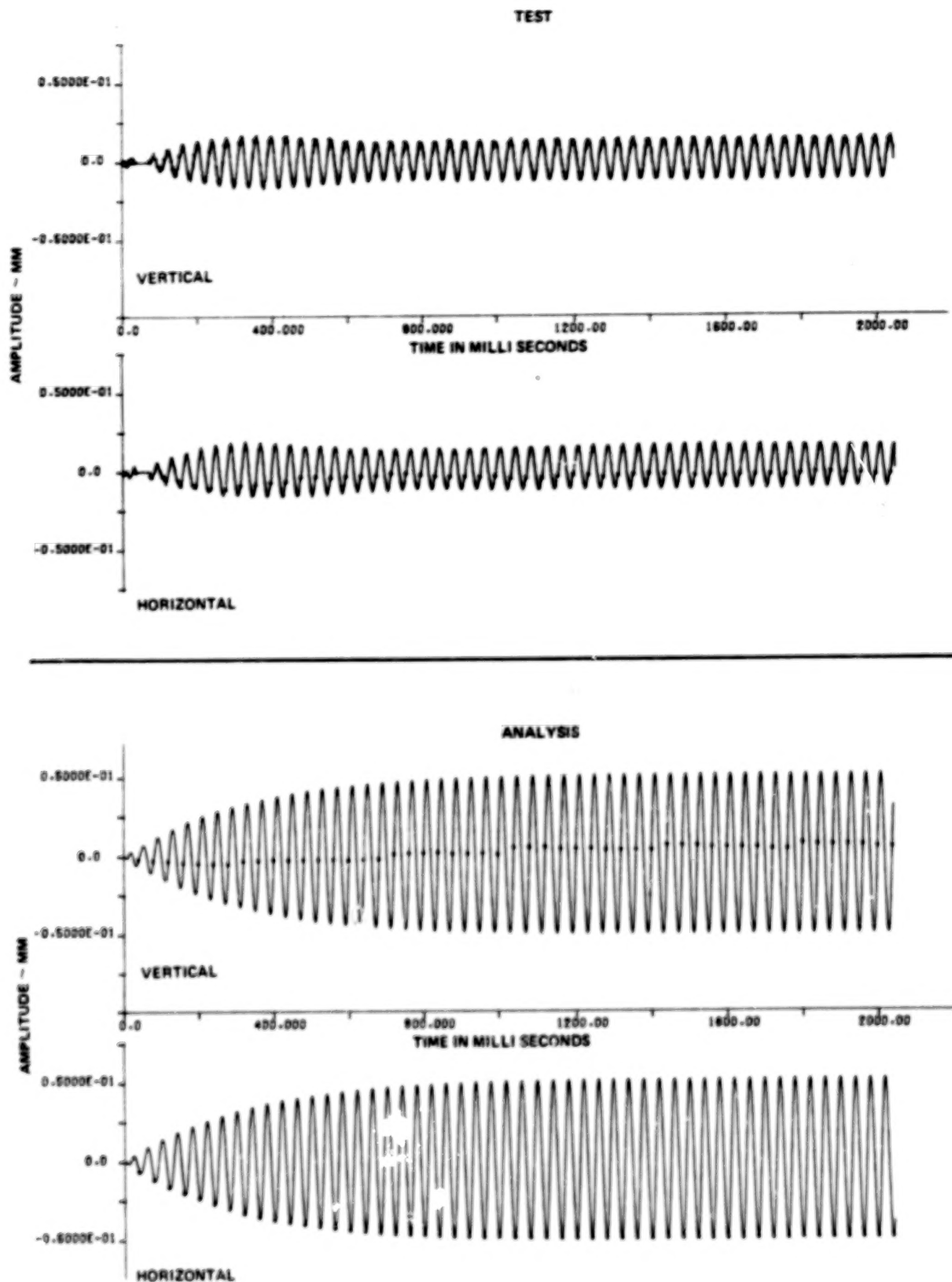


Figure 36 Experimental and Analytical Response From Data Station 5 During Damped Blade Loss At 1500 RPM With 7.41 g cm Imbalance

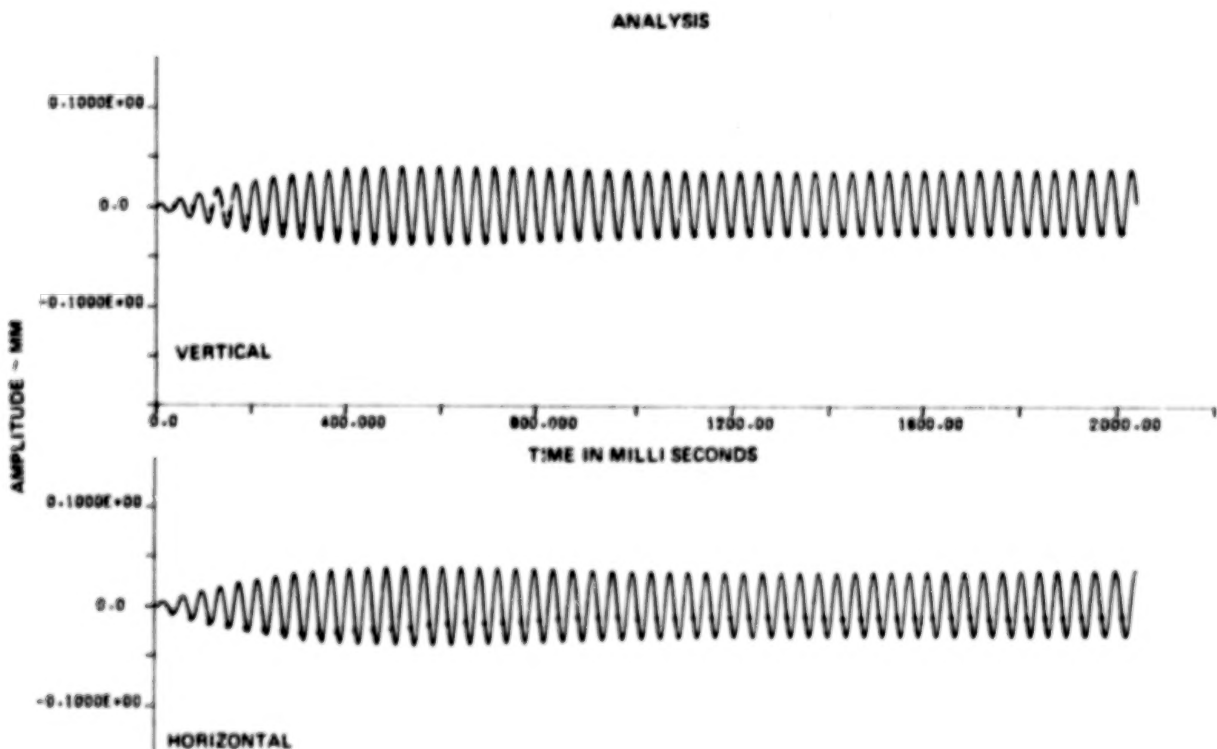
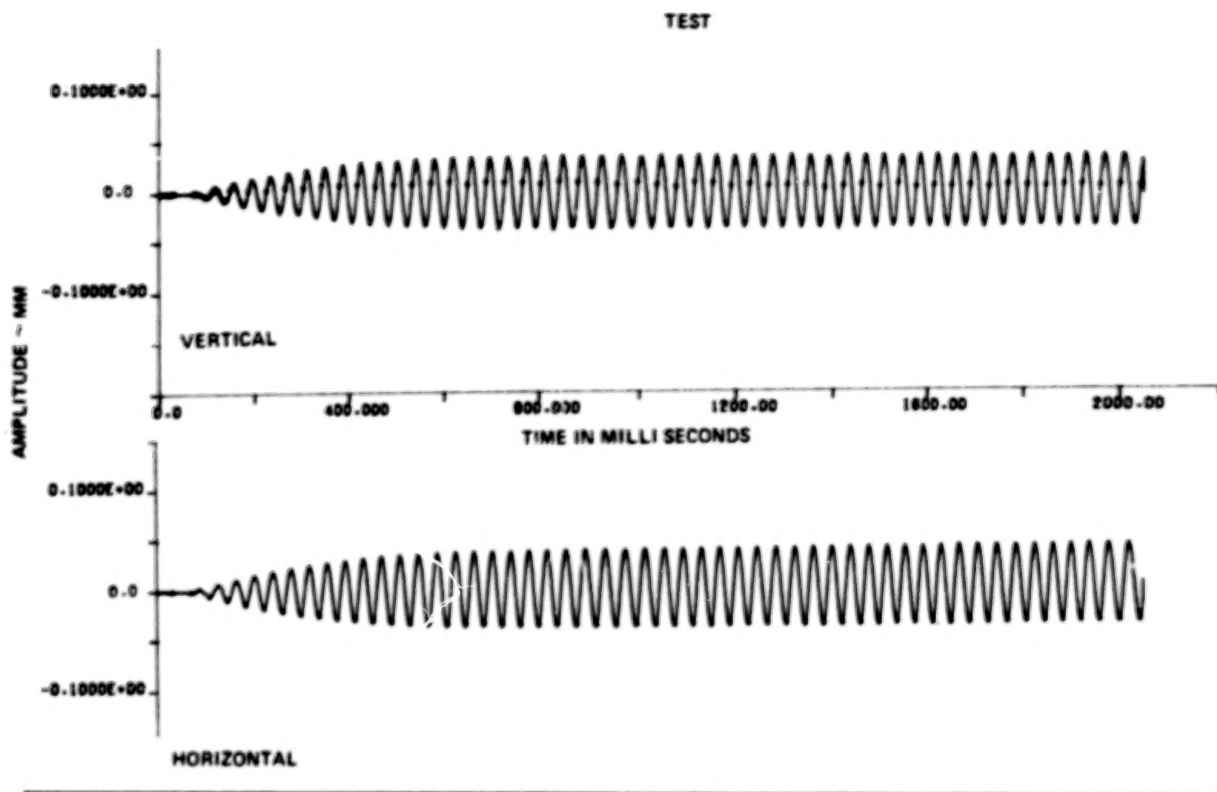


Figure 37 Experimental and Analytical Response From Data Station 1 During Damped Blade Loss At 1550 RPM With 7.41 g cm Imbalance

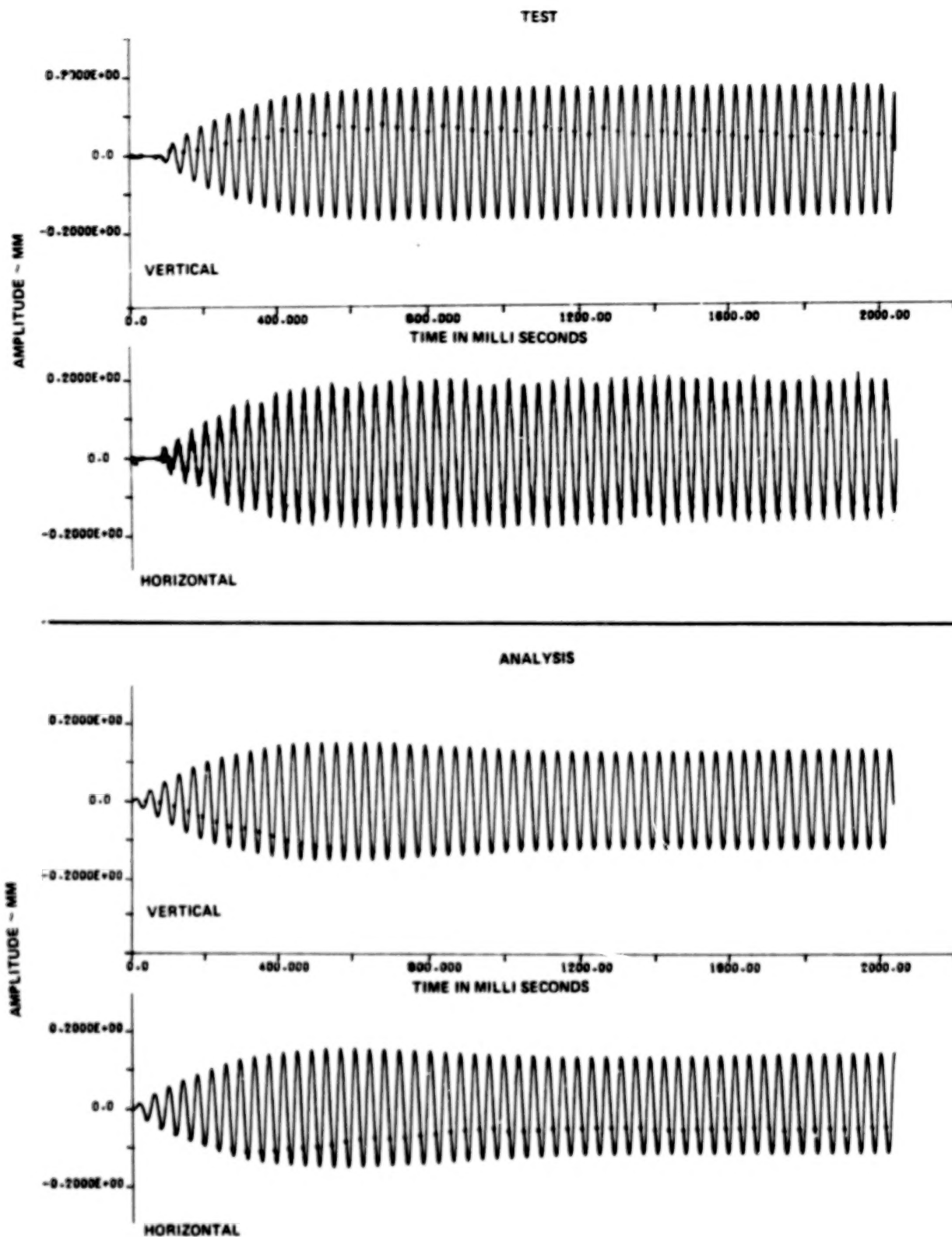


Figure 38 Experimental and Analytical Response From Data Station 2 During Damped Blade Loss At 1550 RPM With 7.41 g cm Imbalance

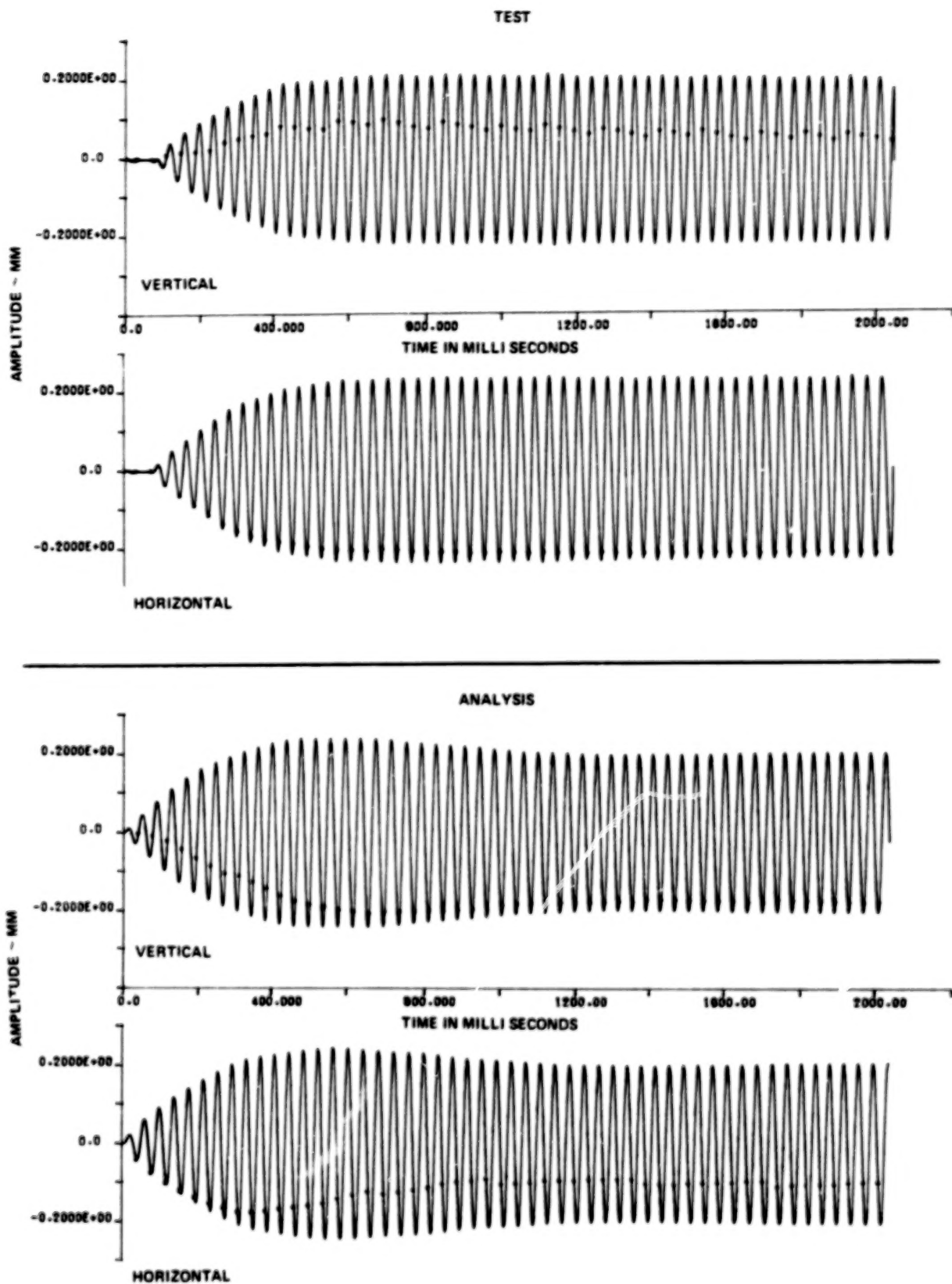


Figure 39 Experimental and Analytical Response From Data Station 3 During Damped Blade Loss At 1550 RPM With 7.41 g cm Imbalance

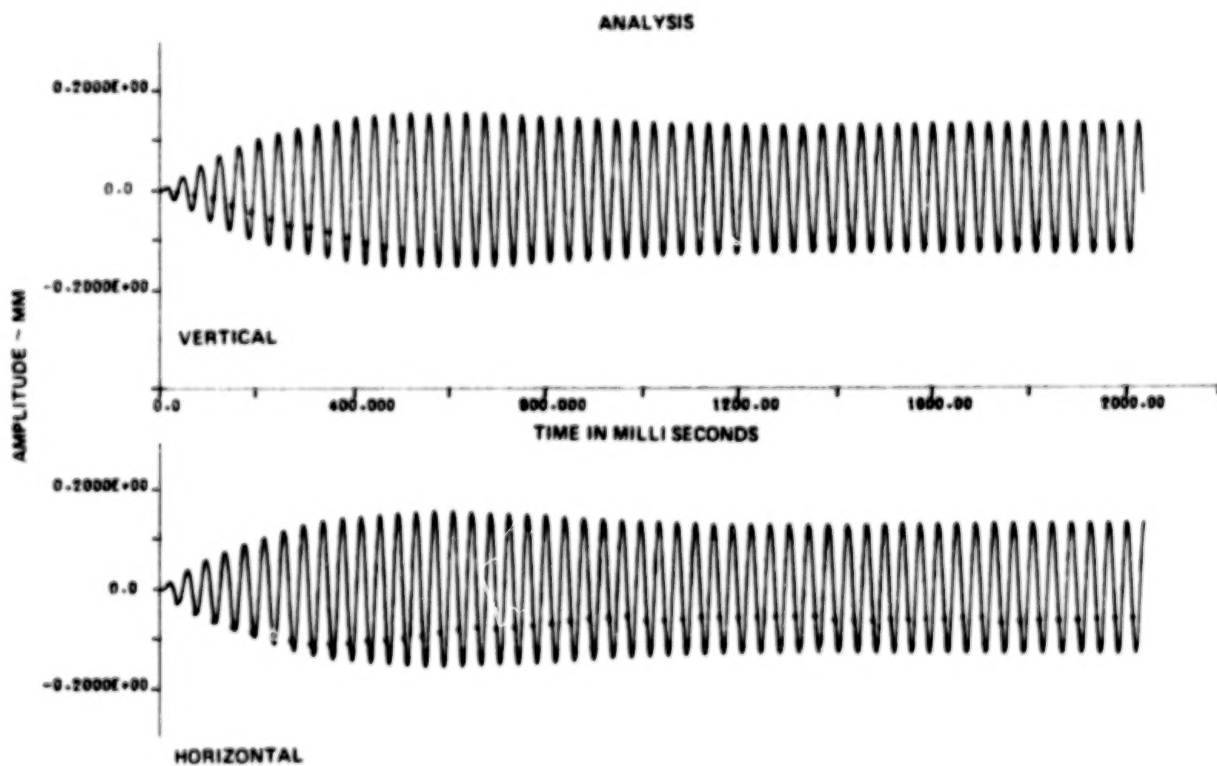
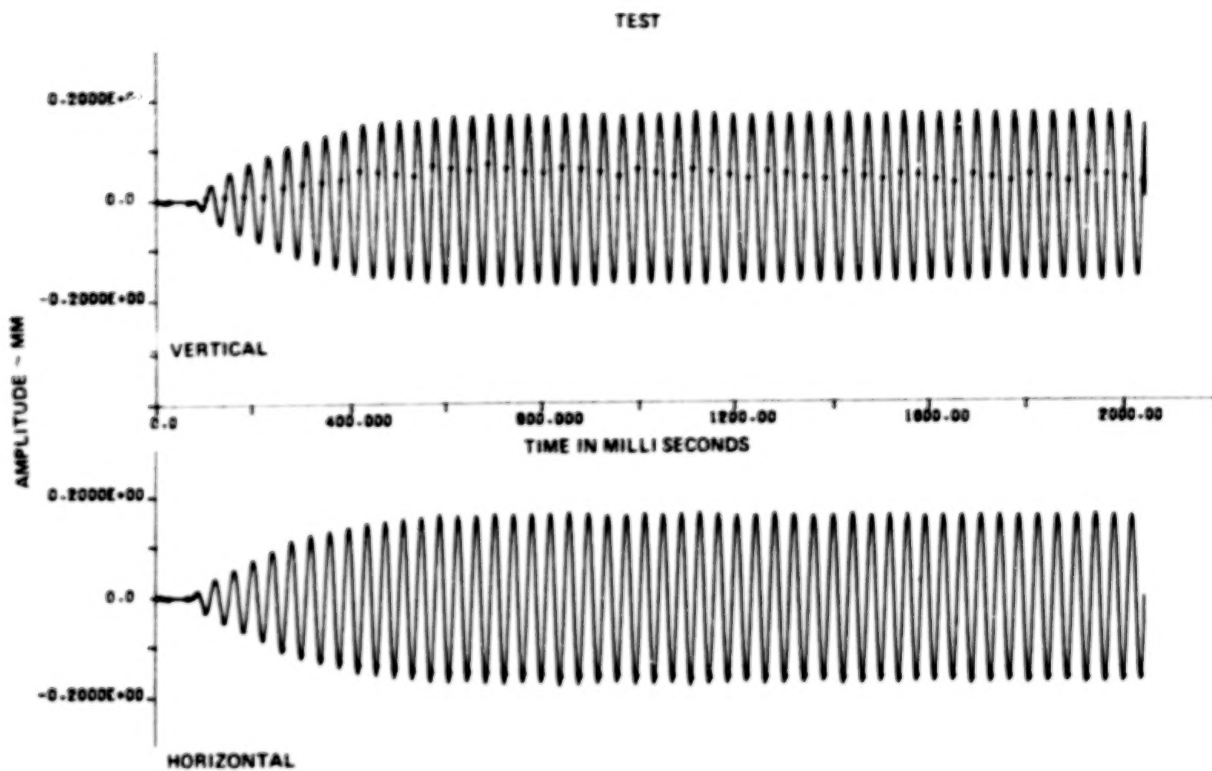


Figure 40 *Experimental and Analytical Response From Data Station 4 During Damped Blade Loss At 1550 RPM With 7.41 g cm Imbalance*

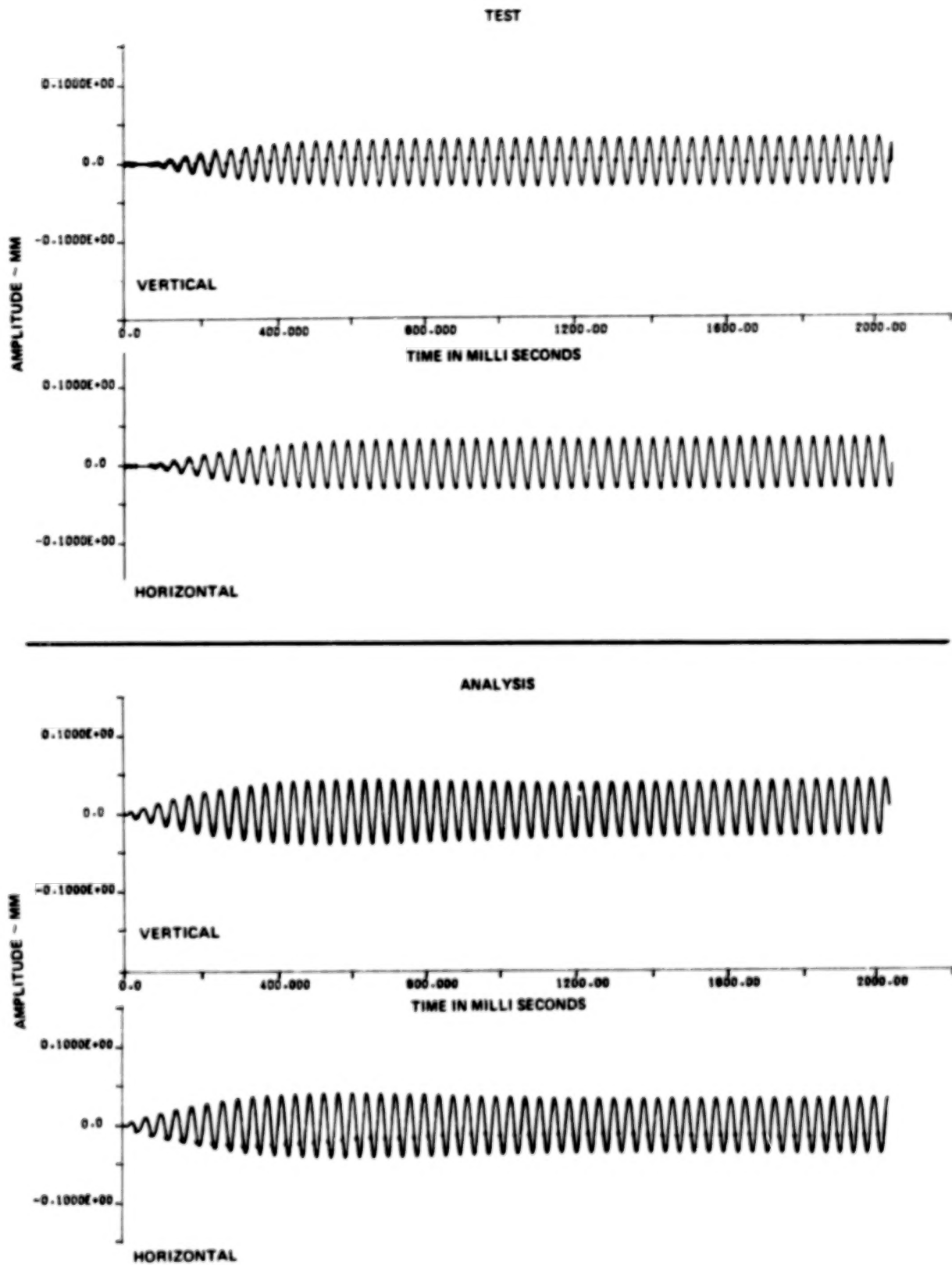


Figure 41 *Experimental and Analytical Response From Data Station 5 During Damped Blade Loss At 1550 RPM With 7.41 g cm Imbalance*

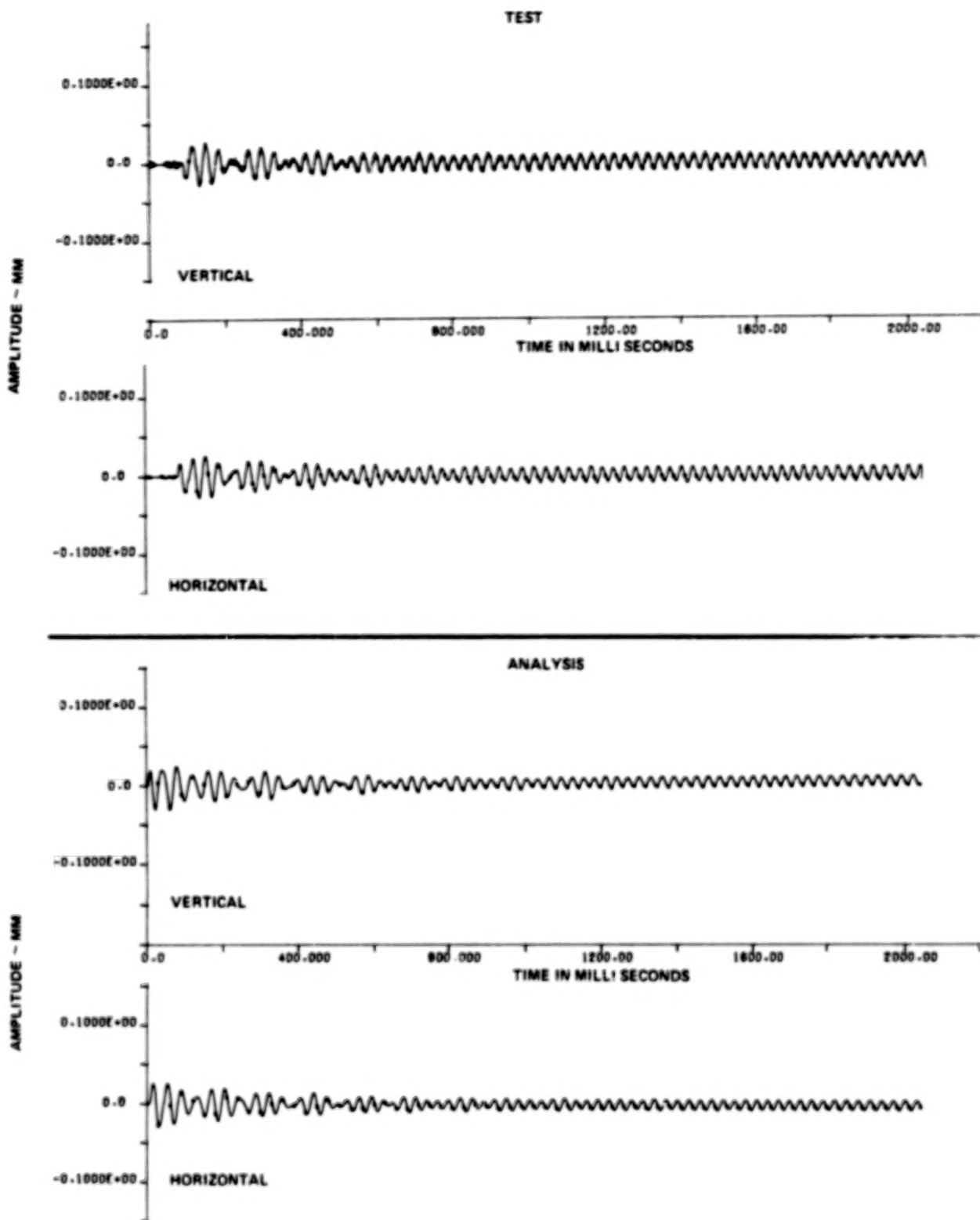
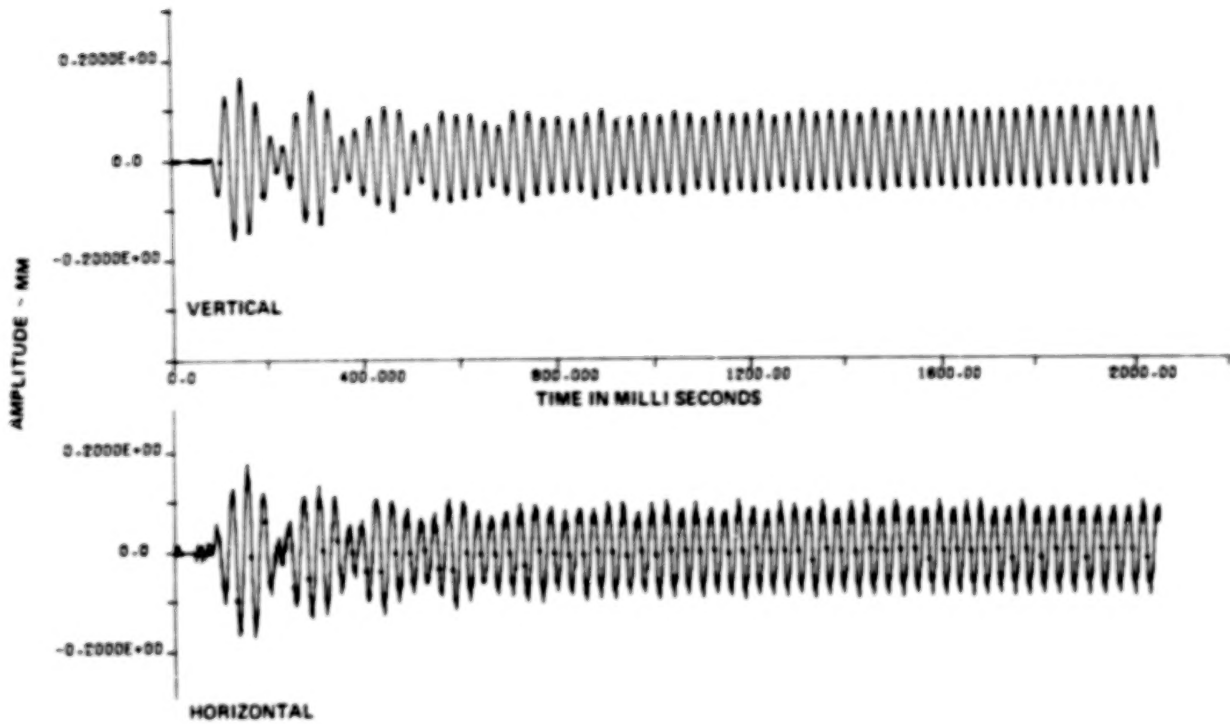


Figure 42 Experimental and Analytical Response From Data Station 1 During Damped Blade Loss At 2000 RPM With 27.65 g cm Imbalance

TEST



ANALYSIS

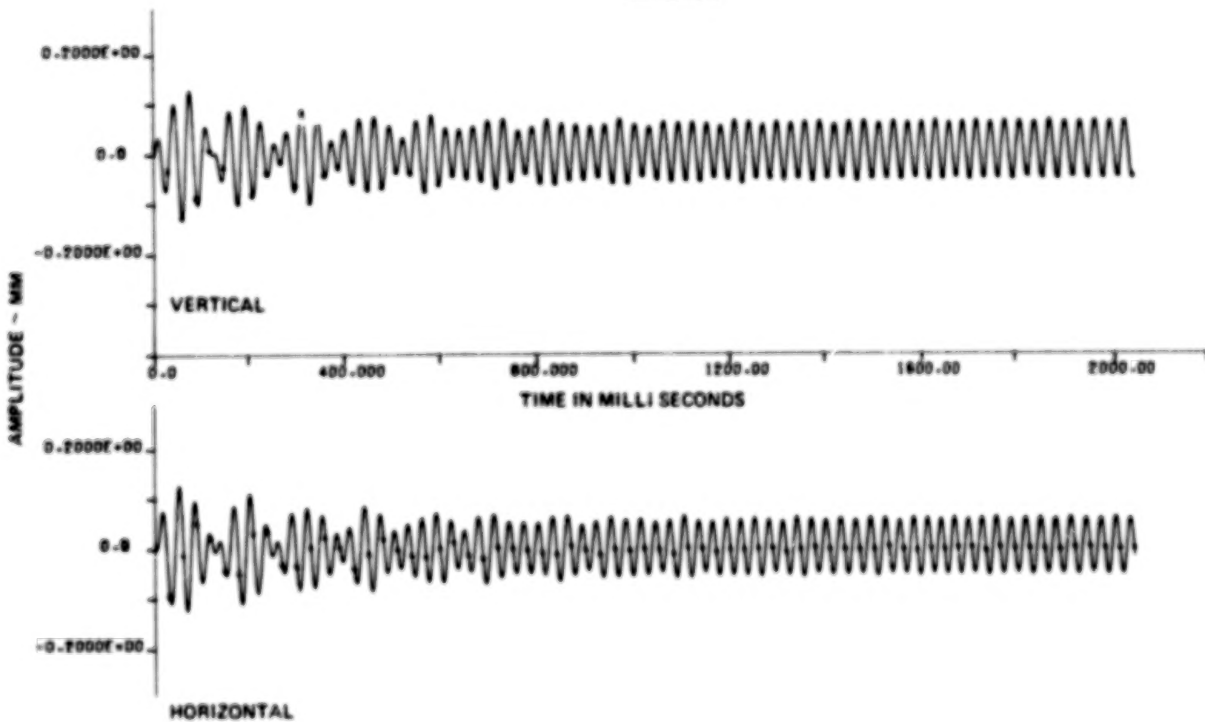


Figure 43 Experimental and Analytical Response From Data Station 2 During Damped Blade Loss At 2000 RPM With 27.65 g cm Imbalance

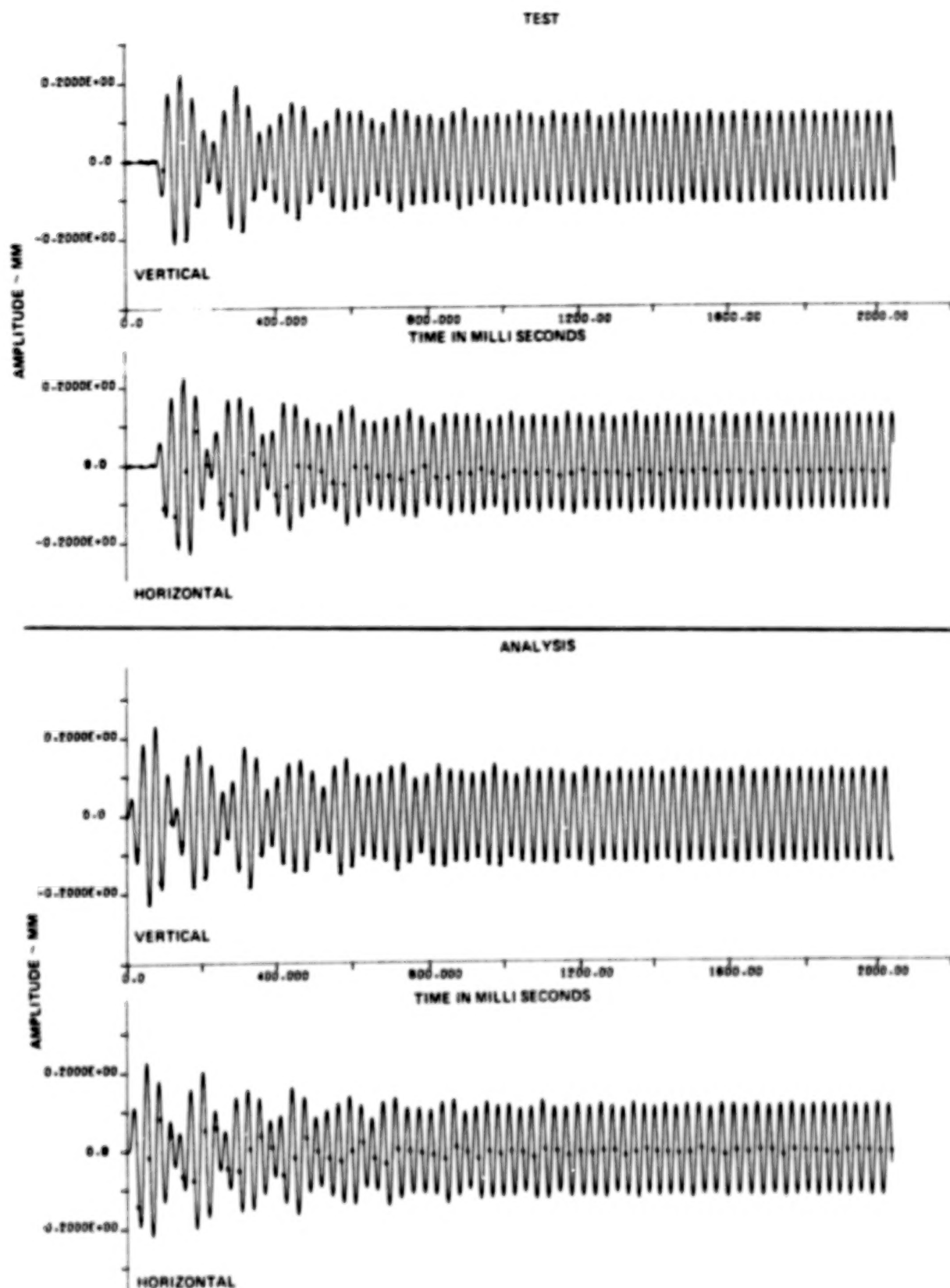


Figure 44 Experimental and Analytical Response From Data Station 3 During Damped Blade Loss At 2000 RPM With 27.65 g cm Imbalance

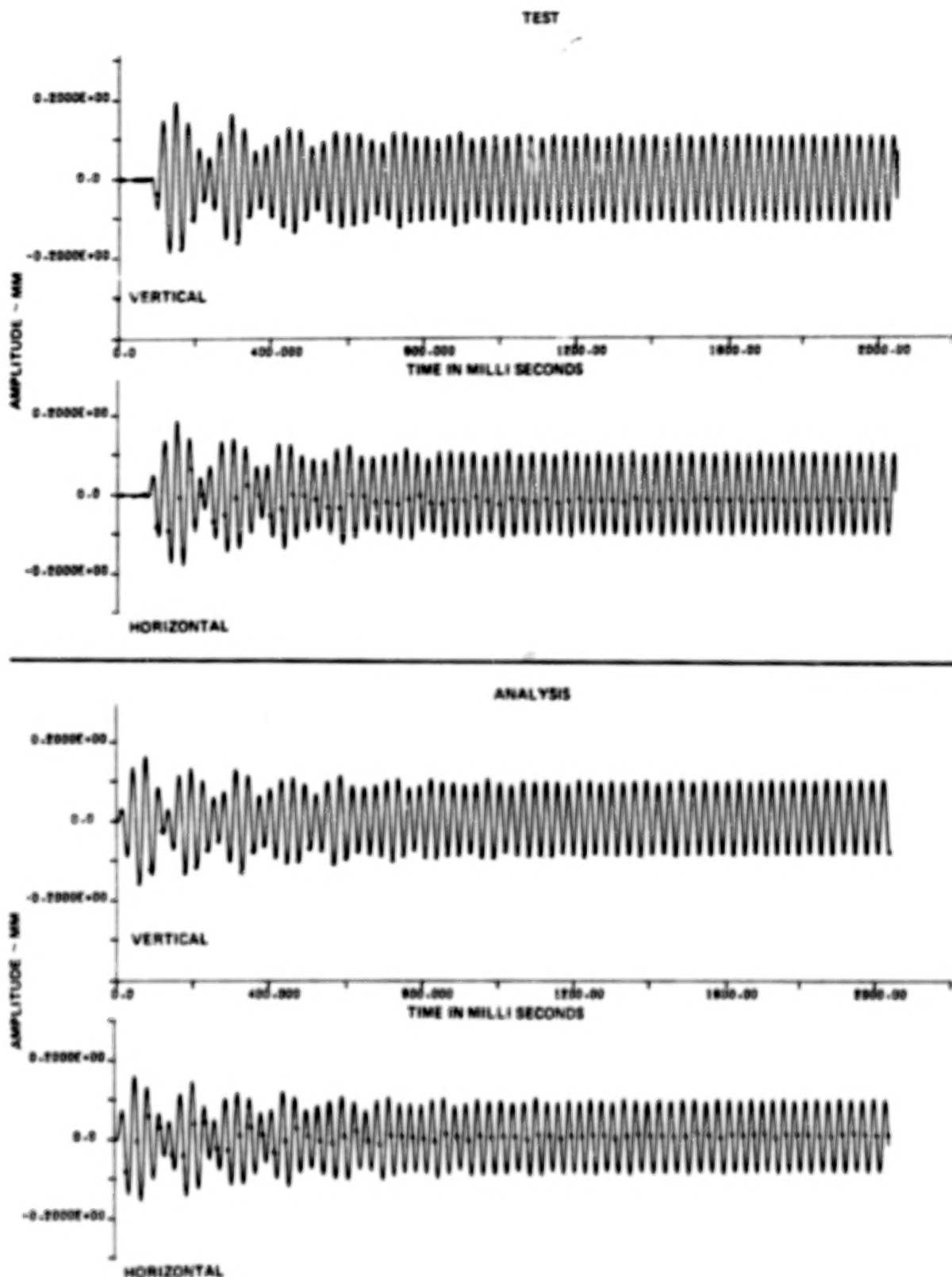


Figure 45 Experimental and Analytical Response From Data Station 4 During Damped Blade Loss At 2000 RPM With 27.65 g cm Imbalance

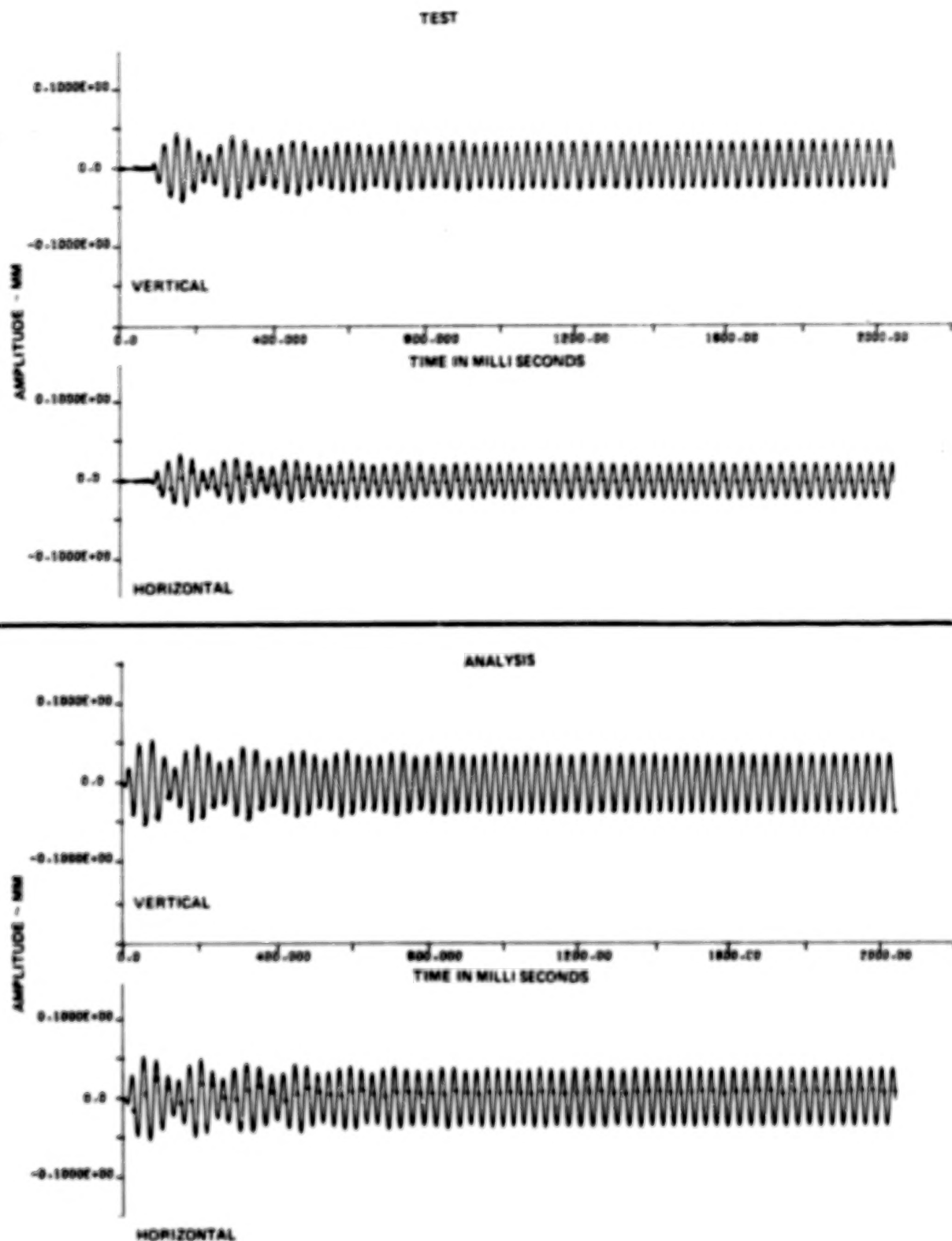
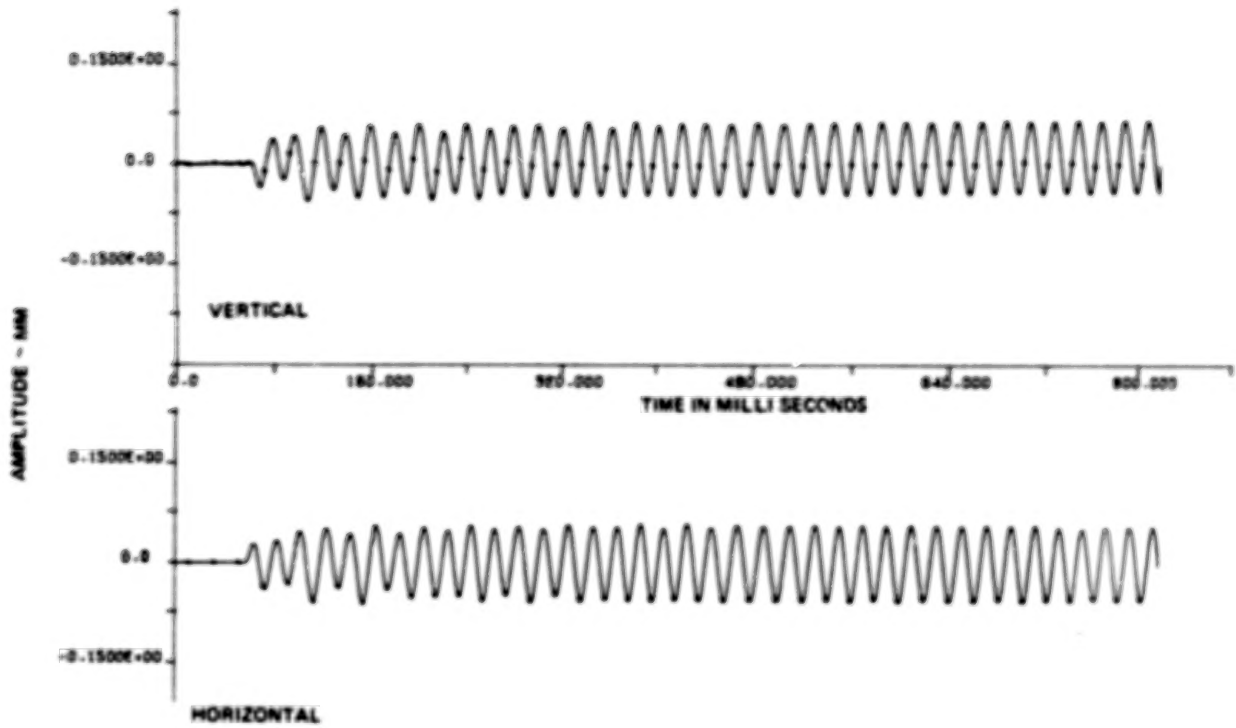


Figure 46 Experimental and Analytical Response From Data Station 5 During Lumped Blade Loss At 2000 RPM With 27.65 g cm Imbalance

TEST



ANALYSIS

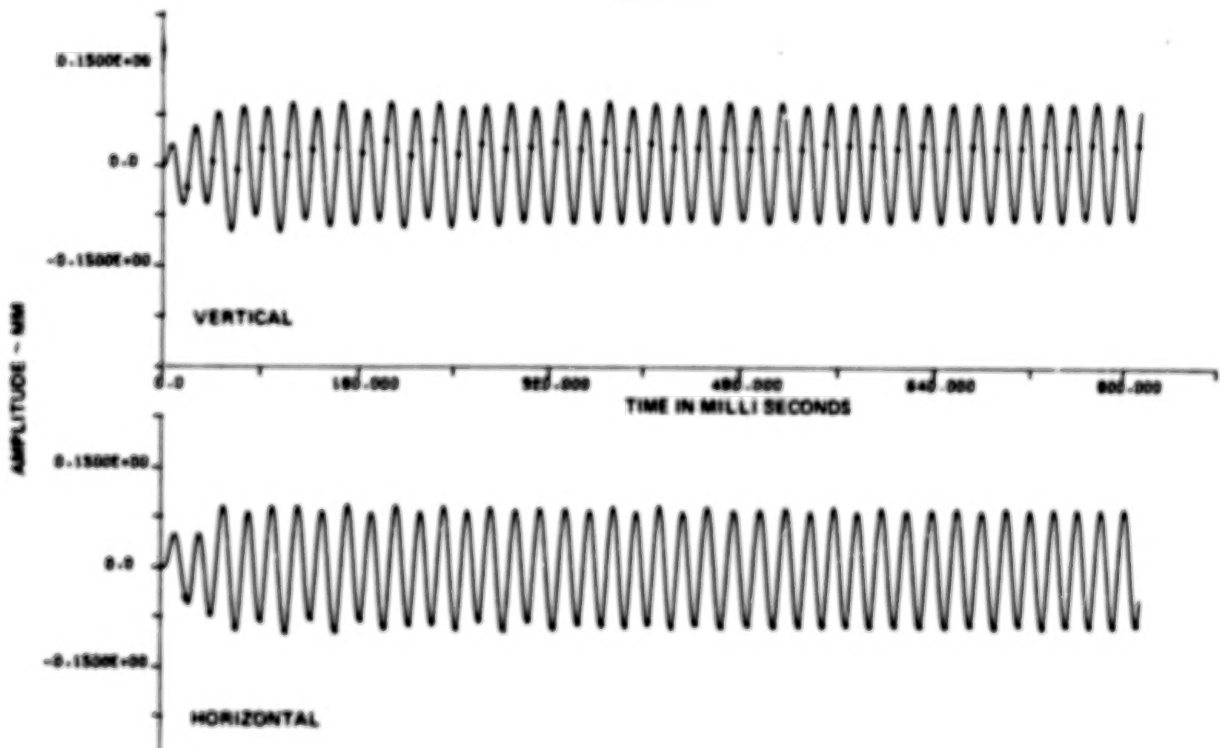


Figure 47 Experimental and Analytical Response From Data Station 1 During Damped Blade Loss At 2950 RPM With 27.65 g cm Imbalance

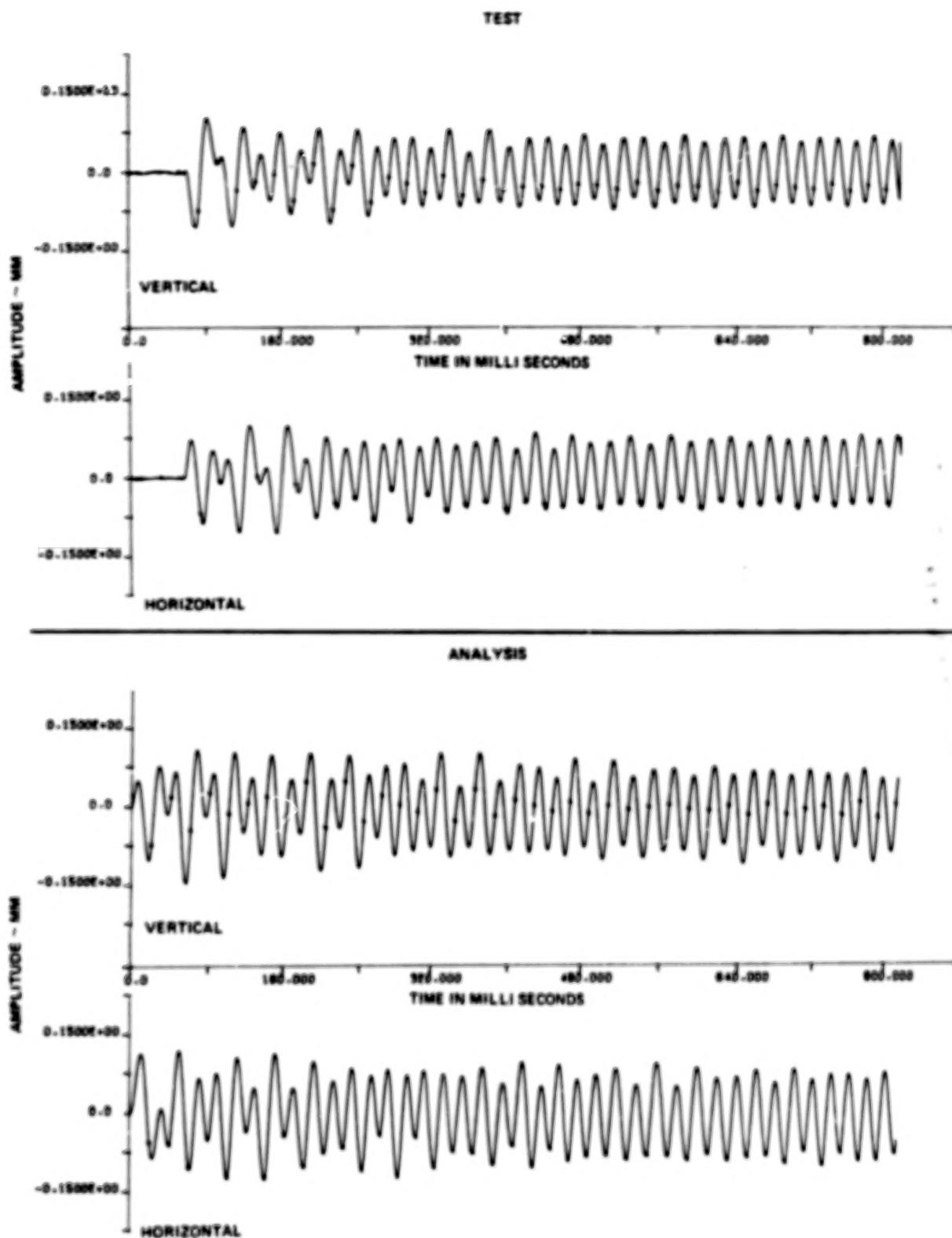


Figure 48 *Experimental and Analytical Response From Data Station 2 During Damped Blade Loss At 2950 RPM With 27.65 g cm Imbalance*

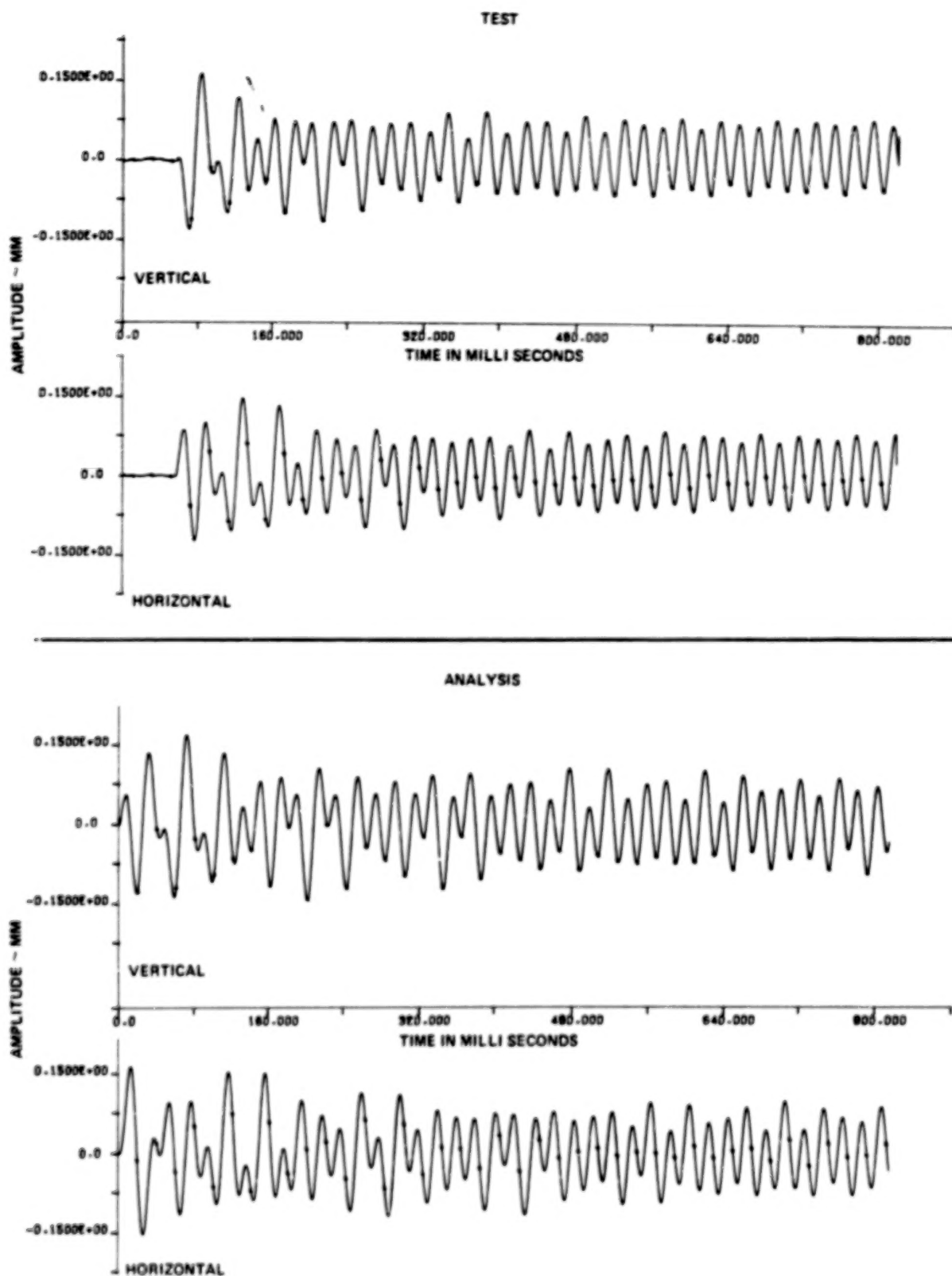


Figure 49 *Experimental and Analytical Response From Data Station 3 During Damped Blade Loss At 2950 RPM With 27.65 g cm Imbalance*

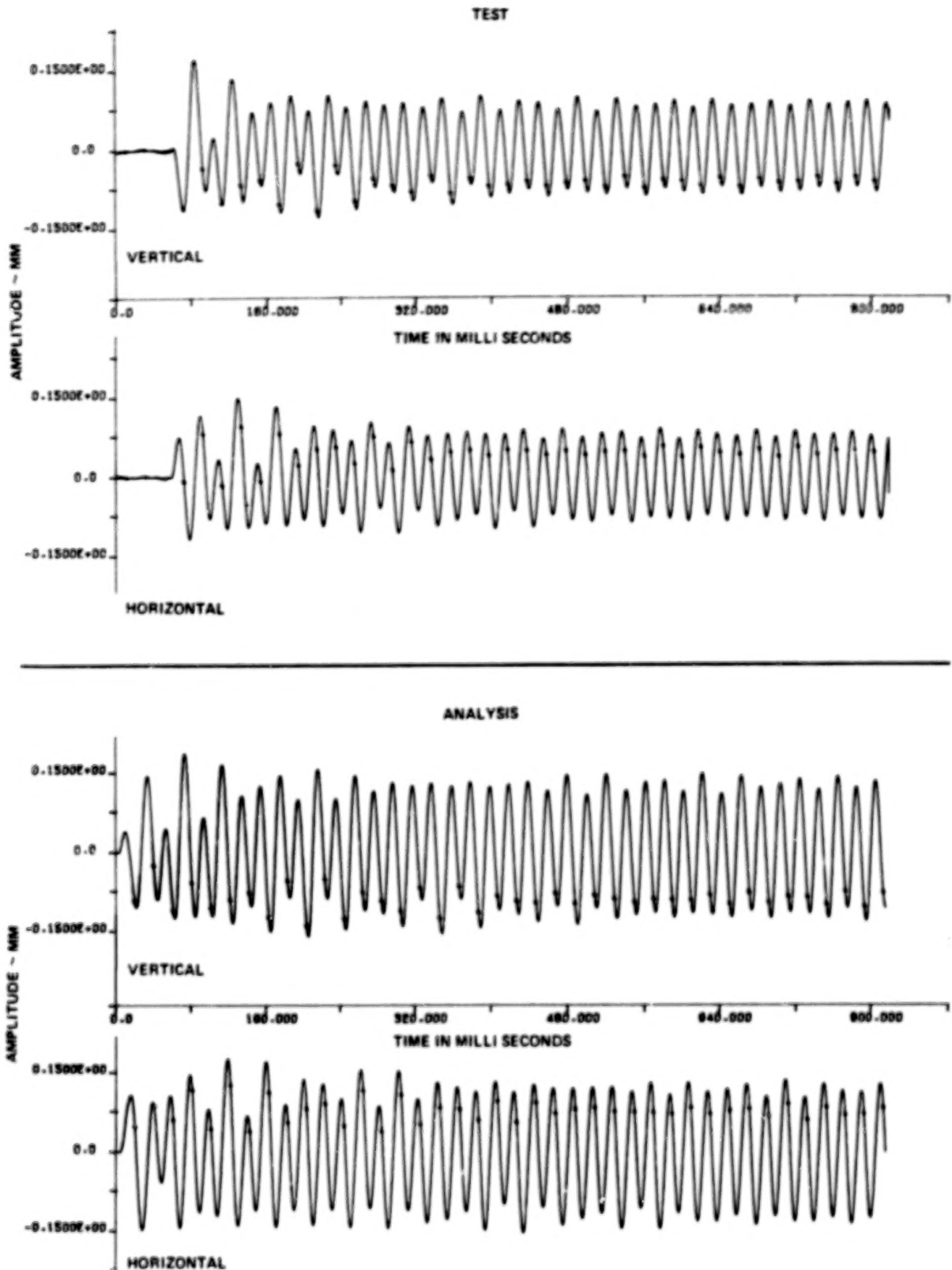


Figure 50 *Experimental and Analytical Response From Data Station 4 During Damped Blade Loss At 2950 RPM With 27.65 g cm Imbalance*

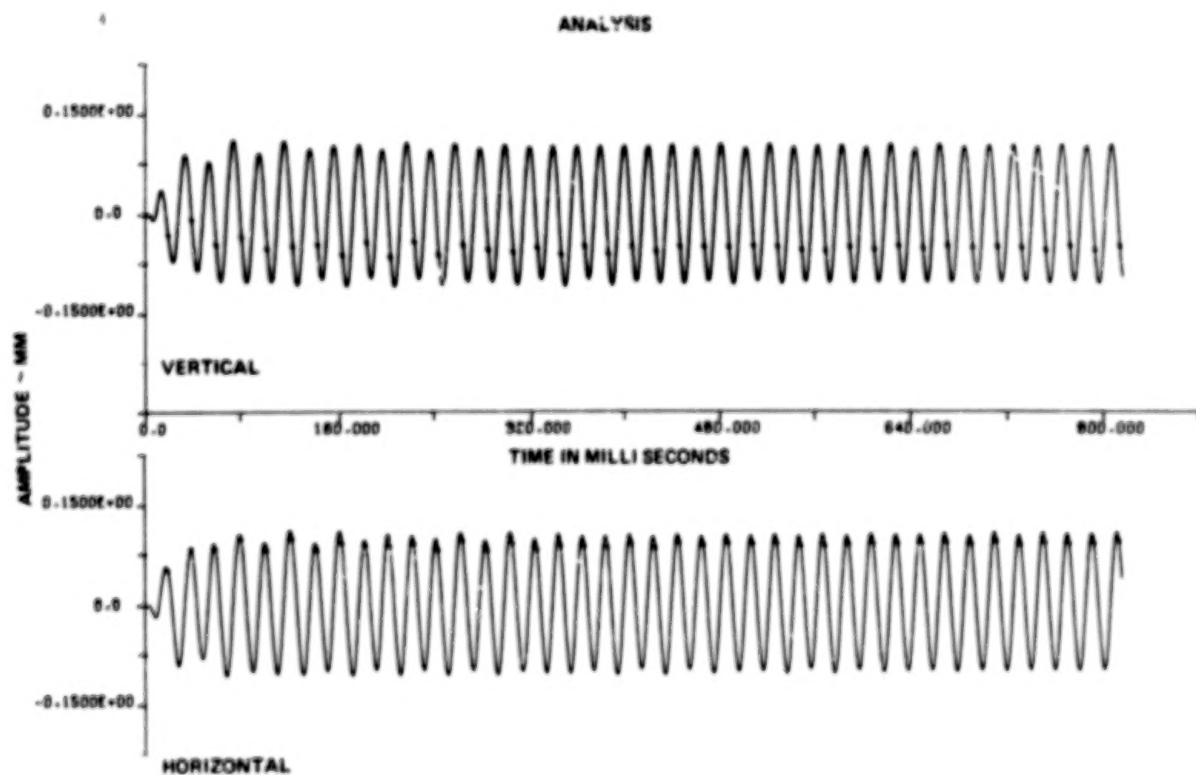
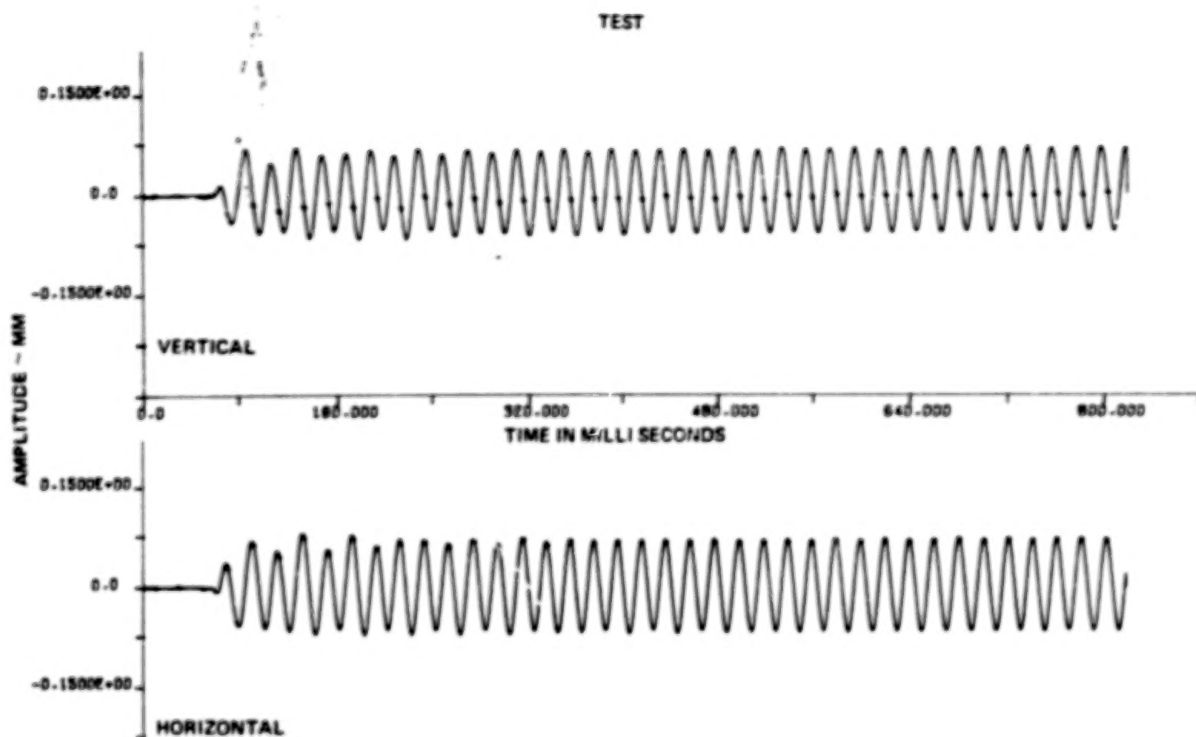


Figure 51 Experimental and Analytical Response From Data Station 5 During Damped Blade Loss At 2950 RPM With 27.65 g cm Imbalance

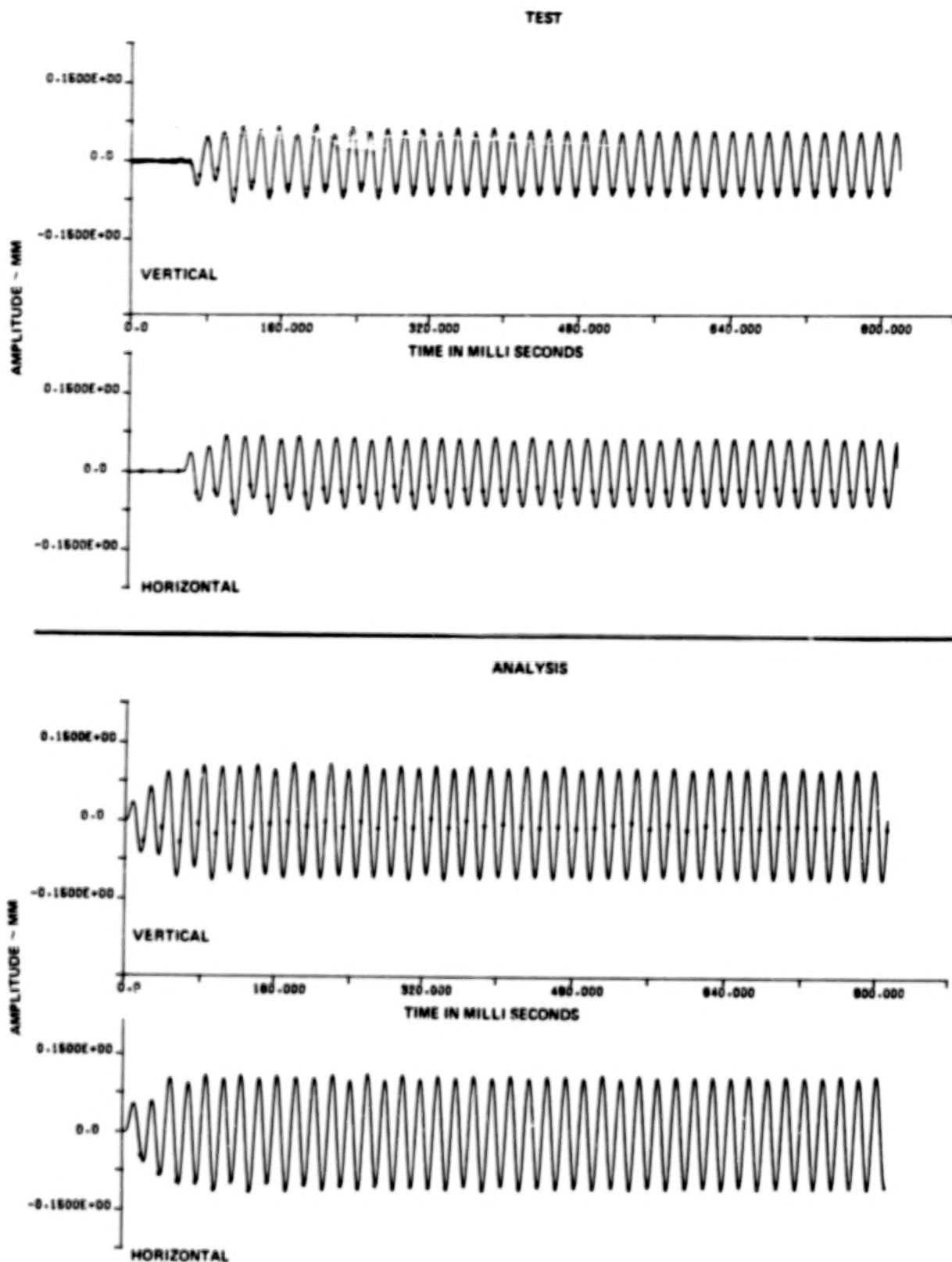


Figure 52 *Experimental and Analytical Response From Data Station 1 During Damped Blade Loss At 3100 RPM With 27.65 g cm Imbalance*

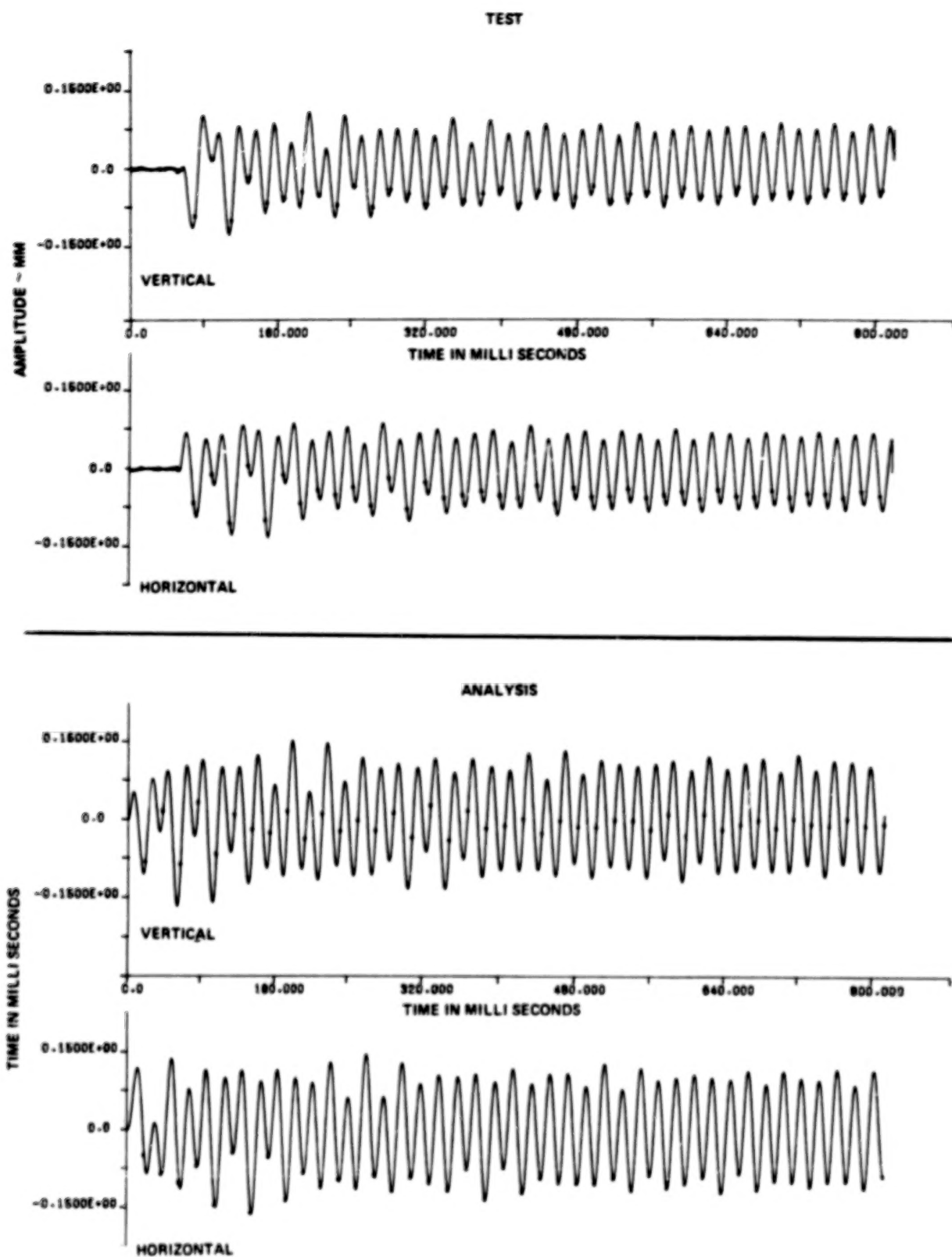


Figure 53 Experimental and Analytical Response From Data Station 2 During Damped Blade Loss At 3100 RPM With 27.65 g cm Imbalance

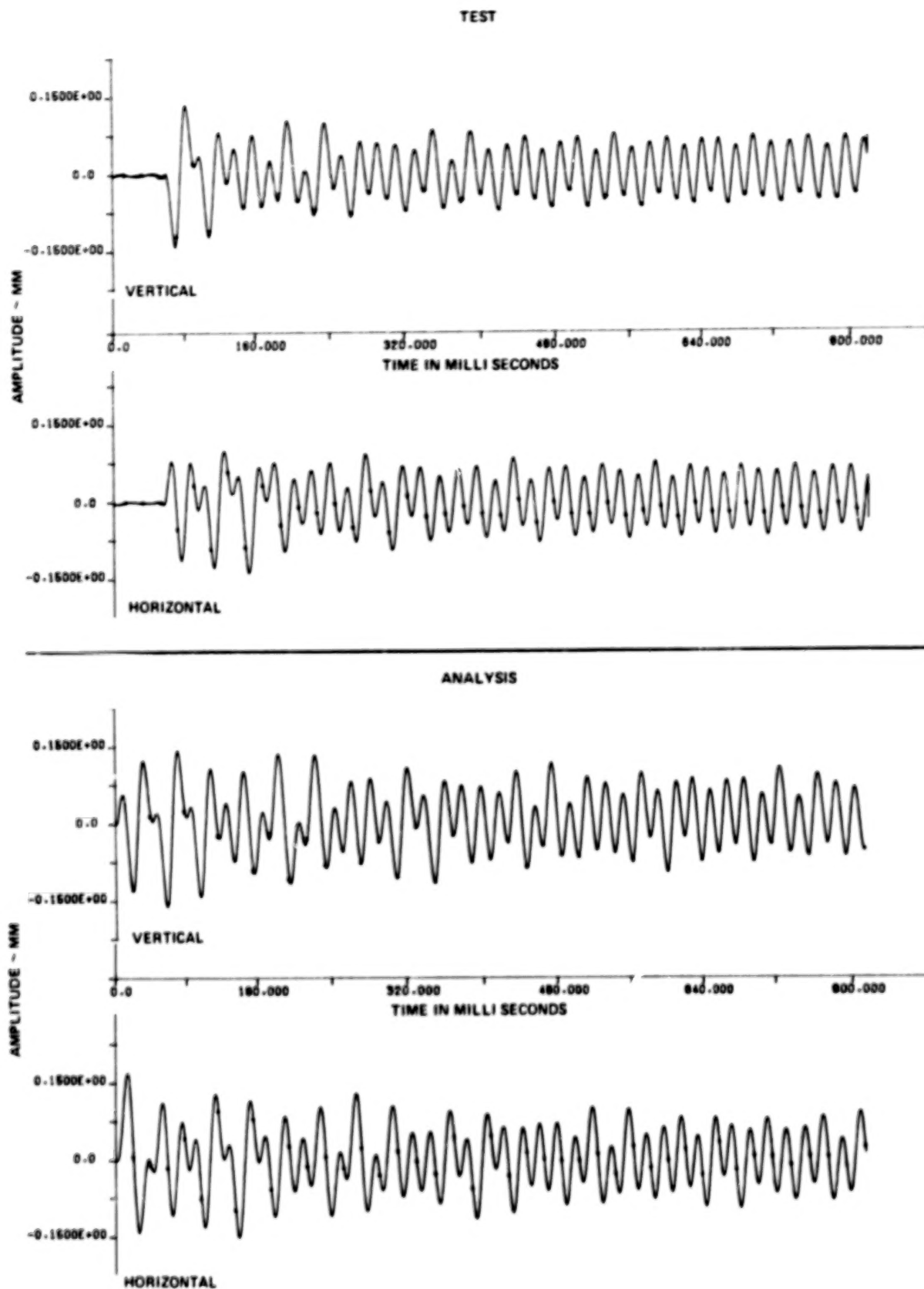


Figure 54 *Experimental and Analytical Response From Data Station 3 During Damped Blade Loss At 3100 RPM With 27.65 g cm Imbalance*

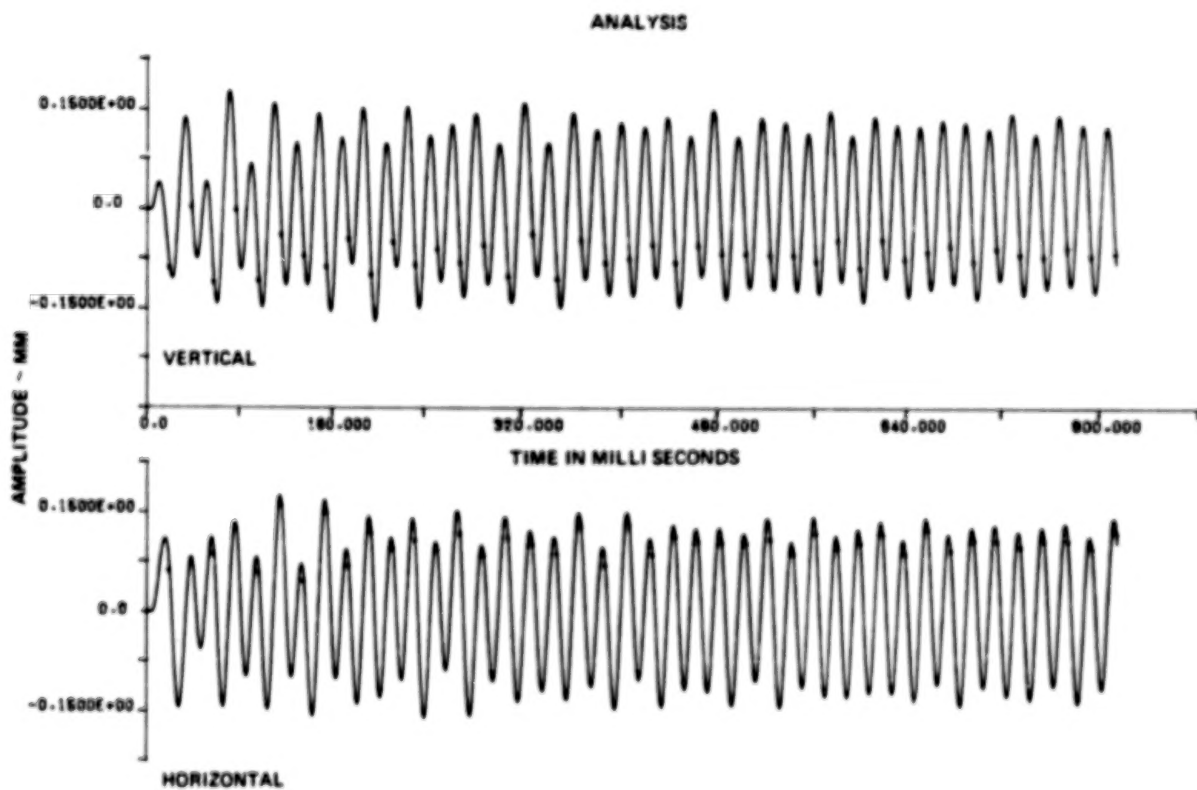
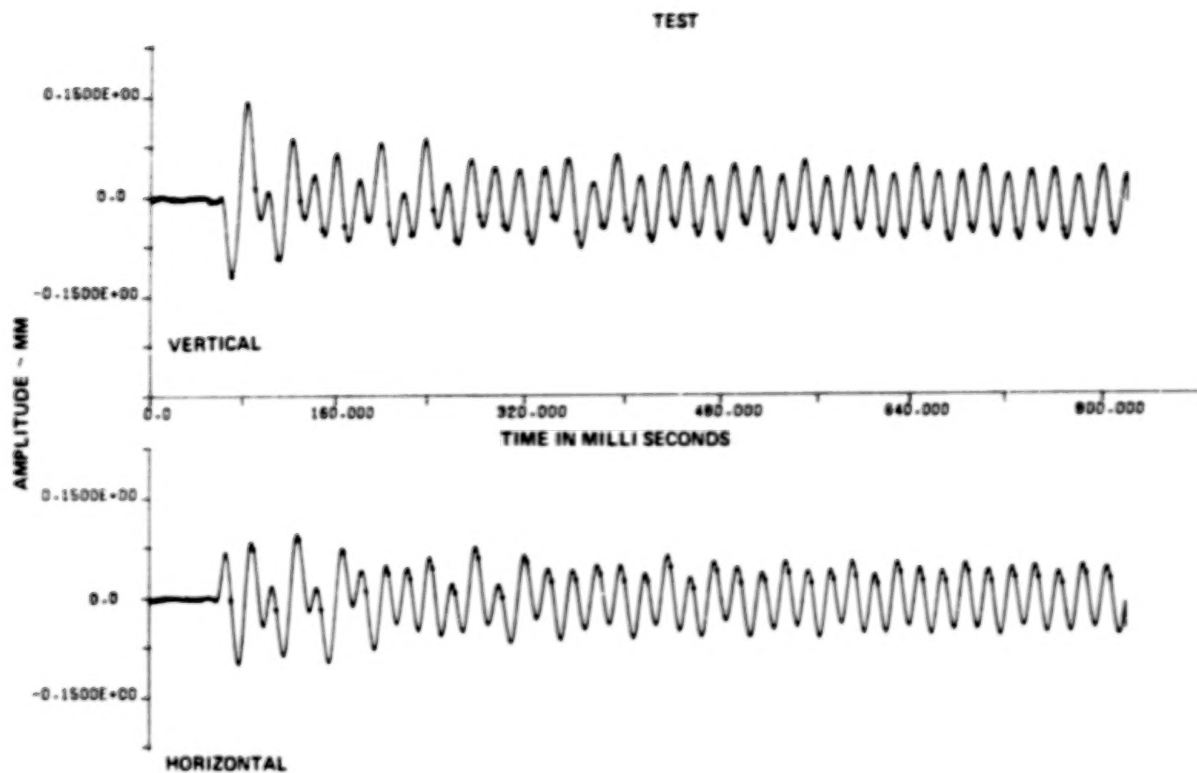


Figure 55 Experimental and Analytical Response From Data Station 4 During Damped Blade Loss At 3100 RPM With 27.65 g cm Imbalance

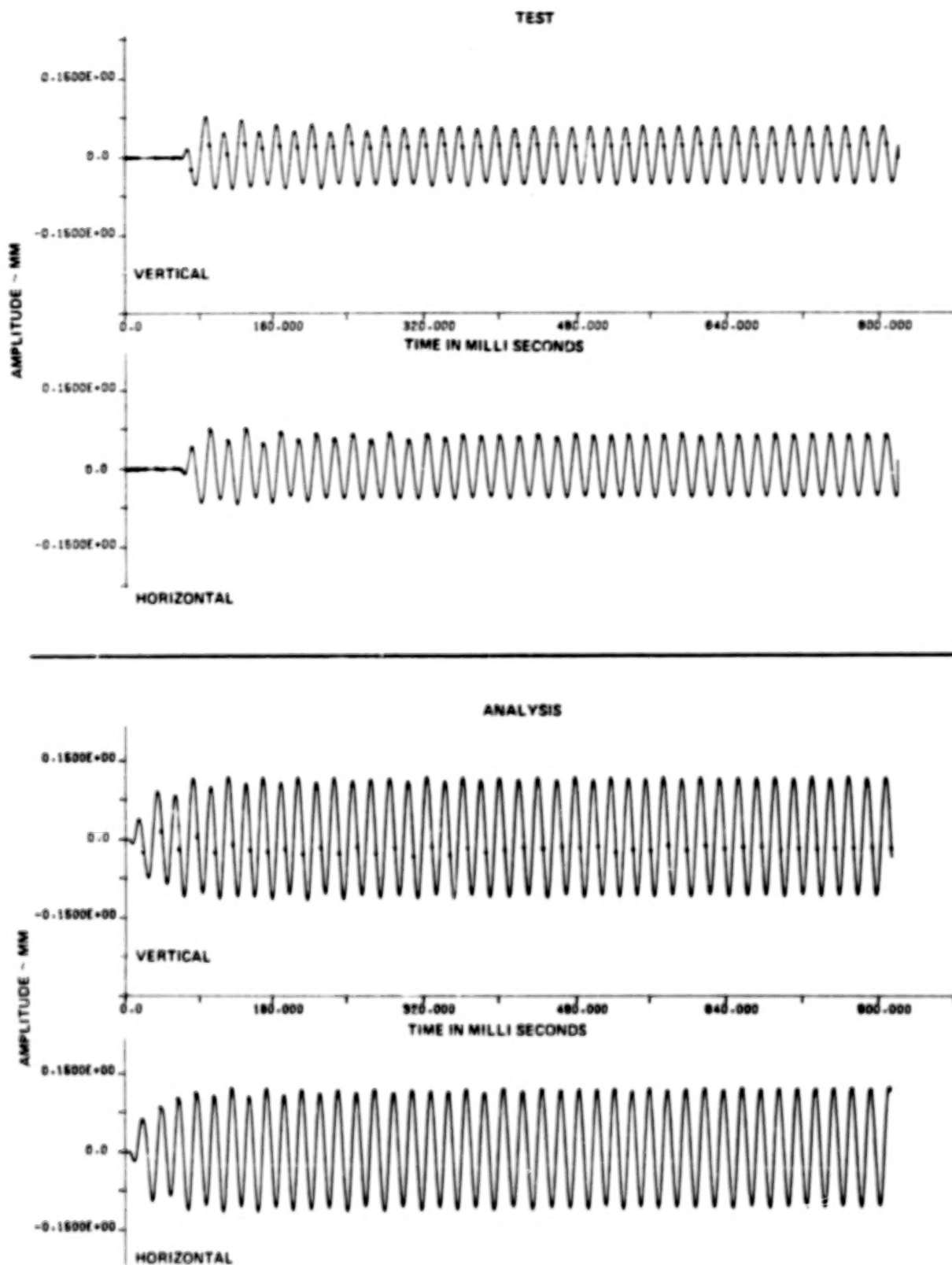


Figure 56 Experimental and Analytical Response From Data Station 5 During Damped Blade Loss At 3100 RPM With 27.65 g cm Imbalance

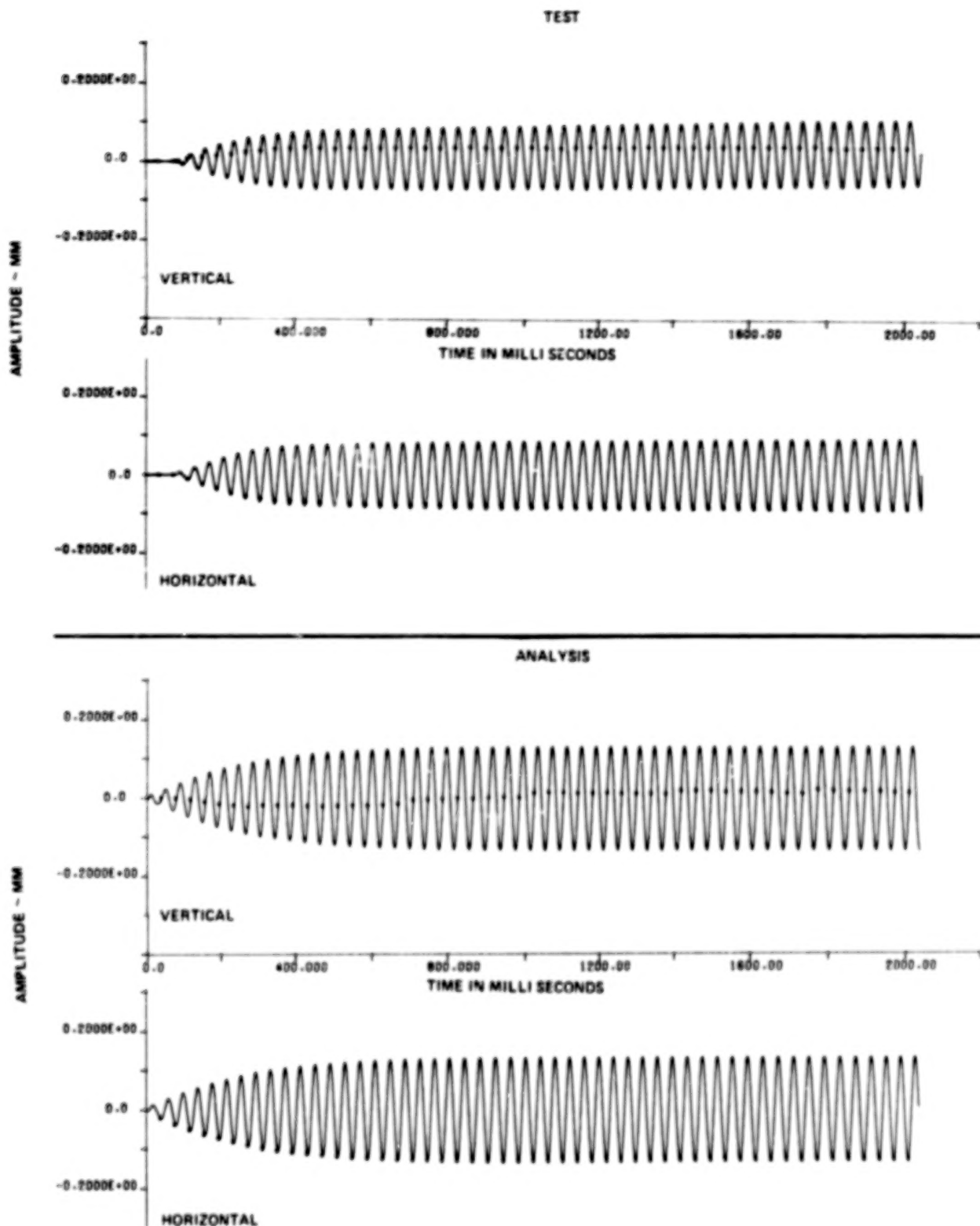


Figure 57 Experimental and Analytical Response From Data Station 1 During Damped Blade Loss At 1520 RPM With 22.22 g cm Imbalance

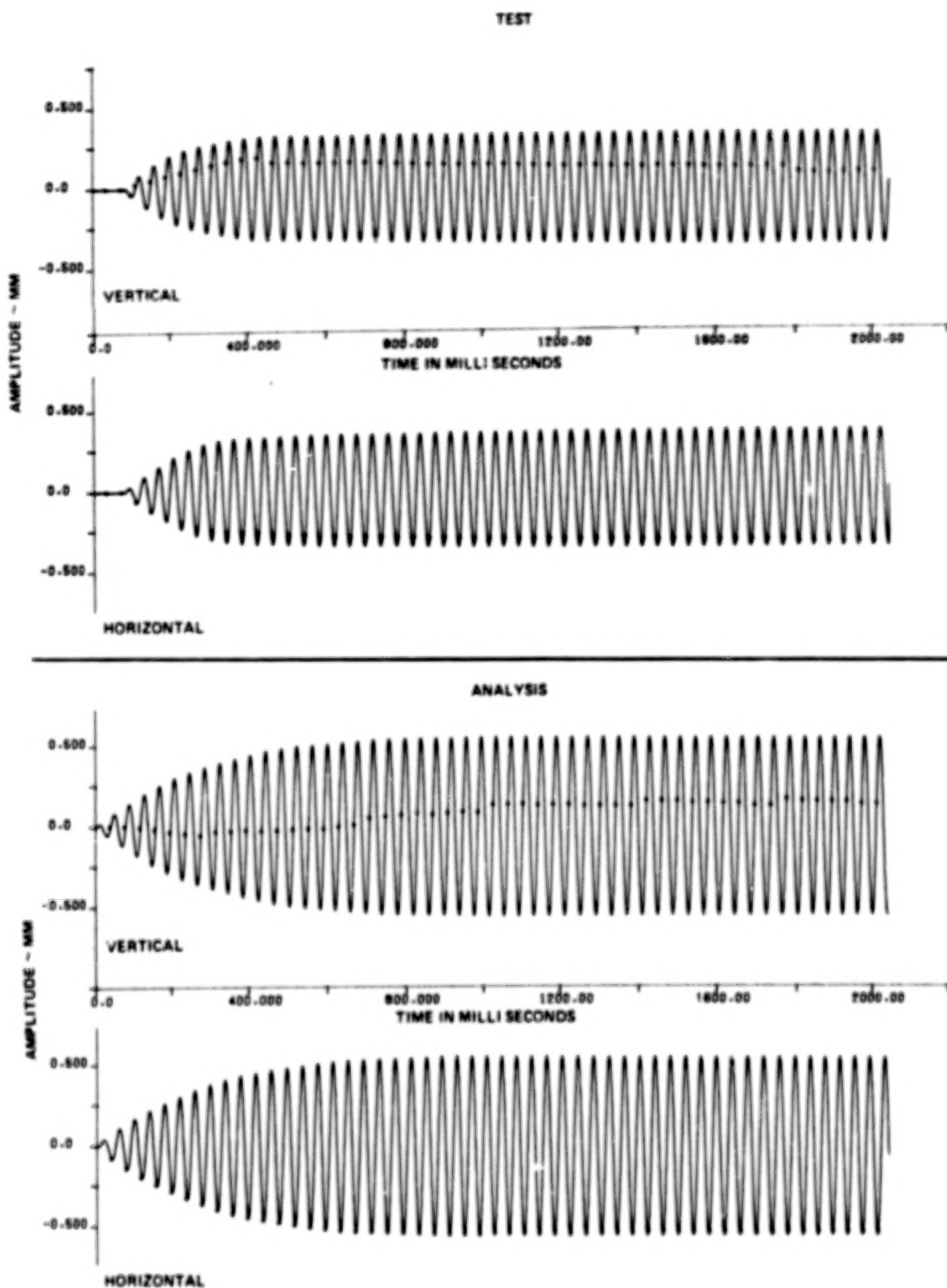
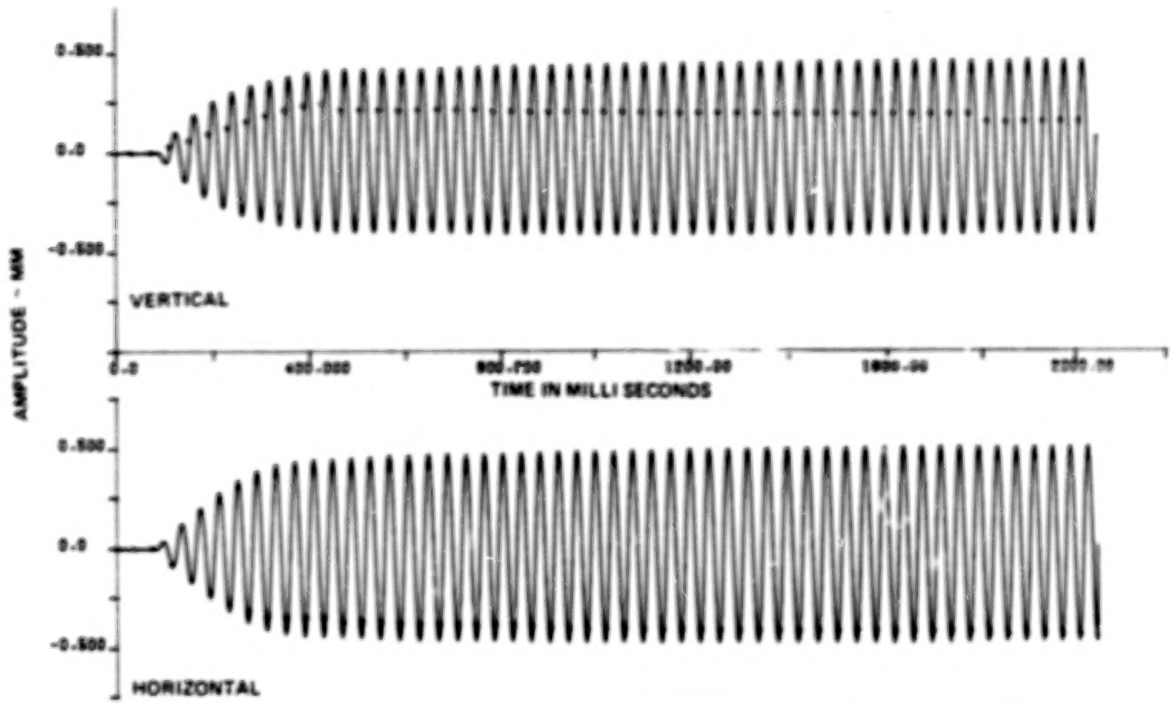


Figure 58 *Experimental and Analytical Response From Data Station 1 During Damped Blade Loss At 1520 RPM With 22.22 g cm Imbalance*

TEST



ANALYSIS

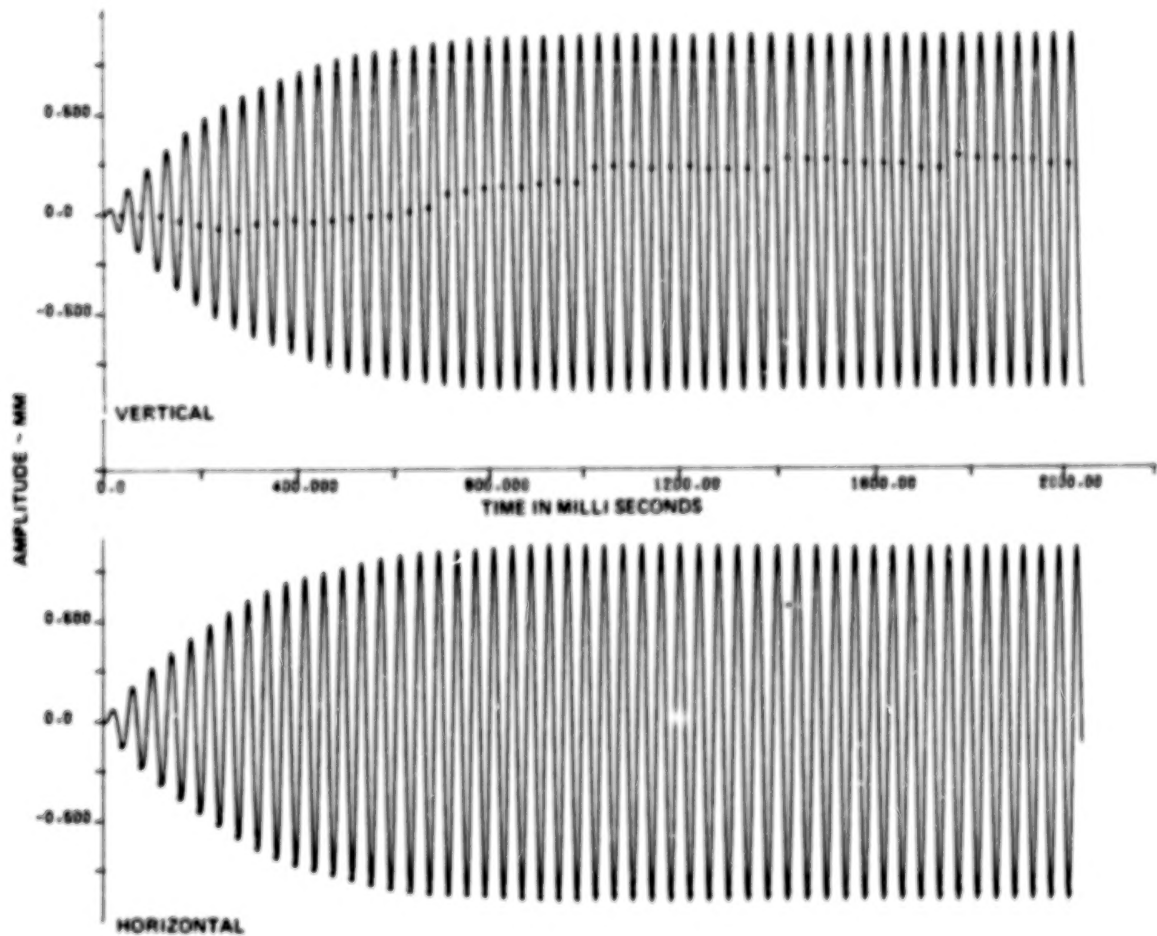


Figure 59 Experimental and Analytical Response From Data Station 3 During Damped Blade Loss At 1520 RPM With 22.22 g cm Imbalance

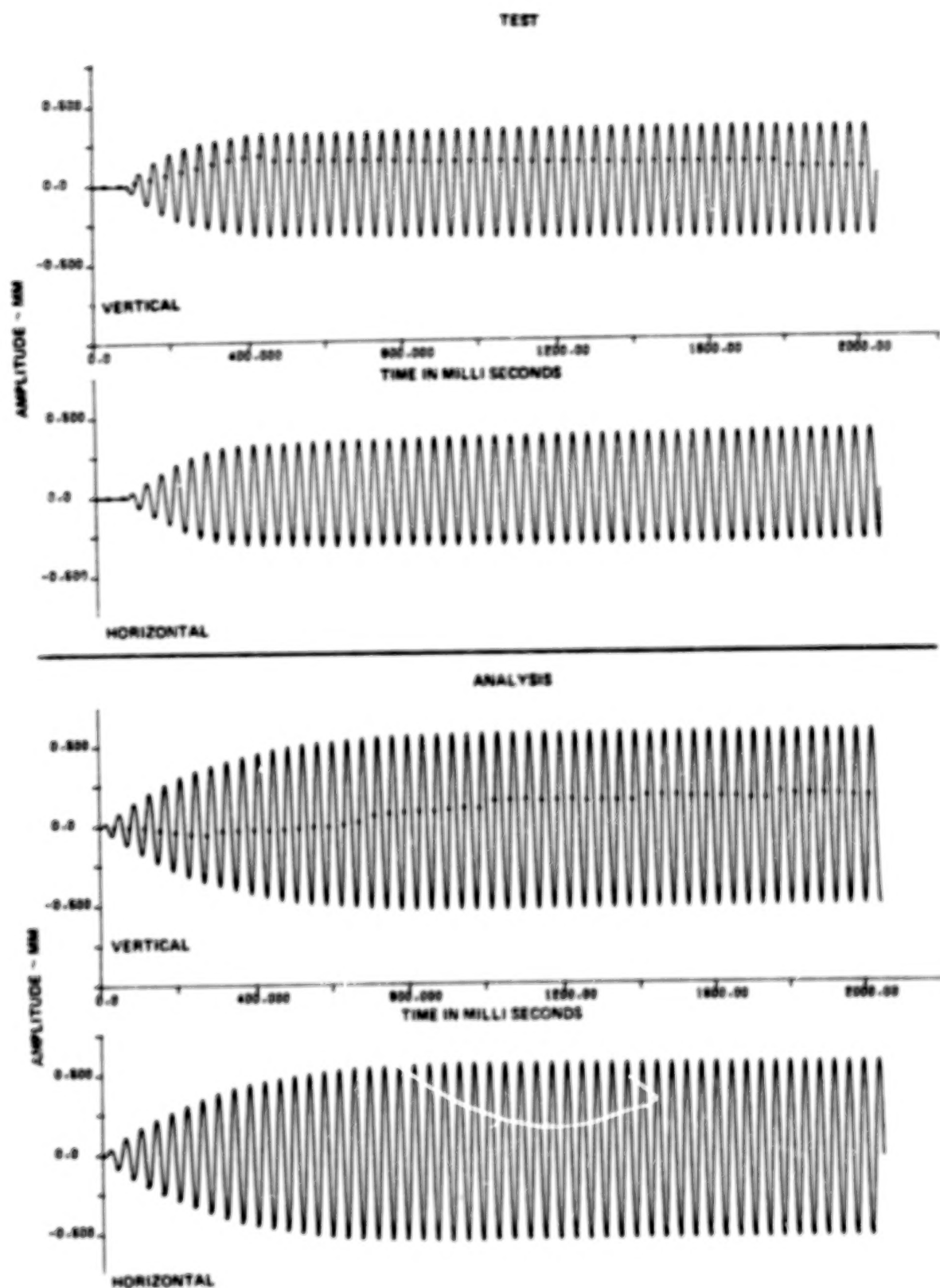
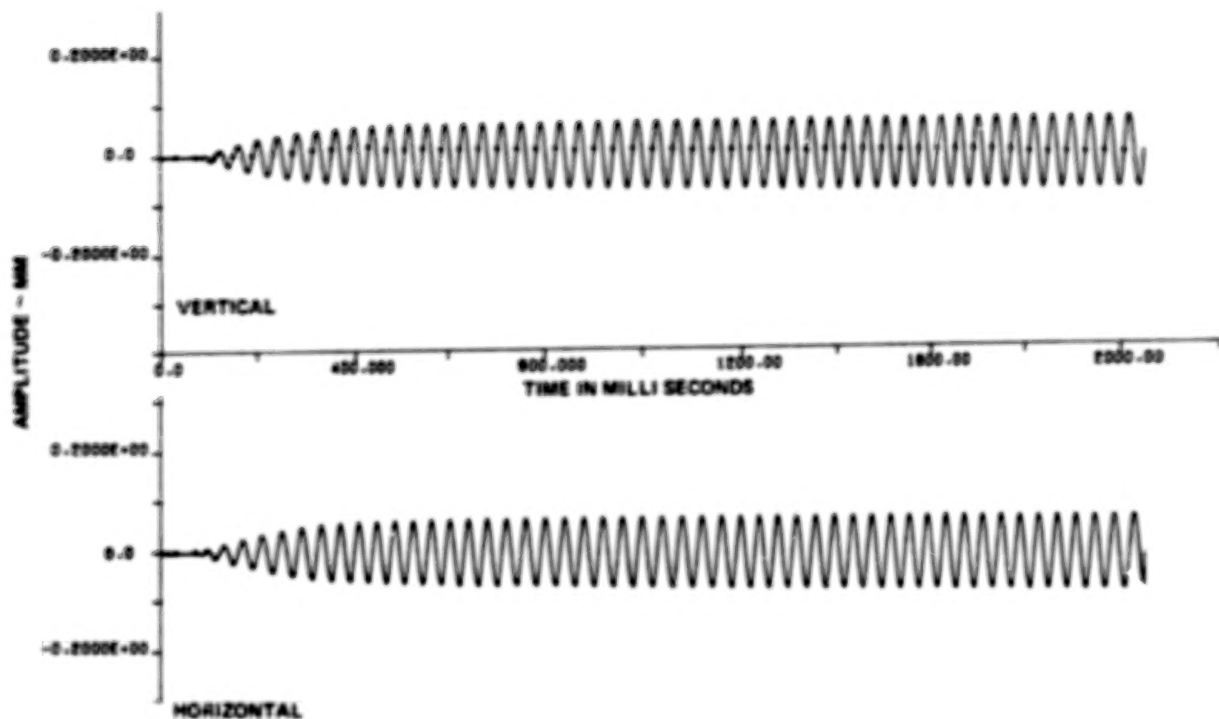


Figure 60 Experimental and Analytical Response From Data Station 4 During Damped Blade Loss At 1520 RPM With 22.22 g cm Imbalance

TEST



ANALYSIS

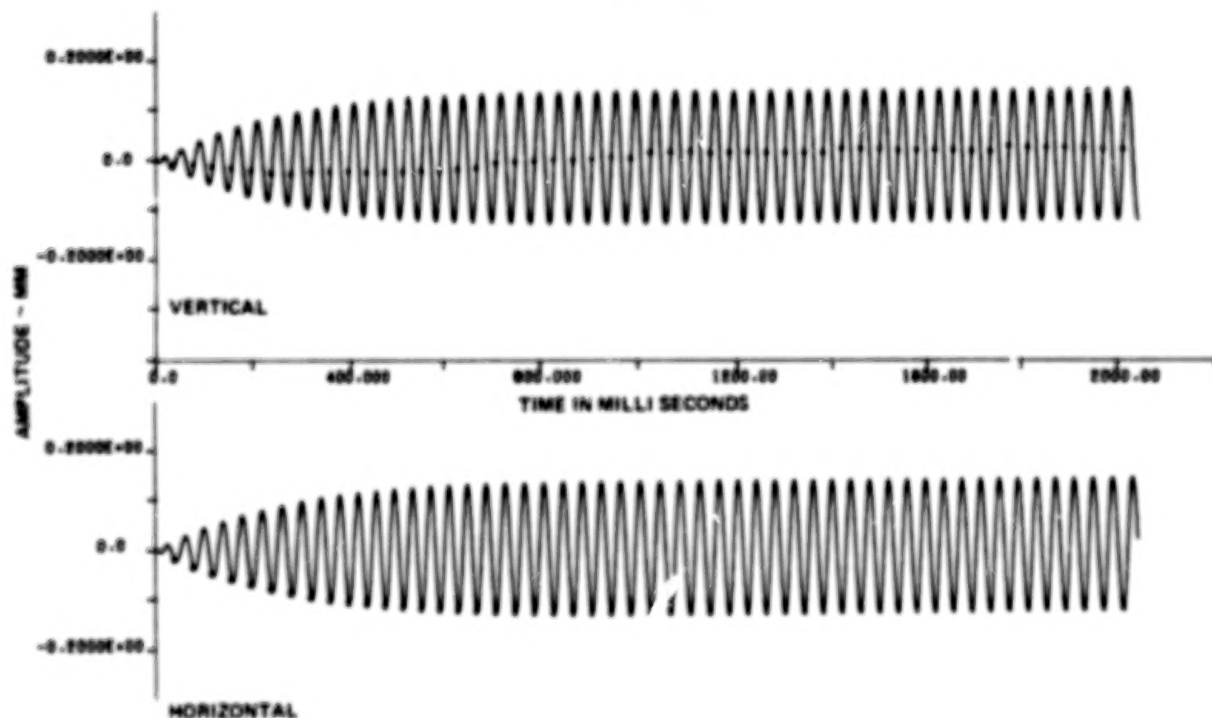


Figure 61 Experimental and Analytical Response From Data Station 5 During Damped Blade Loss At 1520 RPM With 22.22 g cm Imbalance

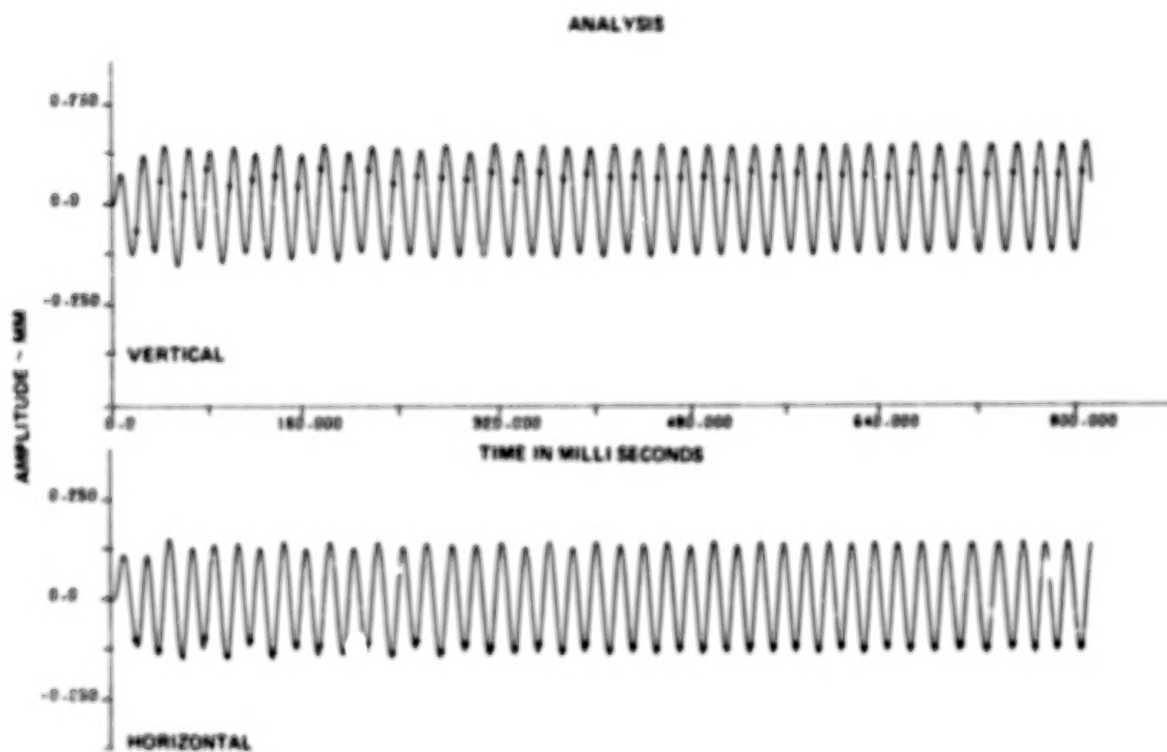
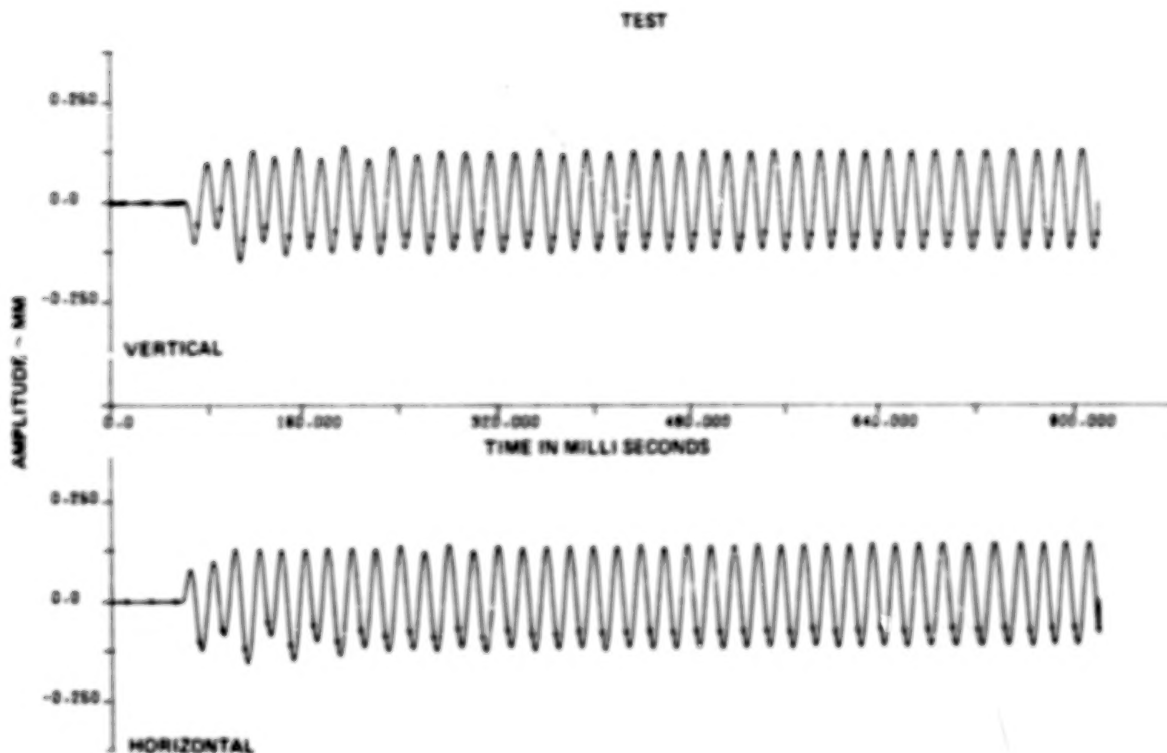


Figure 62 *Experimental and Analytical Response From Data Station 1 During Damped Blade Loss At 3050 RPM With 66.07 g cm Imbalance*

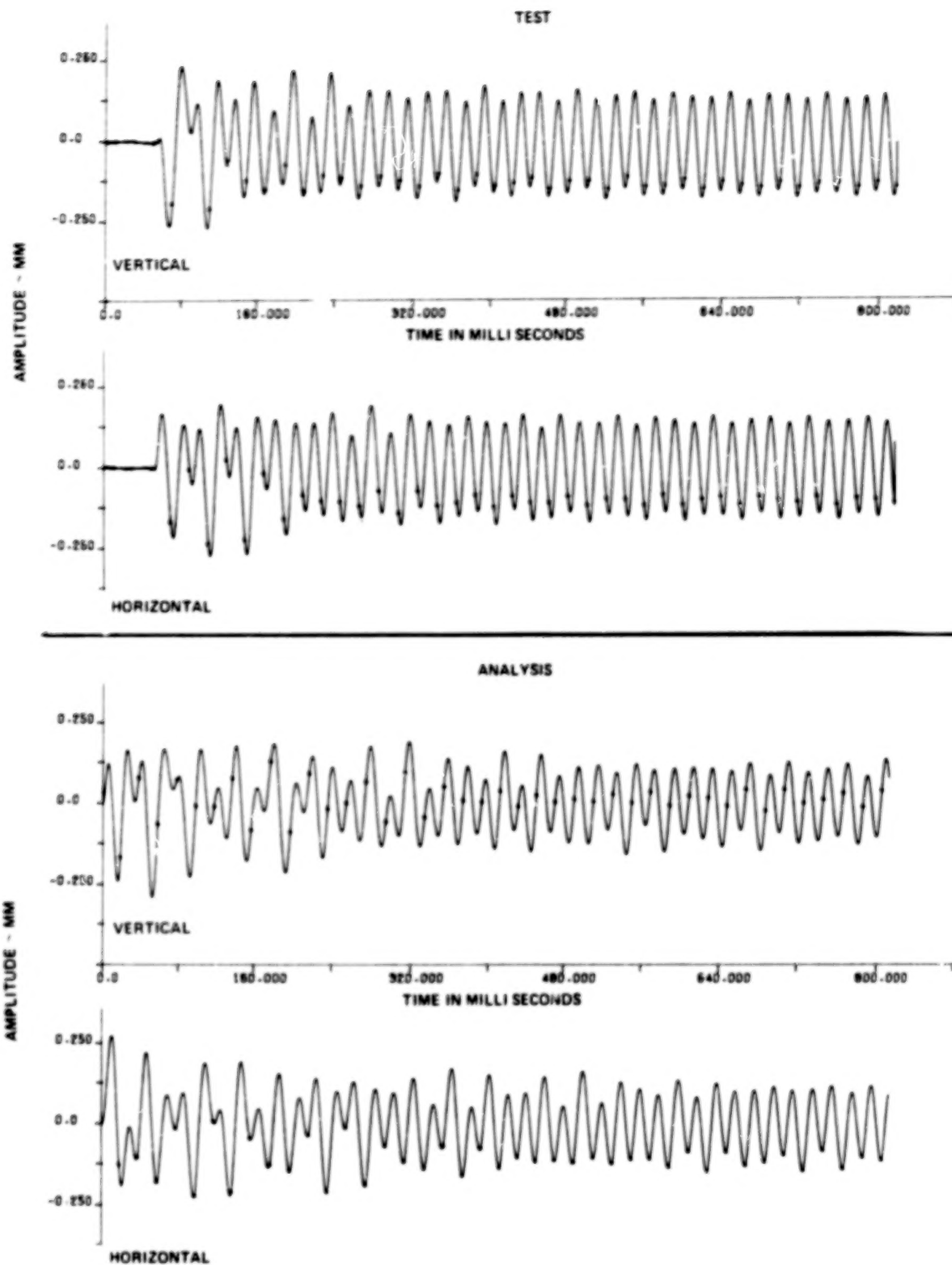


Figure 63 Experimental and Analytical Response From Data Station 2 During Damped Blade Loss At 3050 RPM With 66.07 g cm Imbalance

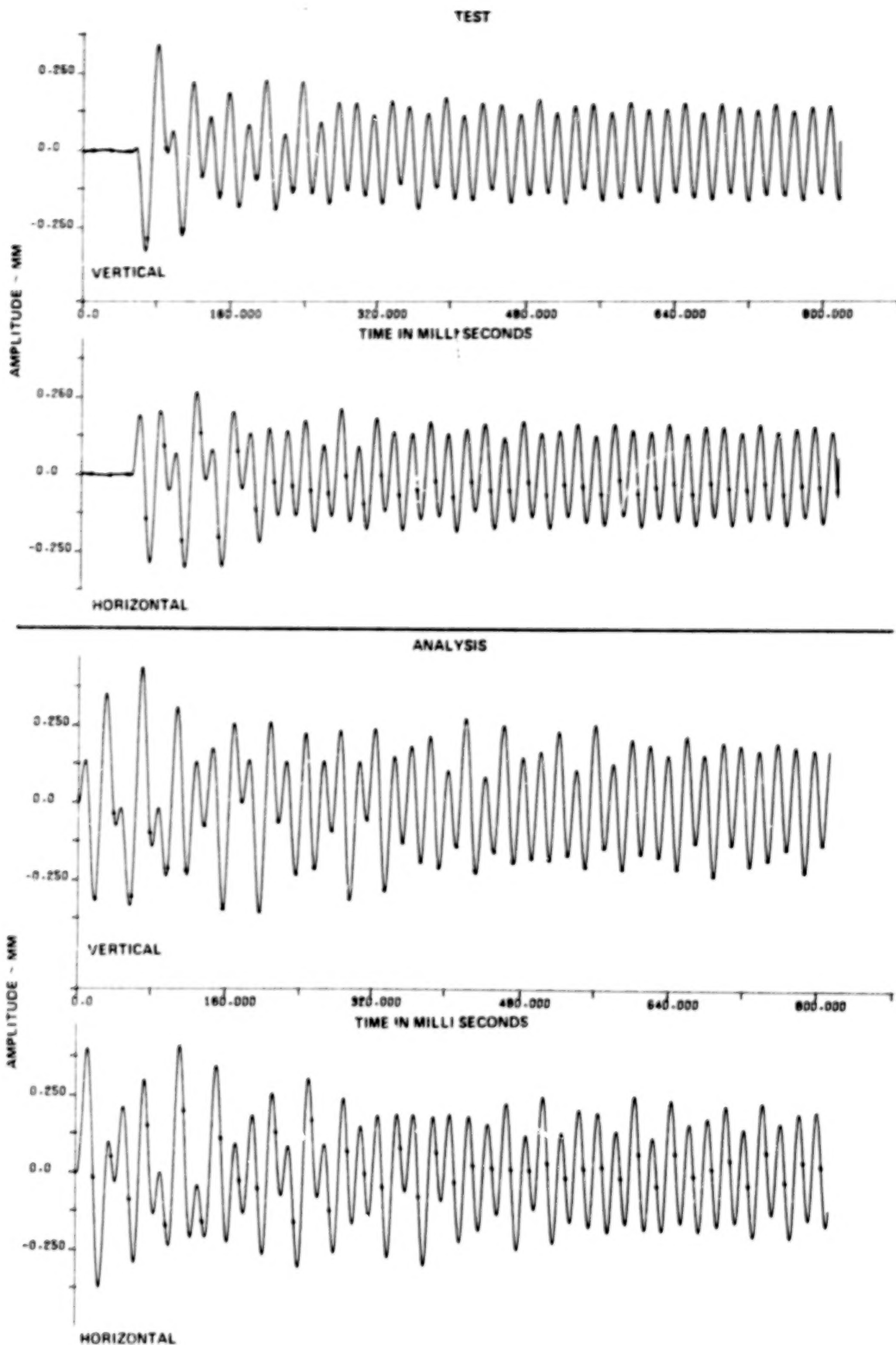


Figure 64 *Experimental and Analytical Response From Data Station 3 During Damped Blade Loss At 3050 RPM With 66.07 g cm Imbalance*

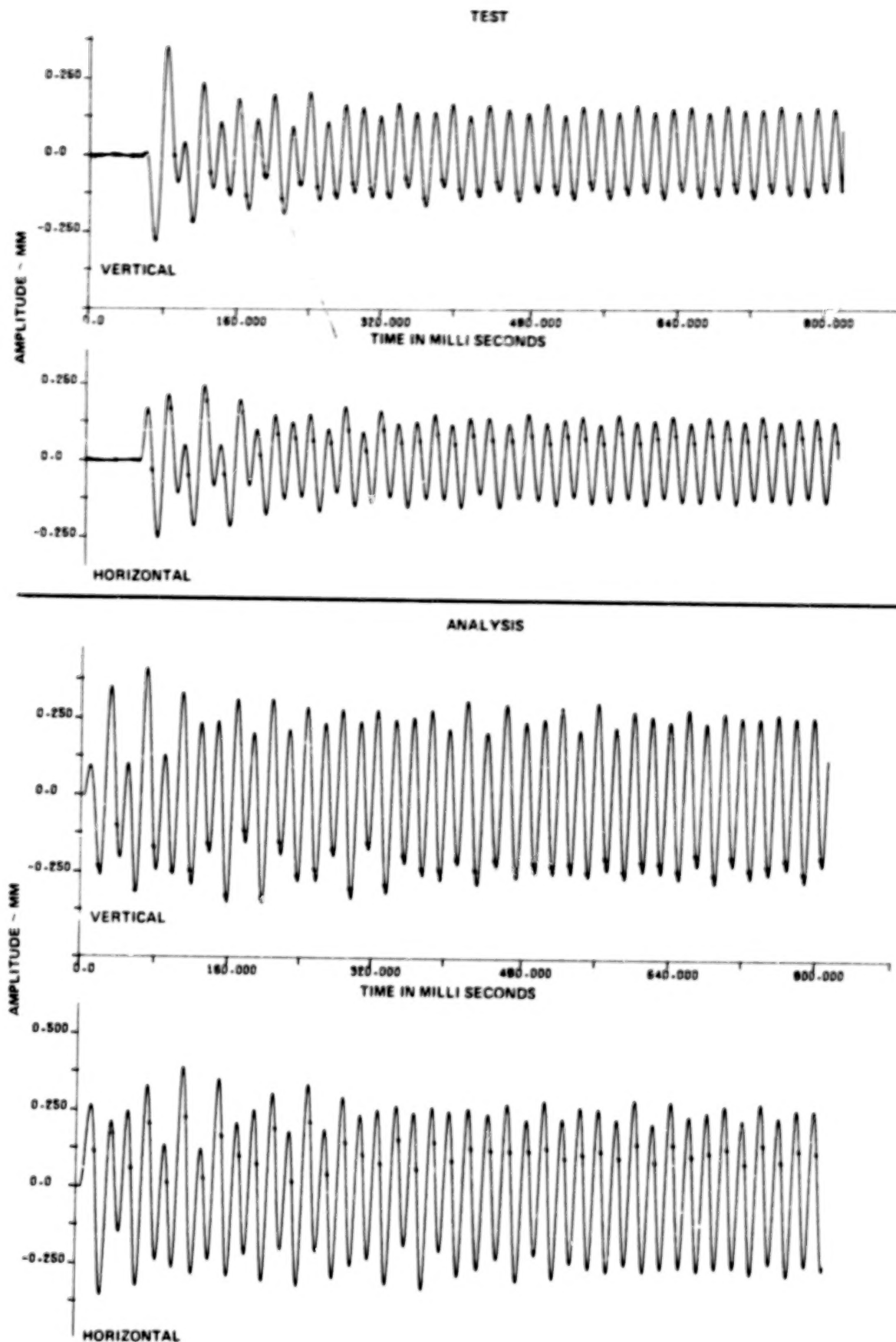


Figure 65 *Experimental and Analytical Response From Data Station 4 During Damped Blade Loss At 3050 RPM With 66.07 g cm Imbalance*

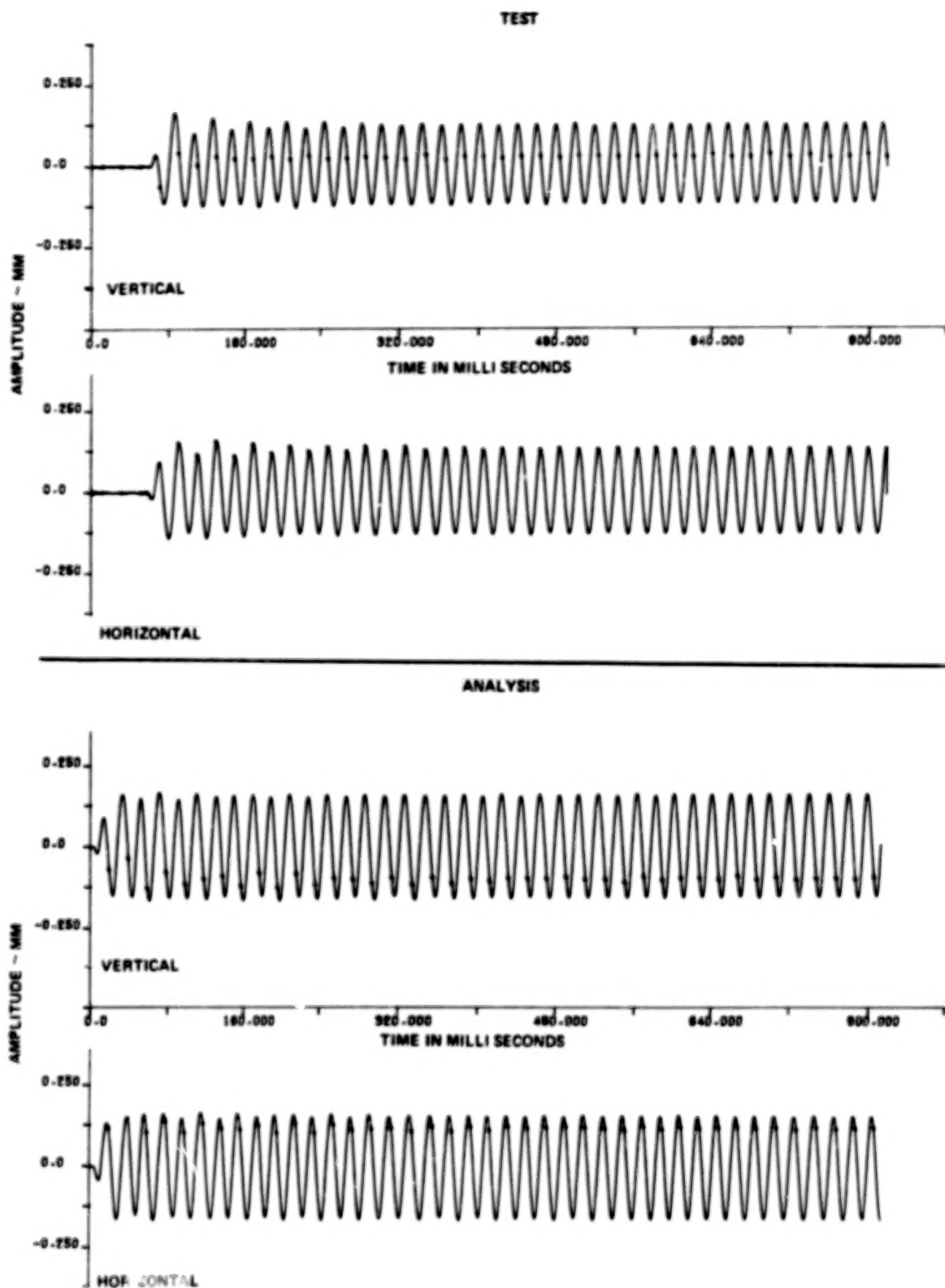
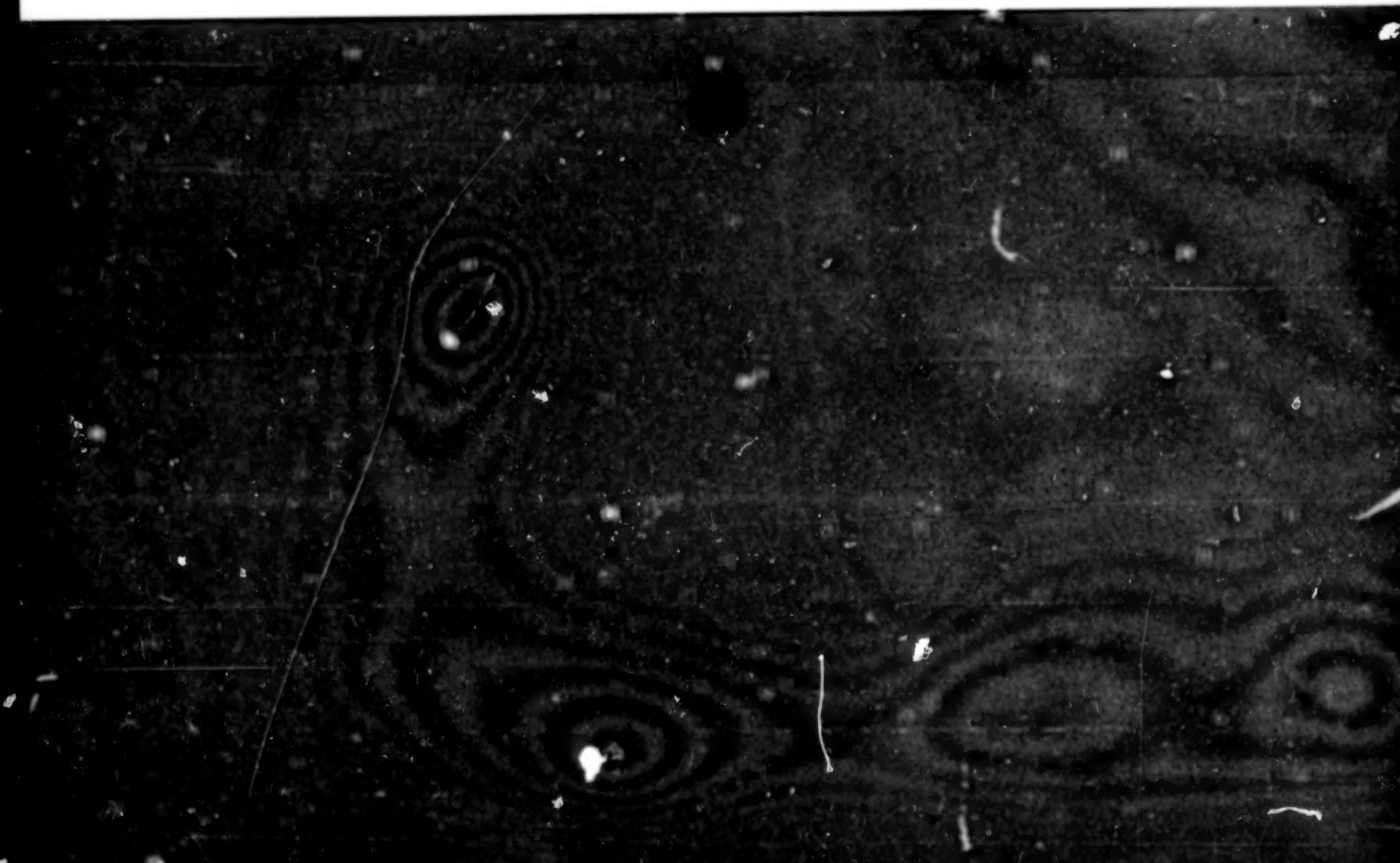


Figure 66 Experimental and Analytical Response From Data Station 5 During Damped Blade Loss At 3050 RPM With 66.07 g cm Imbalance

1. Report No. NASA CR-3050	2. Government Accession No.	3. Recipient's Catalog No.	
4. Title and Subtitle TRANSIENT DYNAMICS OF A FLEXIBLE ROTOR WITH SQUEEZE FILM DAMPERS		5. Report Date September 1978	
		6. Performing Organization Code	
7. Author(s) D. F. Buono, L. D. Schlitzer, R. G. Hall III, and D. H. Hibner		8. Performing Organization Report No. PWA 5548-9	
		10. Work Unit No.	
9. Performing Organization Name and Address United Technologies Corporation Pratt & Whitney Aircraft East Hartford, Connecticut 06108		11. Contract or Grant No. NAS3-18523	
		13. Type of Report and Period Covered Contractor Report	
12. Sponsoring Agency Name and Address National Aeronautics and Space Administration Washington, D. C. 20546		14. Sponsoring Agency Code	
15. Supplementary Notes Final report. Project Manager, Albert F. Kascak, Propulsion Laboratory, AVRADCOM Research and Technology Laboratories, NASA Lewis Research Center, Cleveland, Ohio 44135.			
16. Abstract <p>This report contains the results of an experimental and analytical investigation of the transient response of a flexible rotor with squeeze film dampers. The experimental part of the program consisted of a series of simulated blade loss tests on a test rotor designed to operate above its second bending critical speed. The analytical part of the program comprised a series of analyses which predicted the transient behavior of the test rig for each of the blade loss tests. The scope of the program included the investigation of transient rotor dynamics of a flexible rotor system, similar to modern flexible jet engine rotors, both with and without squeeze film dampers. The results substantiate the effectiveness of squeeze film dampers and document the ability of available analytical methods to predict their effectiveness and behavior.</p>			
17. Key Words (Suggested by Author(s)) Transient response Blade loss Flexible rotor Rotor vibration Squeeze film damper		18. Distribution Statement Unclassified - unlimited STAR Category 37	
19. Security Classif. (of this report) Unclassified	20. Security Classif. (of this page) Unclassified	21. No. of Pages 83	22. Price* A05



END

MAR 2 1979